High Reynolds Number Wall-Bounded Turbulence: Approach to Asymptotic State, Universality and ICET

by

Hassan Nagib
Illinois Institute of Technology, Chicago, USA
and
ICET (International Collaboration of Experiments on Turbulence)

for

NORDITA Programme on Turbulent Boundary Layers
and
Linné Flow Centre at KTH
Friday, 23 April, 2010
Stockholm, Sweden

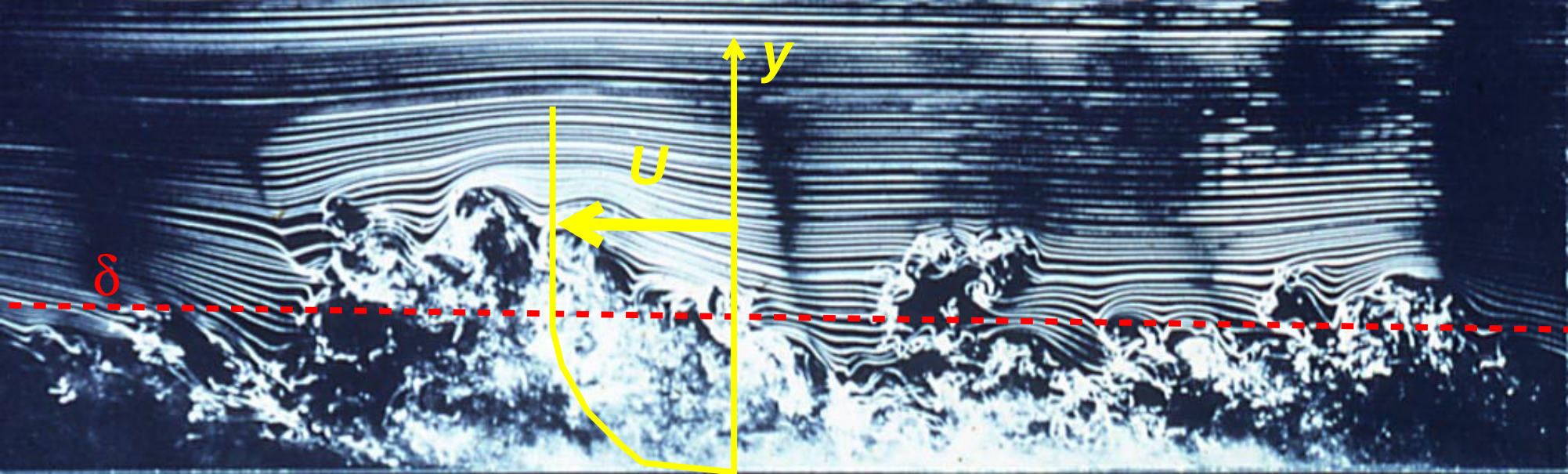
y
u
δ

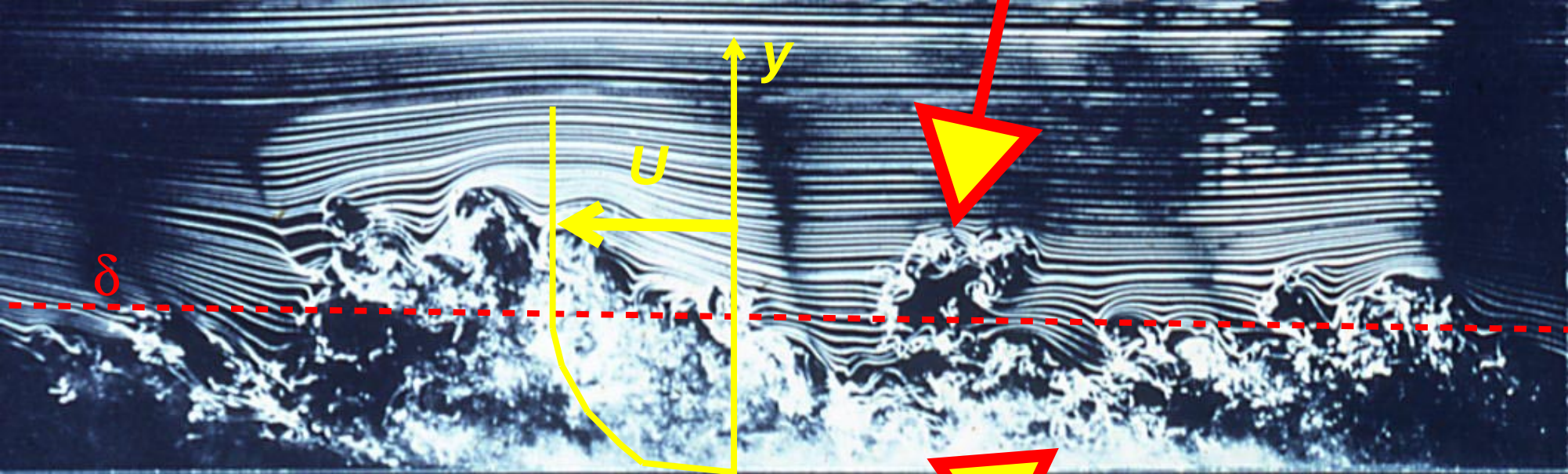
y
u
δ

Typical description of wall-bounded flows

The boundary layer is divided into different regions based on the the dynamics of mean flow and turbulence.

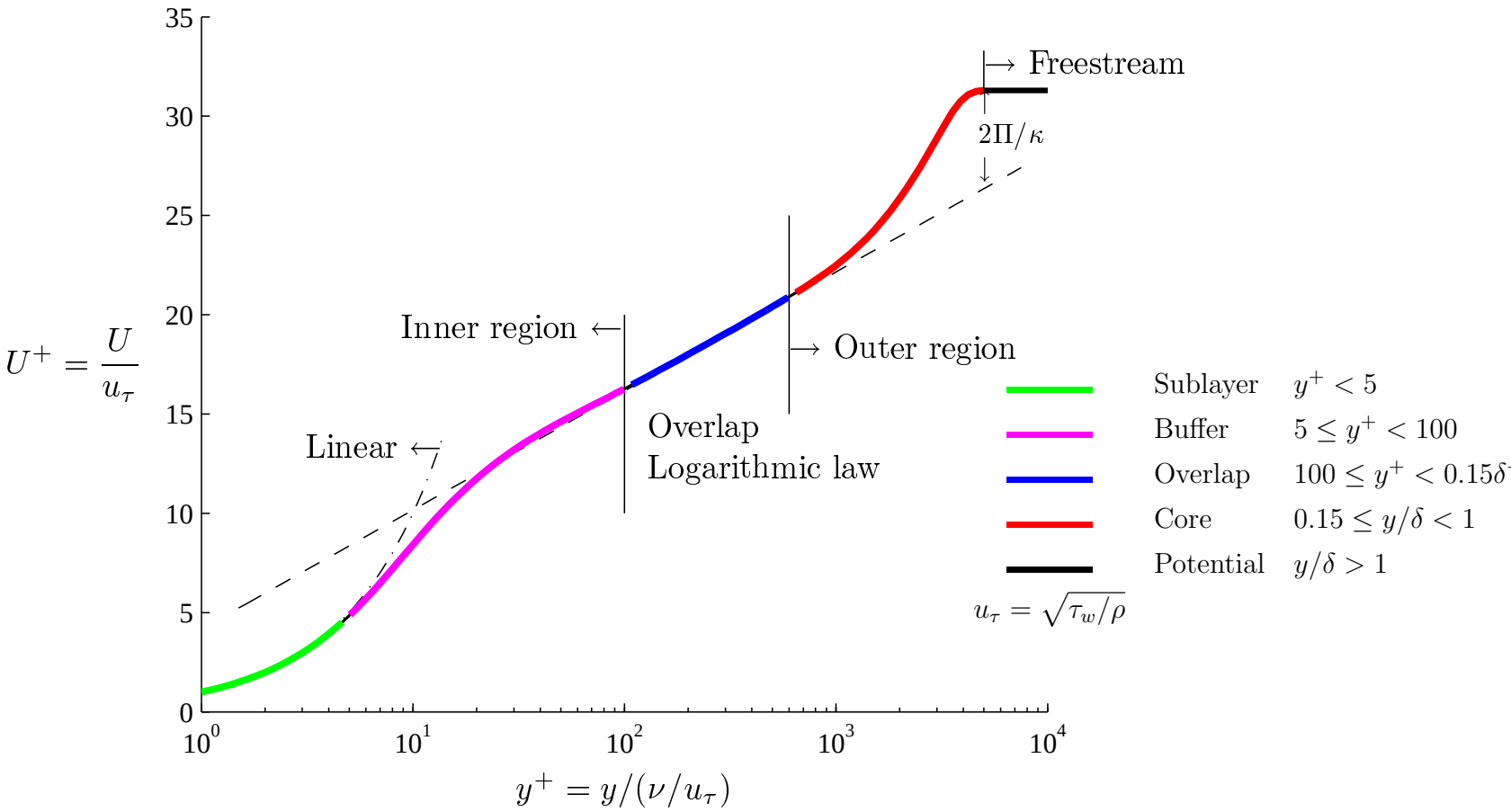

At least two length and velocity scales needed

Freedom to choose can lead to incorrect solutions!!
In the following, an example of the required rigorous experimental & analytical work is described.

Inner : Viscous effects are dominant

$$\frac{U}{U_{\text{si}}} = F_{\text{inner}}(y/L_{\text{si}}, Re, *)$$

Outer : Inertial effects are dominant. Effects of viscosity are negligible

$$\frac{U_\infty - U}{U_{\text{so}}} = F_{\text{outer}}(y/L_{\text{so}}, Re, *)$$

$$\textbf{Matching :} \quad U_\infty^+ = \frac{U_{\text{si}}}{u_\tau}\left[\lim_{y/L_{\text{si}}\to\infty} F_{\text{inner}}\right] + \frac{U_{\text{so}}}{u_\tau}\left[\lim_{y/L_{\text{so}}\to 0} F_{\text{outer}}\right] = F(Re)$$

Also, scaling velocity for the Reynolds stresses , $\overline{u_i' u_j'}$, (R_{si}, R_{so}) are needed.

Equilibrium : Self-similarity of mean flow & Self-preservation of turbulence

	U_{si}	L_{si}	U_{so}	L_{so}
Classical	u_τ	ν/u_τ	u_τ	δ, Δ
George & Castillo (1997)	u_τ	ν/u_τ	U_∞	δ_{99}
Zagarola & Smits (1998)	u_τ	ν/u_τ	$U_\infty \delta^*/\delta$	δ

Other mean flow descriptions by T. B. Nickels (2004), Oberlack (2001), Barenblatt, Chorin, & Prostokishin (2000)

Completely self-consistent description of ZPG TBLs based on the classical (logarithmic) theory recently established by Monkewitz *et al.*, 2007 and Chauhan, Monkewitz, & Nagib, 2007

Past Wisdom in ZPG Boundary Layers Based on Logarithmic Law

Wall Shear Stress:

$$C_f = 2*\left(\frac{1}{\kappa} Ln(\mathrm{Re}_\theta) + C\right)^{-2} = 2*(u_\tau/U_{inf})^2$$

Mean Velocity Profile:

$$U^+ = \frac{1}{\kappa}\ln(y^+) + B$$

κ = 0.41 & B = 5
C is not equal to B

Recently The Power-Law Velocity Profile Was Revived by:

George et al. (and Barenblatt et al.)

The 'Classical' logarithmic overlap region : $\frac{U}{u_\tau} = \frac{1}{\kappa}\ln(y^+) + B$

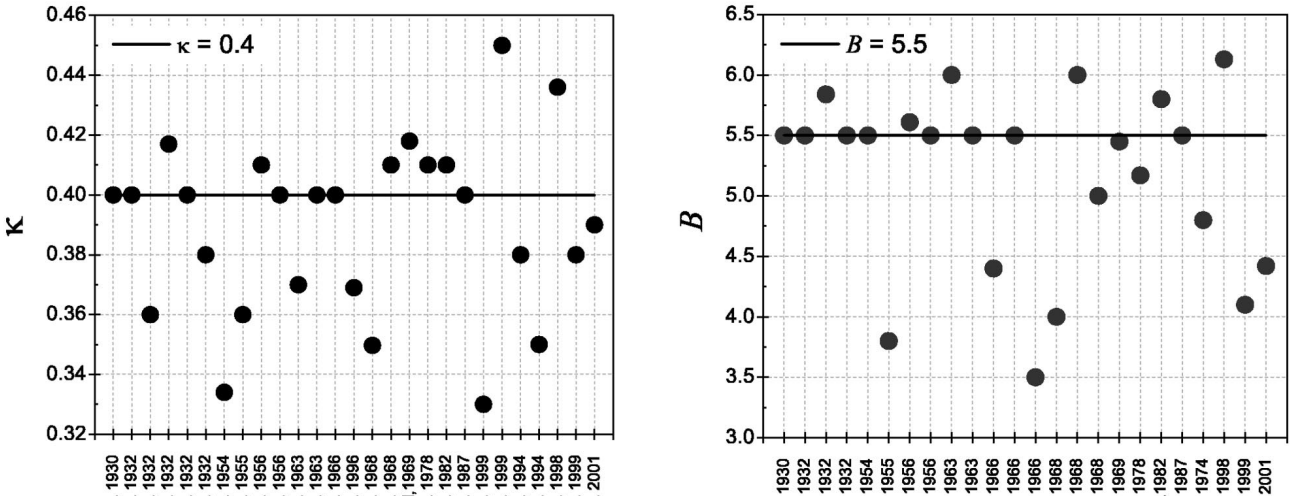

There is no consensus for the value of von Kármán constant, κ (& B) in wall-bounded flows in the literature.

The past experimental interpretations were primarily based on low Reynolds number data.

Less than a decade ago we were very lost!!

Figure from Zanoun, Durst, & Nagib (2003), Physics of Fluids

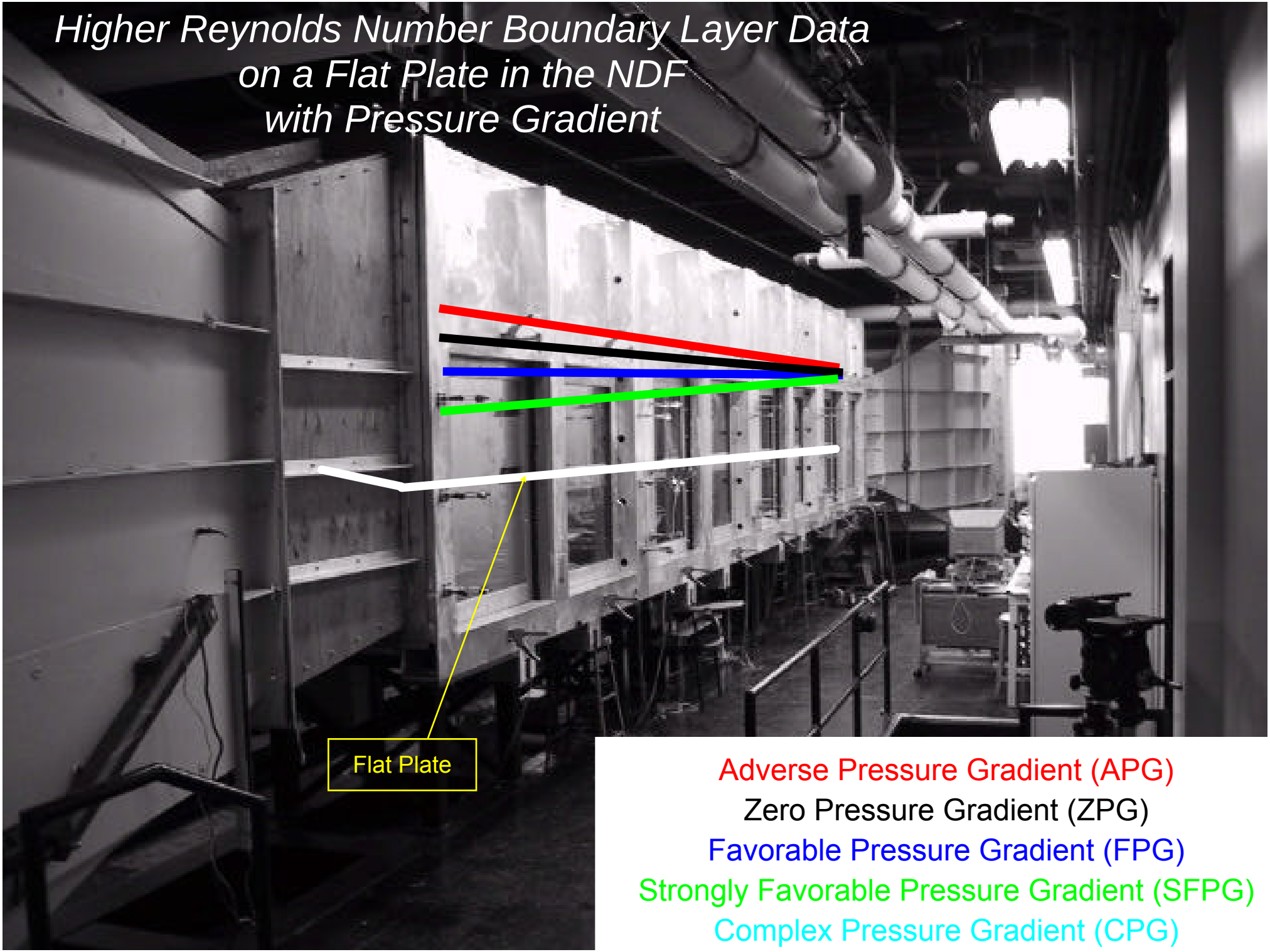
Higher Reynolds Number Boundary Layer Data
on a Flat Plate in the NDF
with Pressure Gradient
Flat Plate
Adverse Pressure Gradient (APG)
Zero Pressure Gradient (ZPG)
Favorable Pressure Gradient (FPG)
Strongly Favorable Pressure Gradient (SFPG)
Complex Pressure Gradient (CPG)

Stream-wise development : *Free-stream velocity*

The Acceleration and Deceleration for various Pressure Gradients is obtained by adjusting the tunnel ceiling height

Development of Free-Stream Velocity for different Pressure Gradients

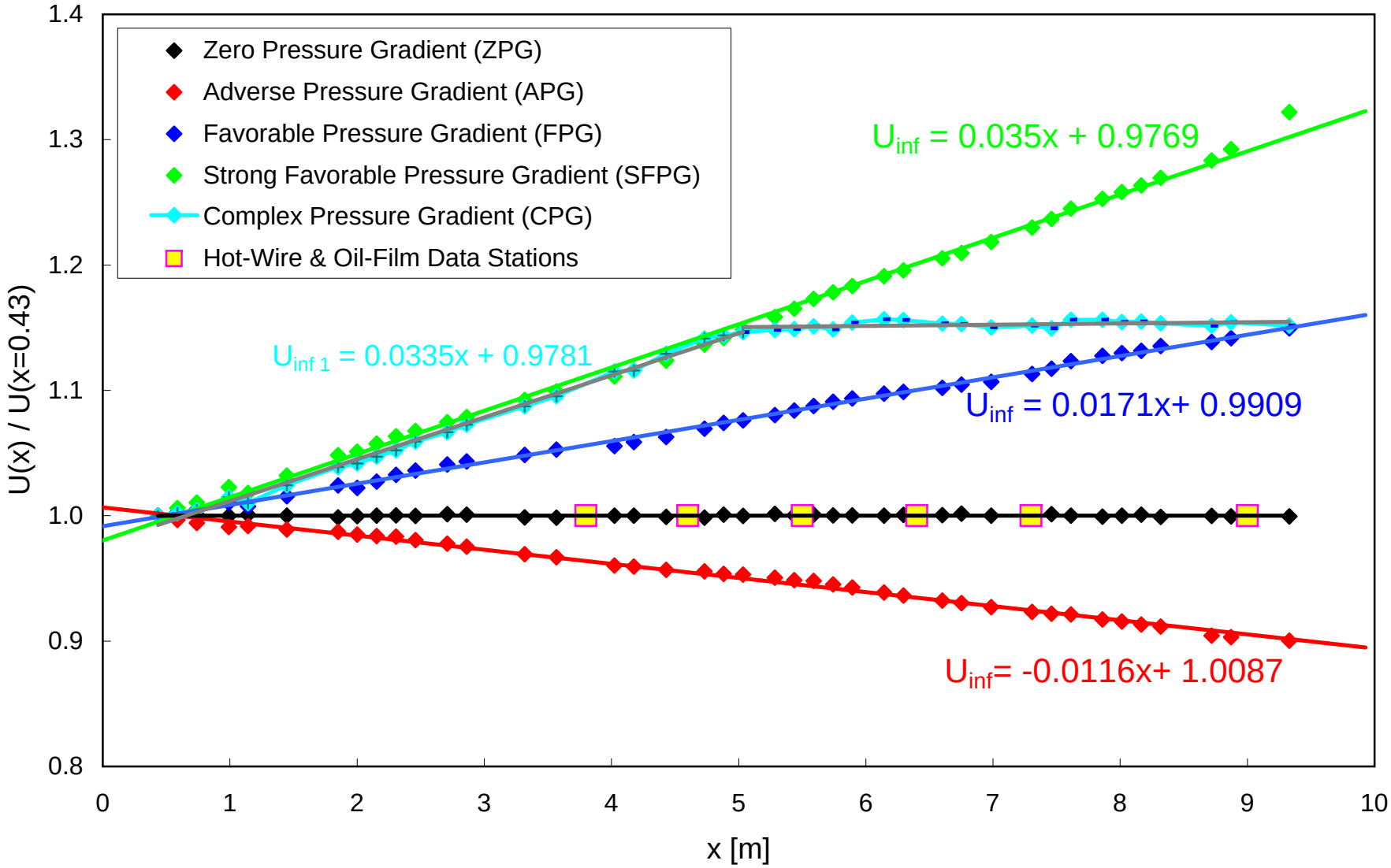

Measurements at U_{ref} = 40, 50 & 60 m/s, and
X=3.8, 4.6, 5.5, 6.4, 7.3 & 9 m

Lessons learned from recent experience:

We believe that the value of experimental data in all wall bounded turbulent flows (except the fully developed pipe) is greatly diminished without accurate and independent measurement of the wall shear stress.

Oil-film interferometry** is the best technique to achieve these measurements as long as the oil viscosity is measured accurately for range of temperatures of experiments; accuracy **~ 1.5%.

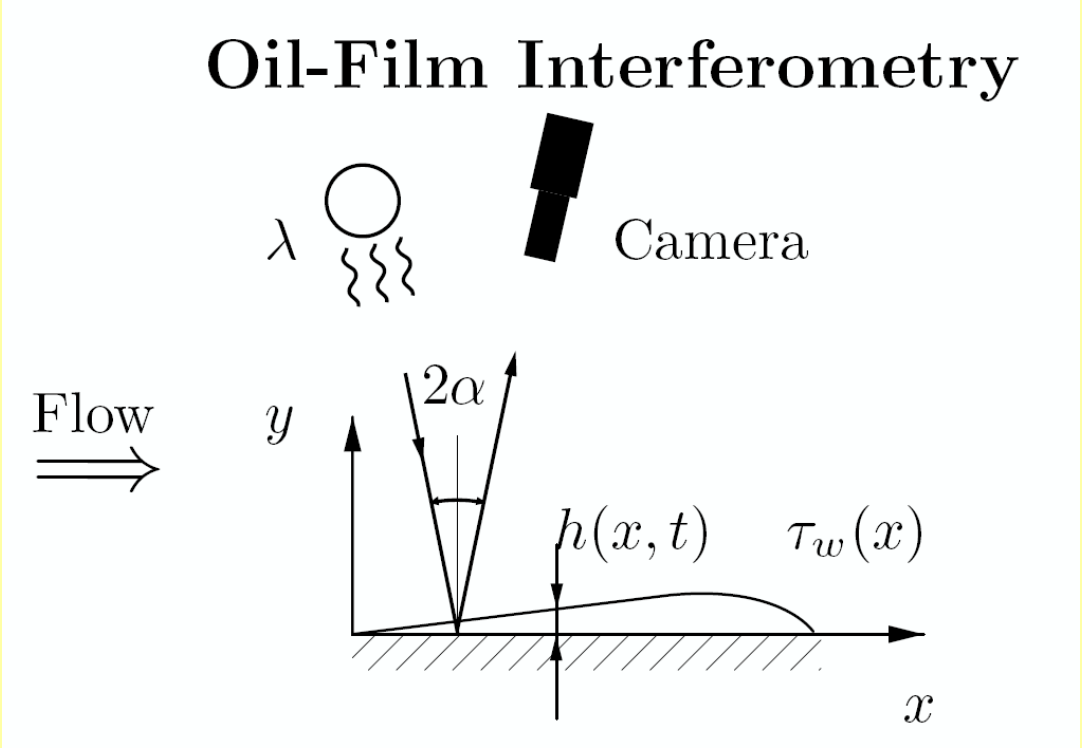

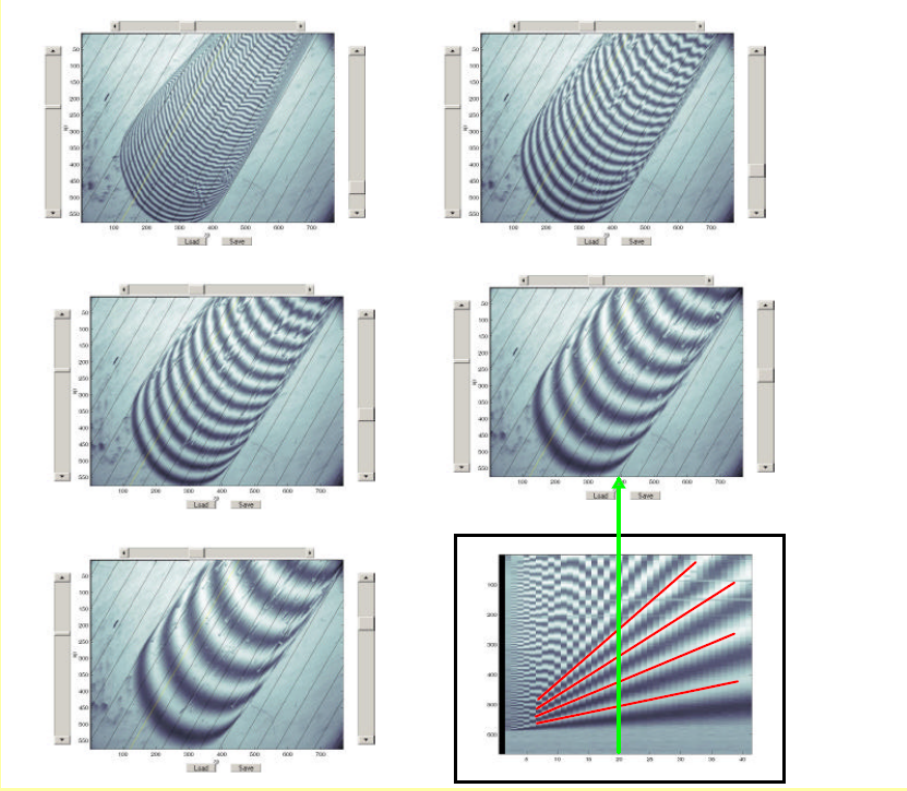

ZPG TBLs - Results

Skin-friction behavior in ZPG TBLs

Coles-Fernholz 1	$C_f = 2[1/\kappa \ln(Re_{\delta^*}) + C]^{-2}$	$\kappa = 0.384$, $C^* = 3.3$
Coles-Fernholz 2	$C_f = 2[1/\kappa \ln(Re_\theta) + C_1]^{-2}$	$\kappa = 0.384$, $C = 4.1$
Kármán-Schoenherr	$C_f = 0.558C'_f/\left[0.558 + 2(C'_f)^{-1/2}\right]$	
	$C'_f = \left[\log(2Re_\theta)/\mathbf{0.242}\right]^{-2}$	0.2385
Prandtl-Schlichting	$C_f = \mathbf{0.455}(\log Re_x)^{-2.58} - A/Re_x$	0.3596
Prandtl-Kármán	$C_f^{-1/2} = 4\log(Re_x\sqrt{C_f}) - \mathbf{0.4}$	2.12
F. Schultz-Grunow	$C_f = \mathbf{0.427}(\log Re_x - 0.407)^{-2.64}$	0.3475
Nikuradse	$C_f = 0.02666Re_x^{\mathbf{-0.139}}$	-0.1502
Schlichting's fit	$C_f = (2\log Re_x - 0.65)^{\mathbf{-2.3}}$	-2.3333
White	$C_f = \mathbf{0.455}[\ln(0.06Re_x)]^{-2}$	0.4177
$1/7^{\text{th}}$ Law	$C_f = \mathbf{0.027}Re_x^{-1/7}$	0.02358
$1/5^{\text{th}}$ Law	$C_f = \mathbf{0.058}Re_x^{-1/5} - A/Re_x$	0.0655
GC97	$C_f^{1/2} = 2(\mathbf{55}/C_{i\infty})\left[\delta^+\right]^{-\gamma_\infty} \exp\left[A/(\ln\delta^+)^\alpha\right]$	56.7

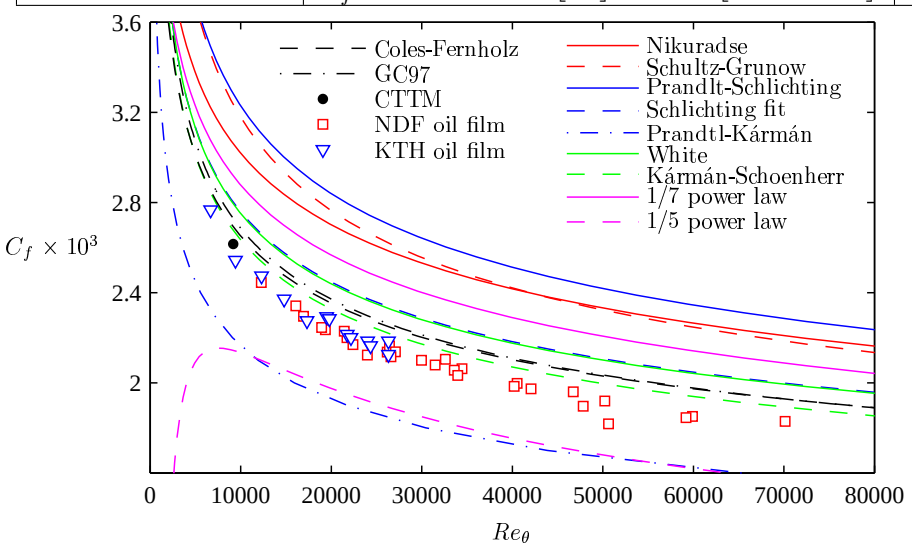

Various skin-friction relations are fitted to the oil-film measurements from NDF and KTH.

Modified by changing only one empirical coefficient to obtain a least-square fit with the high Reynolds number data of KTH and NDF.

Skin-friction behavior in ZPG TBLs .....

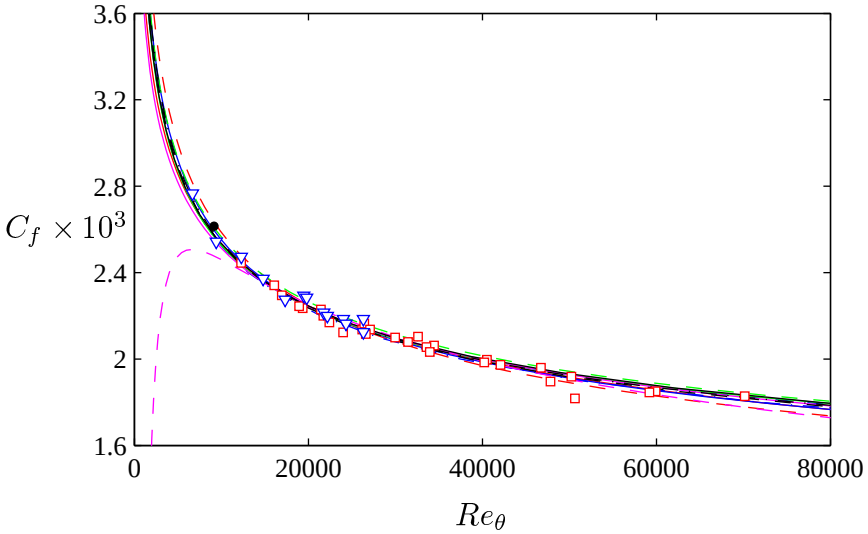

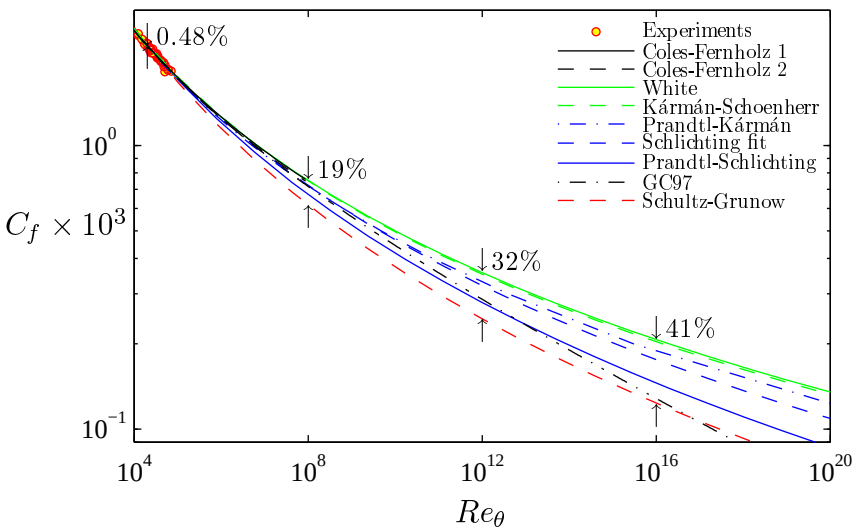

All the modified relations fit the data within experimental accuracy for all laboratory Reynolds numbers if they are underpinned by the *same* measurements.

The appropriateness of a relation (theory) *only* from skin-friction measurements cannot be established.

At finite Reynolds numbers one has to couple the skin-friction relation with mean velocity description (and turbulence if possible) and put it at test with the experimental data.

The differences between the various predictions increase steadily : While they are less than 0.5% at $Re_\theta = 20,000$, they increase to over 40% beyond an Re_θ of 10^{16}.

?

Improved Validity Asymptotic Theory

The Coles-Fernholz type relation and velocity defect in the outer part

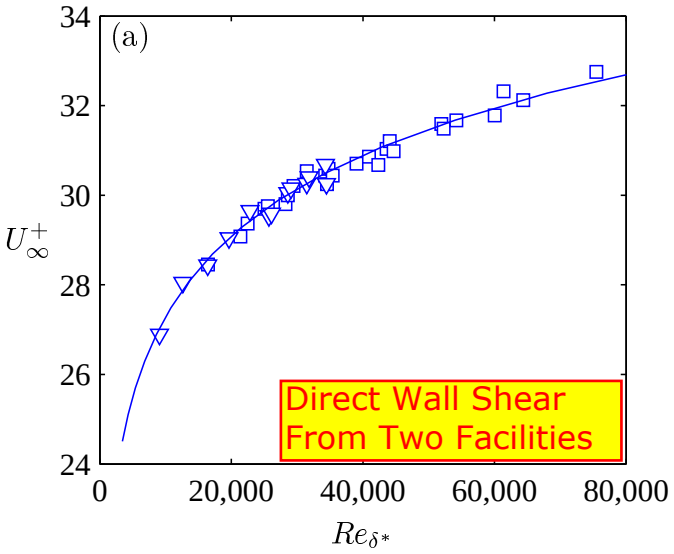

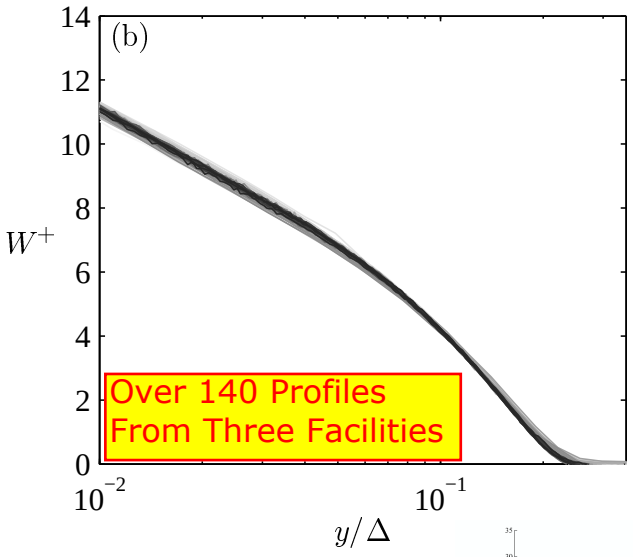

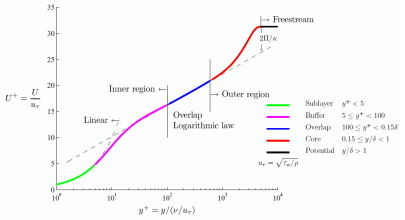

$$U_\infty^+ = \frac{1}{\kappa}\ln(Re_{\delta*}) + C$$

$$\text{Inner}: \quad \frac{U}{u_\tau} = F_{\text{inner}}(y^+) \qquad \lim_{y^+\to\infty} F_{\text{inner}} = U^+ = \frac{1}{\kappa}\ln(y^+) + B$$

$$\text{Outer}: \quad W^+ = \frac{U_\infty - U}{u_\tau} = F_{\text{outer}}(y/\Delta) \qquad \lim_{\eta\to 0} F_{\text{outer}} = U_\infty^+ - U^+ = -\frac{1}{\kappa}\ln(y/\Delta) + C_\Delta$$

$$\text{Matching}: \quad U_\infty^+ = \lim_{y^+\to\infty} F_{\text{inner}} + \lim_{\eta\to 0} F_{\text{outer}} = U_\infty^+(Re_{\delta*})$$

$$\text{For ZPG TBLs,} \quad \frac{\Delta}{\delta} \to \textit{constant}.$$

Therefore, either of $\Delta = U_\infty^+\delta^*$ (Rotta-Clauser Delta) or δ (local boundary layer thickness) can be used in the outer part.

$$\kappa = 0.384, \quad B = 4.17, \quad C = 3.3$$

Inner profile (Monkewitz, Chauhan, & Nagib, 2007), *Physics of fluids*

$$\frac{\mathrm{d}U^+_{inner}}{\mathrm{d}y^+} = P_{23} + P_{25}, \qquad \Xi = y^+ \frac{\mathrm{d}U^+}{\mathrm{d}y^+}$$

$$P_{23} = b_0 \frac{1 + b_1 y^+ + b_2 y^{+2}}{1 + b_1 y^+ + b_2 y^{+2} + \kappa b_0 b_2 y^{+3}}$$

$$b_0 = 1.000\ 10^{-2}\ \kappa^{-1} \quad (\kappa = 0.384)$$

$$b_1 = 1.100\ 10^{-2}$$

$$b_2 = 1.100\ 10^{-4}$$

$$P_{25} = (1 - b_0) \frac{1 + h_1 y^+ + h_2 y^{+2}}{1 + h_1 y^+ + h_2 y^{+2} + h_3 y^{+3} + h_4 y^{+4} + h_5 y^{+5}}$$

$$h_1 = -\,1.000 \times 10^{-2}$$

$$h_2 = 6.000 \times 10^{-3}$$

$$h_3 = 9.977 \times 10^{-4}$$

$$h_4 = 2.200 \times 10^{-5}$$

$$h_5 = 1.000 \times 10^{-6}\ .$$

$\Xi_{23}+\Xi_{25}$ (——); Ξ_{23} (−+−+−); Ξ_{25} (−×−×−); KTH (△); NDF (○) ; Carlier & Stanislas (2005) (×); T. Nickels *et al.*, 2007(□). Comparison of new fit $\Xi_{23} + \Xi_{25}$ (——) with previous proposals in the literature. Other functional forms shown for $\kappa = 0.384$ and $B = 4.17$ are : —×—, Musker (1979); ∗, Modified Musker from Chauhan, Monkewitz, & Nagib, 2007; − − − −, Spalding (1961); − · − · − · −, Van Driest from White (2006); —+—, Gersten & Herwig from Schlichting & Gersten (2000).

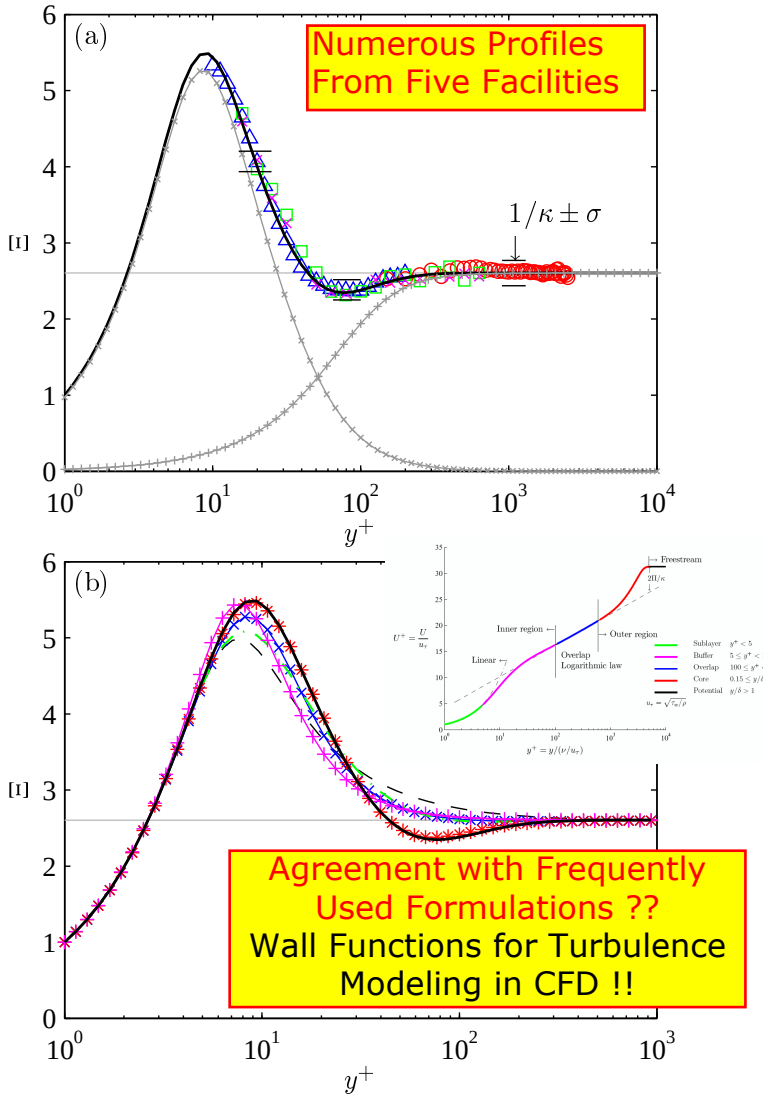

Outer profile (Monkewitz, Chauhan, & Nagib, 2007), *Physics of fluids*

Monkewitz, Chauhan, & Nagib, 2007, *Physics of fluids*

$$\eta = y/\Delta$$

$$U_\infty^+ - U_{outer}^+ = \left[\frac{1}{\kappa}E_1(\eta)+w_0\right]\frac{1}{2}\left[1-\tanh\left(\frac{w_{-1}}{\eta}+w_2\eta^2+w_8\eta^8\right)\right]$$

$$\begin{aligned} w_0 &= 0.6332 \\ w_{-1} &= \text{-}0.096 \\ w_2 &= 28.5 \\ w_8 &= 33000. \end{aligned}$$

$$E_1(\eta) = \int_\eta^\infty \frac{\exp^{-t}}{t}dt = -\gamma - \ln(\eta) + \eta + O(\eta^2) \quad \text{for} \quad \eta \ll 1$$

$$\sim \frac{\exp^{-\eta}}{\eta}\left[1 - \frac{1}{\eta} + O(\eta^{-2})\right] \quad \text{for} \quad \eta \to \infty \quad ,$$

$\gamma = 0.57721566$ Euler-Mascheroni constant

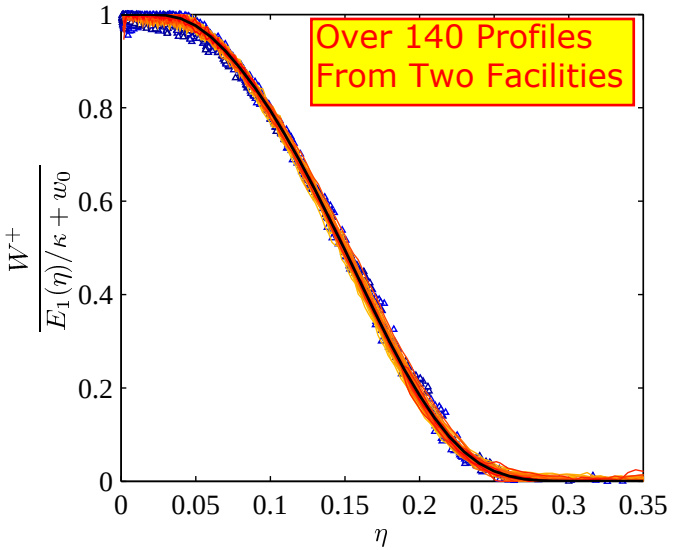

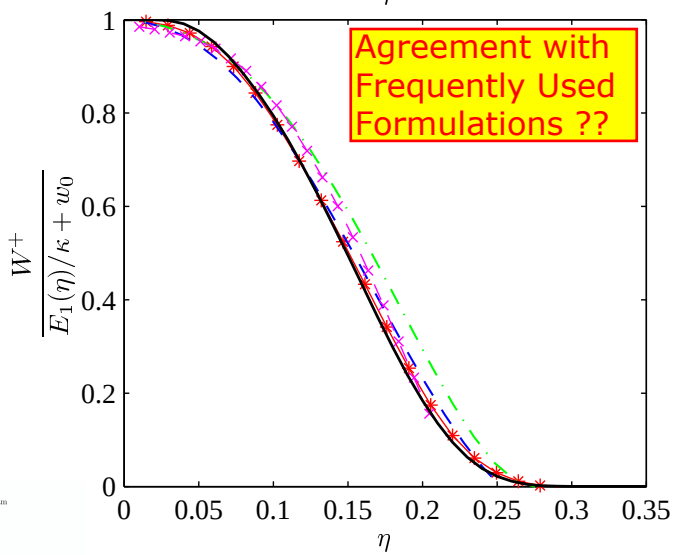

NDF (——); KTH (△); —∗—, exponential wake function of Chauhan, Nagib, & Monkewitz, 2007; —·—·—, quartic polynomial of Lewkowicz (1982); - - - -, sine wake function of Coles (1956); —×—, wake function of T. B. Nickels (2004).

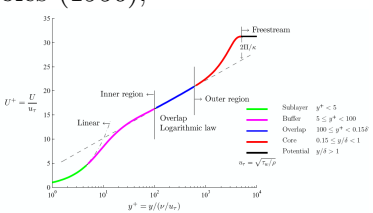

Original **Musker (1979) inner form :** $$\frac{\mathrm{d}U^+_{\text{inner}}}{\mathrm{d}y^+} = \frac{\dfrac{1}{s} + \dfrac{y^{+2}}{\kappa}}{\dfrac{1}{s} + \dfrac{y^{+2}}{\kappa} + y^{+3}}$$

Modified Musker (1979) inner form : $$U^+_{\text{inner}} = \frac{1}{\kappa}\ln\left(\frac{y^+ - a}{-a}\right) + \frac{R^2}{a(4\alpha - a)}\left[(4\alpha + a)\ln\left(-\frac{a}{R}\frac{\sqrt{(y^+ - \alpha)^2 + \beta^2}}{y^+ - a}\right) + \frac{\alpha}{\beta}(4\alpha + 5a)\left(\arctan\left(\frac{y^+ - \alpha}{\beta}\right) + \arctan\left(\frac{\alpha}{\beta}\right)\right)\right] + \frac{\exp\left[-\ln^2(y^+/30)\right]}{2.85},$$

where, $\alpha = (-1/\kappa - a)/2$, $\beta = \sqrt{-2a\alpha - \alpha^2}$, $R = \sqrt{\alpha^2 + \beta^2}$, $s = -aR^2$.

Coles (1956) outer form : $$U^+_{\text{outer}} = \frac{1}{\kappa}\ln(y^+) + B + \frac{2\Pi}{\kappa}\mathcal{W}(\xi), \quad \xi \equiv y/\delta \leq 1$$

New wake function : $$\mathcal{W}_{\exp}(\xi) = \frac{1 - \exp\left[-\dfrac{1}{4}(5a_2 + 6a_3 + 7a_4)\xi^4 + a_2\xi^5 + a_3\xi^6 + a_4\xi^7\right]}{1 - \exp\left[-(a_2 + 2a_3 + 3a_4)/4\right]} \times \left(1 - \frac{1}{2\Pi}\ln(\xi)\right),$$

where, $a_2 = 132.8410$, $a_3 = -166.2041$ and $a_4 = 71.9114$.

Composite form : $$U^+_{\text{inner}}(y^+) + \frac{2\Pi}{\kappa}\mathcal{W}_{\exp}(y/\delta), \quad \xi \equiv y/\delta \leq 1$$

Logarithmic composite profile Gives accurate description

Remarkable agreement between data covering a wide range of Reynolds numbers and the fitted composite profile.

The agreement is also equally good for data from different experimental facilities with different velocity measurement and acquisition techniques with varying number of data points available for fitting or their wall-normal spacing.

Similar to the conventional 'Clauser' plot the composite profile now can be fitted to U versus y to determine, u_τ, δ, & Π.

Gives excellent indirect prediction of U_∞^+.

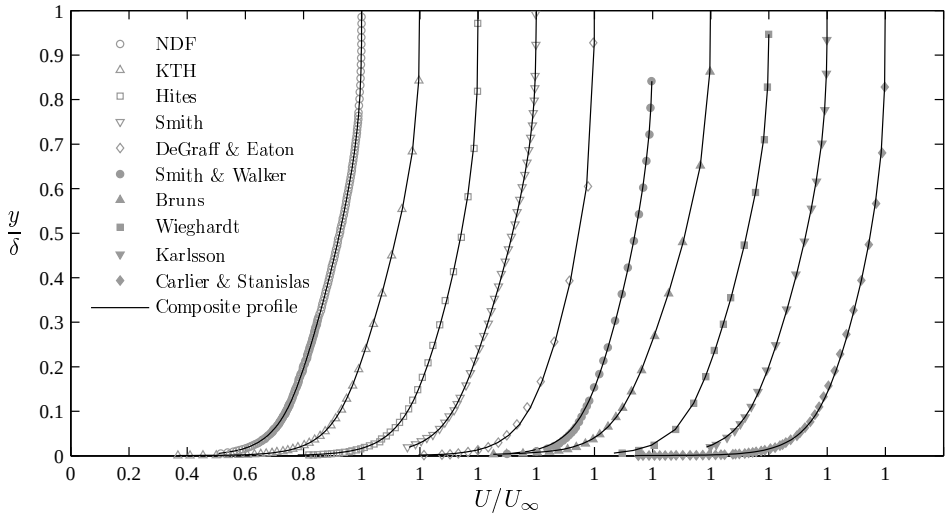

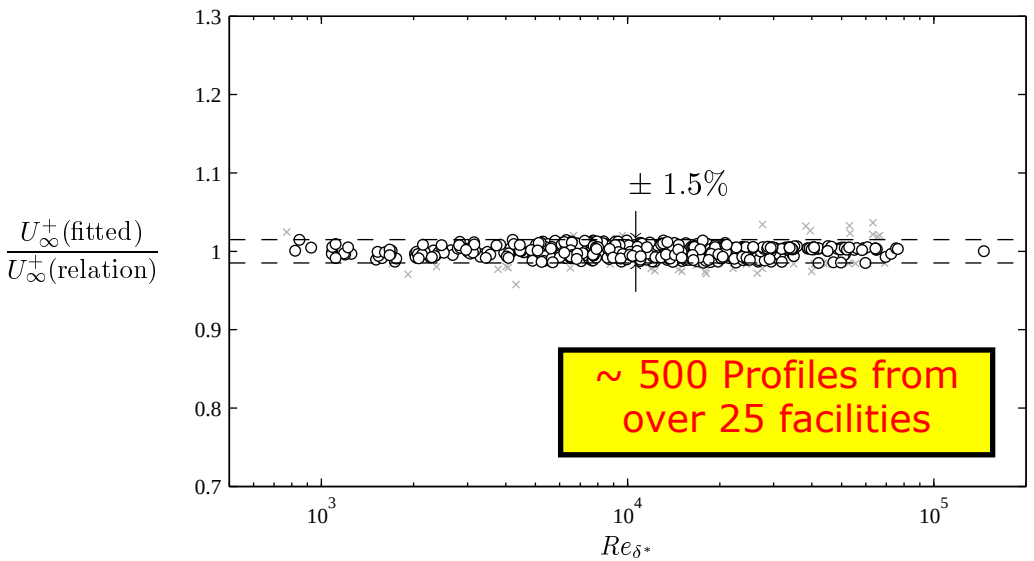

Wall Shear Stress & Momentum Distribution (Shape Factor H)
MUST BE CONSISTENT in order for "theory" to be appropriate

Experiments studied in canonical wall-bounded flows

ZPG TBLs

1950, Schubauer & Klebanoff
1952, Klebanoff & Diehl
1958, D. W. Smith & Walker
1968, Coles & Hirst
- Bell
- Wieghardt
- Riabouchinsky

1980, Karlsson
1981, Purtell, Klebanoff, & Buckley
1986, Ahn
1988, Spalart (DNS)
1988, Wark
1988, Erm
1991, Nagano, Tagawa, & Tsuji
1992, Naguib
1994, R. W. Smith
1995, H.-H. Fernholz, Krause, Nockemann, & Schober
1996, Osaka, Kameda, & Mochizuki
1997, Hites
1998, Bruns
1999, Tsuji
1999, Österlund
2000, DeGraff & Eaton
2001, Skote (DNS)
2002, Knobloch & Fernholz
2004, Nagib, Christophorou, & Monkewitz
2005, Carlier & Stanislas
2007, T. Nickels, Marusic, Hafez, Hutchins, & Chong

PG TBLs

1989, Watmuff
1993, Spalart & Watmuff (DNS)
1994, Skare & Krogstad
1995, Marusic & Perry
1998, Jones
1998, H. H. Fernholz & Warnack
2001, Skote (DNS)
2004, Nagib, Christophorou, & Monkewitz
2008, Spalart, Johnstone, & Coleman (DNS of Ekman layer)

Pipe flows

1998, AGARD-AR-345
- Perry, Henbest, & Chong
- Durst, Jovanović, & Sender
- den Toonder & Nieuwstadt

2003, McKeon, Princeton 'Superpipe'
2005, Monty

Channel flows

1987, Kim, Moin, & Moser (DNS)
1998, AGARD-AR-345
- Wei & Willmarth
- Niederschulte, Adrian, & Hanratty
- Comte-Bellot

2001, Christensen
2001, Fischer, Jovanović, & Durst
2003, Zanoun
2004, Jiménez, del Álamo, & Flores (DNS)
2005, Monty

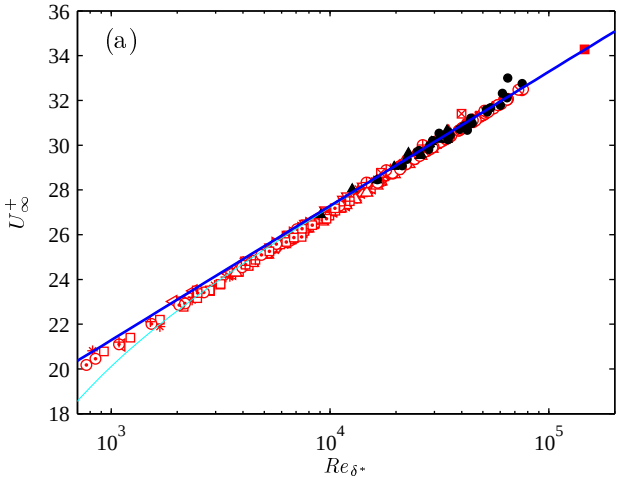

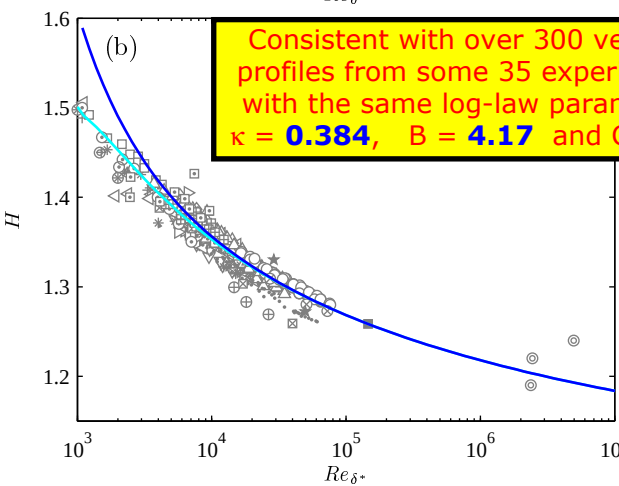

Consistent with over 300 velocity profiles from some 35 experiments with the same log-law parameters κ = **0.384**, B = **4.17** and C = 3.3

Contrast to "traditional' values κ = **0.41**, and B = **5.0**

Other functional forms for ZPG TBLs

At least two length and velocity scales needed

Inner : Viscous effects are dominant

$$\frac{U}{U_{\rm si}} = F_{\rm inner}(y/L_{\rm si}, Re, *)$$

Outer : Inertial effects are dominant. Effects of viscosity are negligible

$$\frac{U_\infty - U}{U_{\rm so}} = F_{\rm outer}(y/L_{\rm so}, Re, *)$$

$$\textbf{Matching :} \quad U_\infty^+ = \frac{U_{\rm si}}{u_\tau}\left[\lim_{y/L_{\rm si}\to\infty} F_{\rm inner}\right] + \frac{U_{\rm so}}{u_\tau}\left[\lim_{y/L_{\rm so}\to 0} F_{\rm outer}\right] = F(Re)$$

Also, scaling velocity for the Reynolds stresses , $\overline{u_i' u_j'}$, ($R_{\rm si}$, $R_{\rm so}$) are needed.

Equilibrium : Self-similarity of mean flow & Self-preservation of turbulence

	$U_{\rm si}$	$L_{\rm si}$	$U_{\rm so}$	$L_{\rm so}$
Classical	u_τ	ν/u_τ	u_τ	δ, Δ
George & Castillo (1997)	u_τ	ν/u_τ	U_∞	δ_{99}
Zagarola & Smits (1998)	u_τ	ν/u_τ	$U_\infty \delta^*/\delta$	δ

Other mean flow descriptions by T. B. Nickels (2004), Oberlack (2001), Barenblatt, Chorin, & Prostokishin (2000)

Completely self-consistent description of ZPG TBLs based on the classical (logarithmic) theory recently established by Monkewitz *et al.*, 2007 and Chauhan, Monkewitz, & Nagib, 2007

Mean flow similarity George & Castillo (1997)

$$U^+ = \frac{1}{\kappa}\ln y^+ + B, \qquad \Xi \equiv y^+\frac{\mathrm{d}U^+}{\mathrm{d}y^+} \quad \Rightarrow \quad \Xi = \frac{1}{\kappa} \quad \text{for log law.}$$

$$U^+ = C_i(y^+ + a^+)^\gamma, \qquad \Gamma \equiv \frac{(y^+ + a^+)}{U^+}\frac{\mathrm{d}U^+}{\mathrm{d}y^+} \quad \Rightarrow \quad \Gamma = \gamma \quad \text{for GC97 power law.}$$

Diagnostic functions establish the validity of logarithmic form in the overlap region.

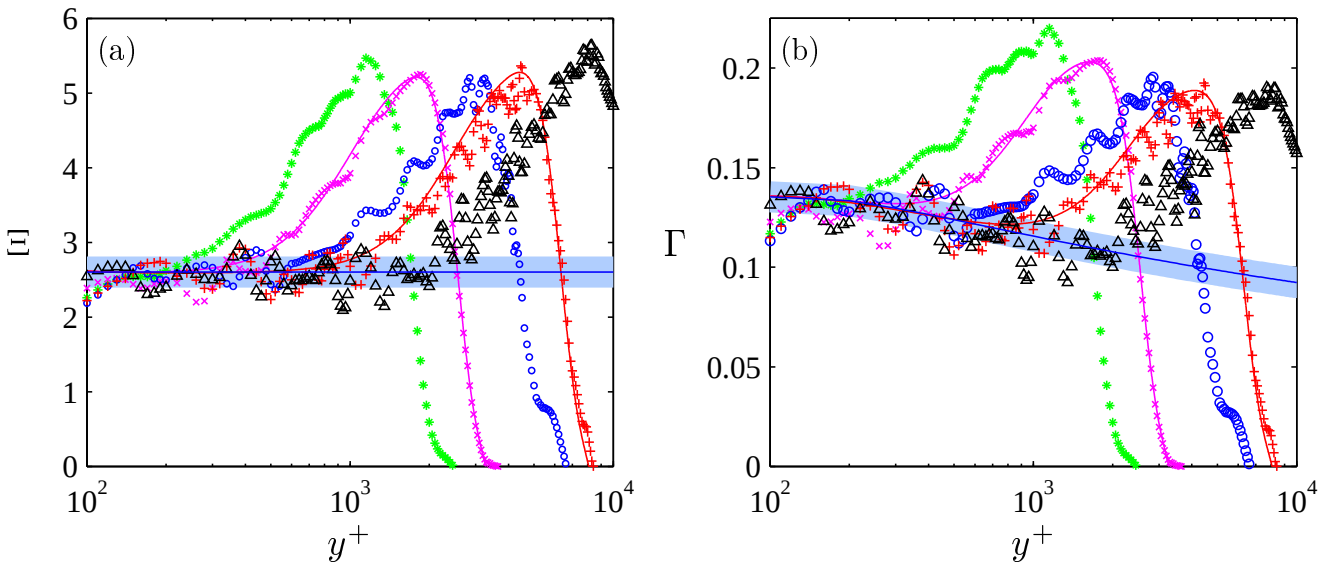

—∗—, $Re_\theta \sim 5,500$; —×—, $Re_\theta \sim 8,200$; —○—, $Re_\theta \sim 14,000$; —+—, $Re_\theta \sim 21,000$; —△—, $Re_\theta \sim 39,500$

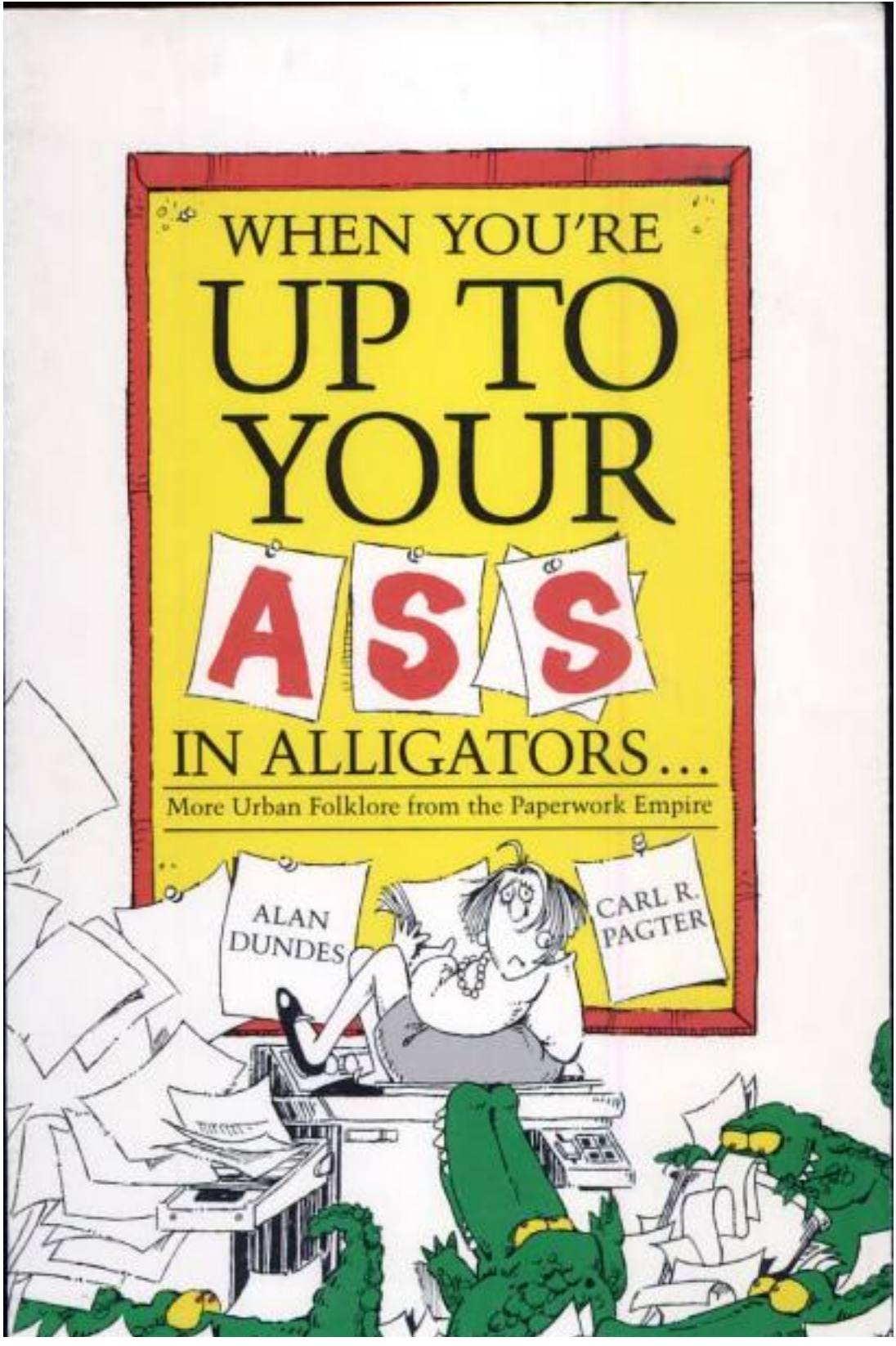

When you are up to your ass in alligators, it is important to remember that your original intent was merely to drain the swamp

Mean flow similarity George & Castillo (1997)

$$U^+ = \frac{1}{\kappa}\ln y^+ + B, \qquad \Xi \equiv y^+\frac{\mathrm{d}U^+}{\mathrm{d}y^+} \quad \Rightarrow \quad \Xi = \frac{1}{\kappa} \quad \text{for log law.}$$

$$U^+ = C_i(y^+ + a^+)^\gamma, \qquad \Gamma \equiv \frac{(y^+ + a^+)}{U^+}\frac{\mathrm{d}U^+}{\mathrm{d}y^+} \quad \Rightarrow \quad \Gamma = \gamma \quad \text{for GC97 power law.}$$

Diagnostic functions establish the validity of logarithmic form in the overlap region.

Re_θ = 14,000

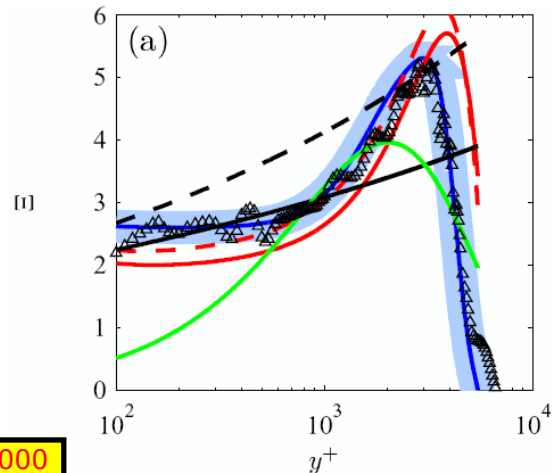

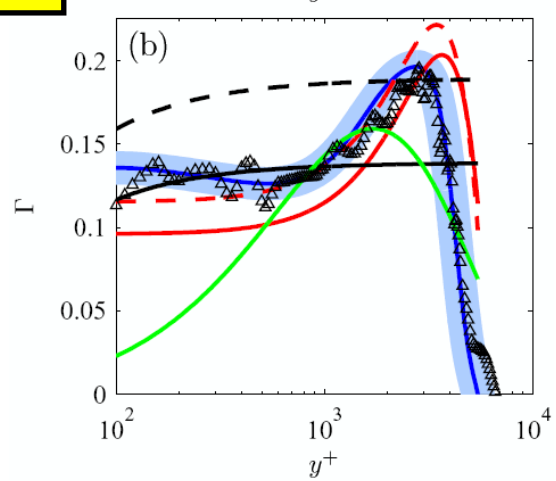

Re_θ = 39,000

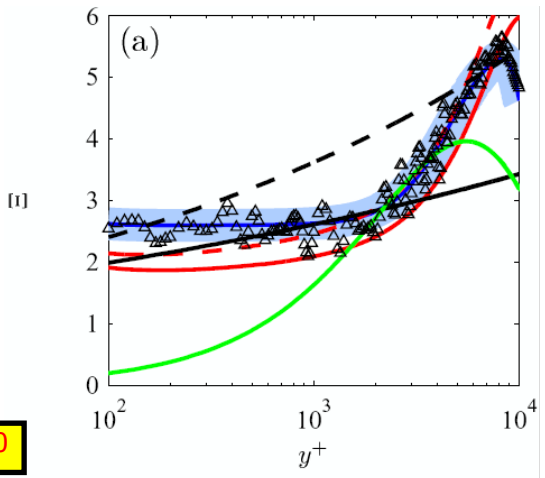

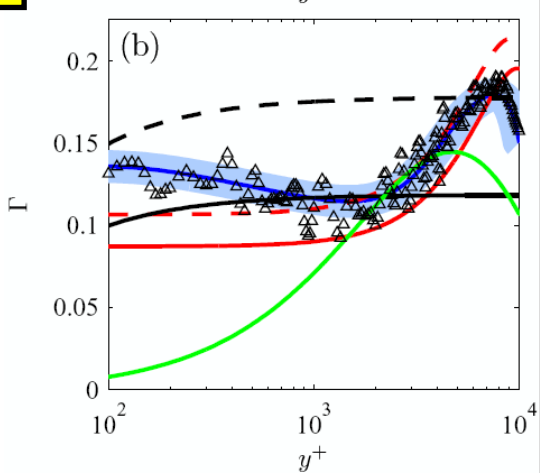

Power Law Results

Mean flow similarity George & Castillo (1997)

With original coefficients

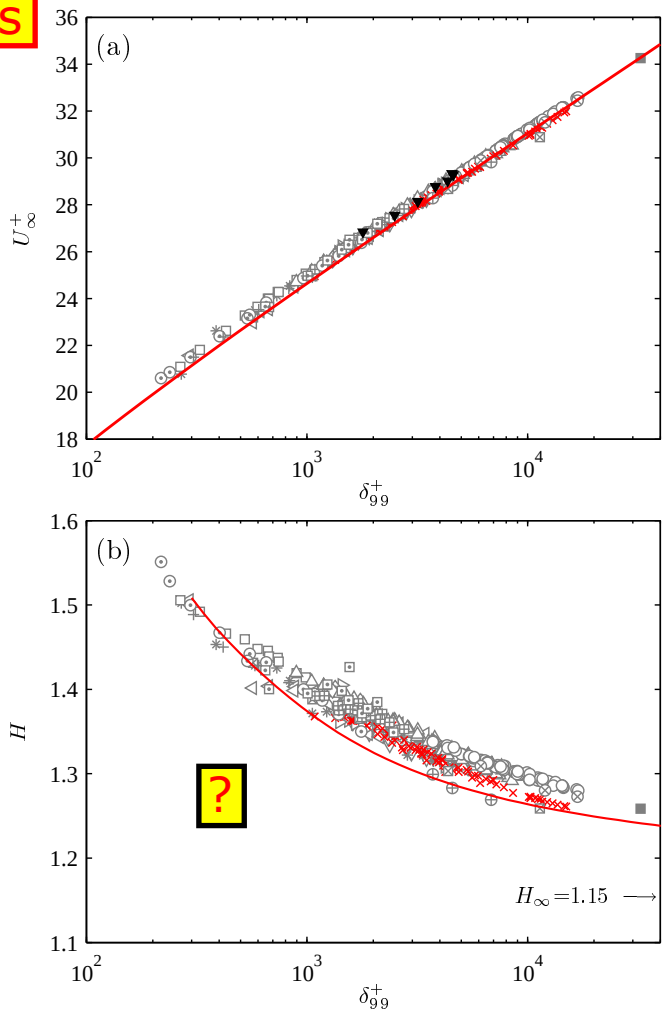

With modified coefficients

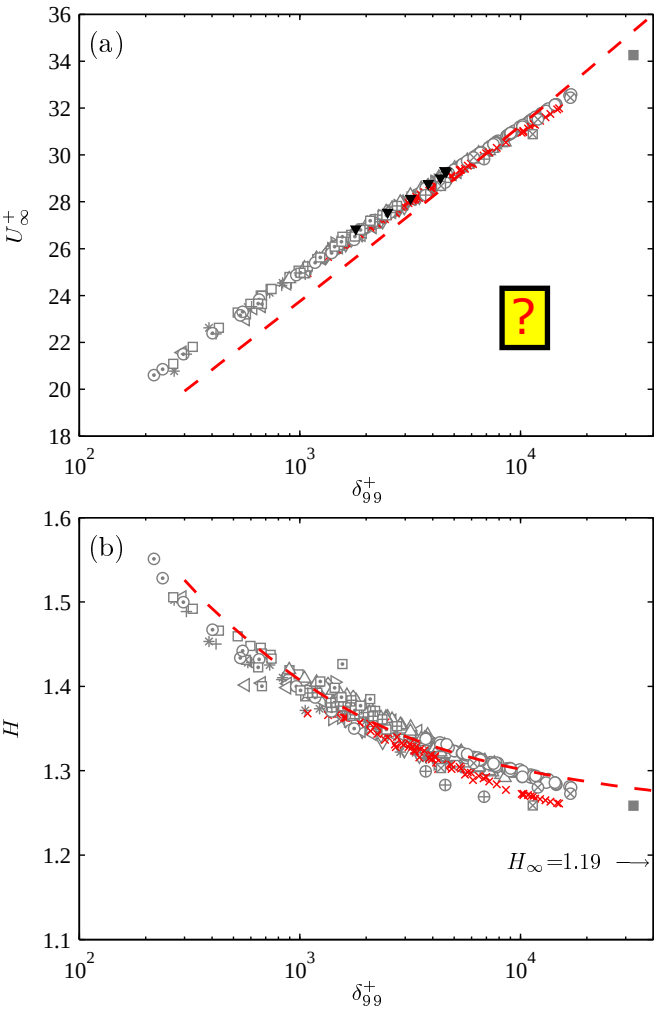

Wall Shear Stress & Momentum Distribution (Shape Factor H)
MUST BE CONSISTENT in order for "theory" to be appropriate

Clauser ratio, Δ/δ

Ratio of Δ over δ is an important parameter indicating the validity of Clauser theory.

Δ/δ reaches its asymptotic value near 3.5 and remains a constant consistent with classical theory

Invalidates arguments of power law theory of George & Castillo (1997)

$$D \equiv \frac{\Delta}{\delta} = \frac{Re_{\delta^*}}{\delta^+} = \exp\left[2\Pi + \kappa(B - C^*)\right]$$

Constant Slope Lines Represent Constant D: Basis of Log Law Scaling

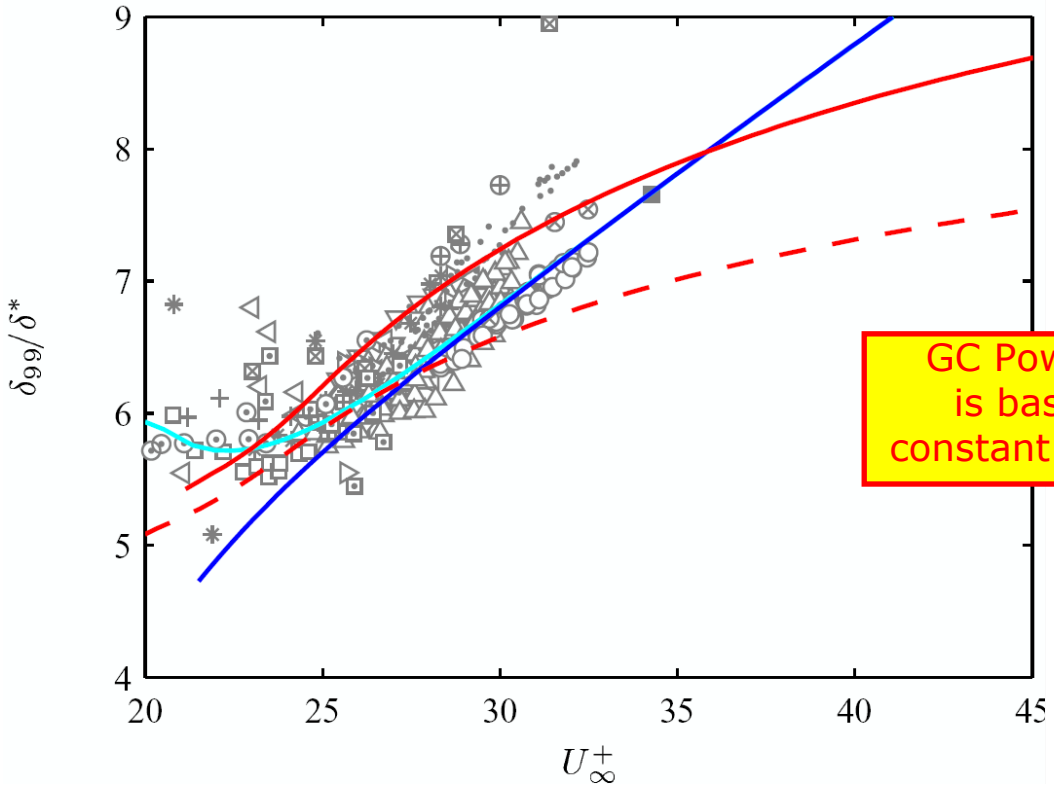

GC Power Law is based on constant δ_{99}/δ^*!!!!

Pressure Gradient Turbulent Boundary Layers

and Pipe & Channel Flows

For the Strongly Favorable Pressure Gradient case, U_∞^+ shows trends with x and U_∞; i.e., non-equilibrium development.

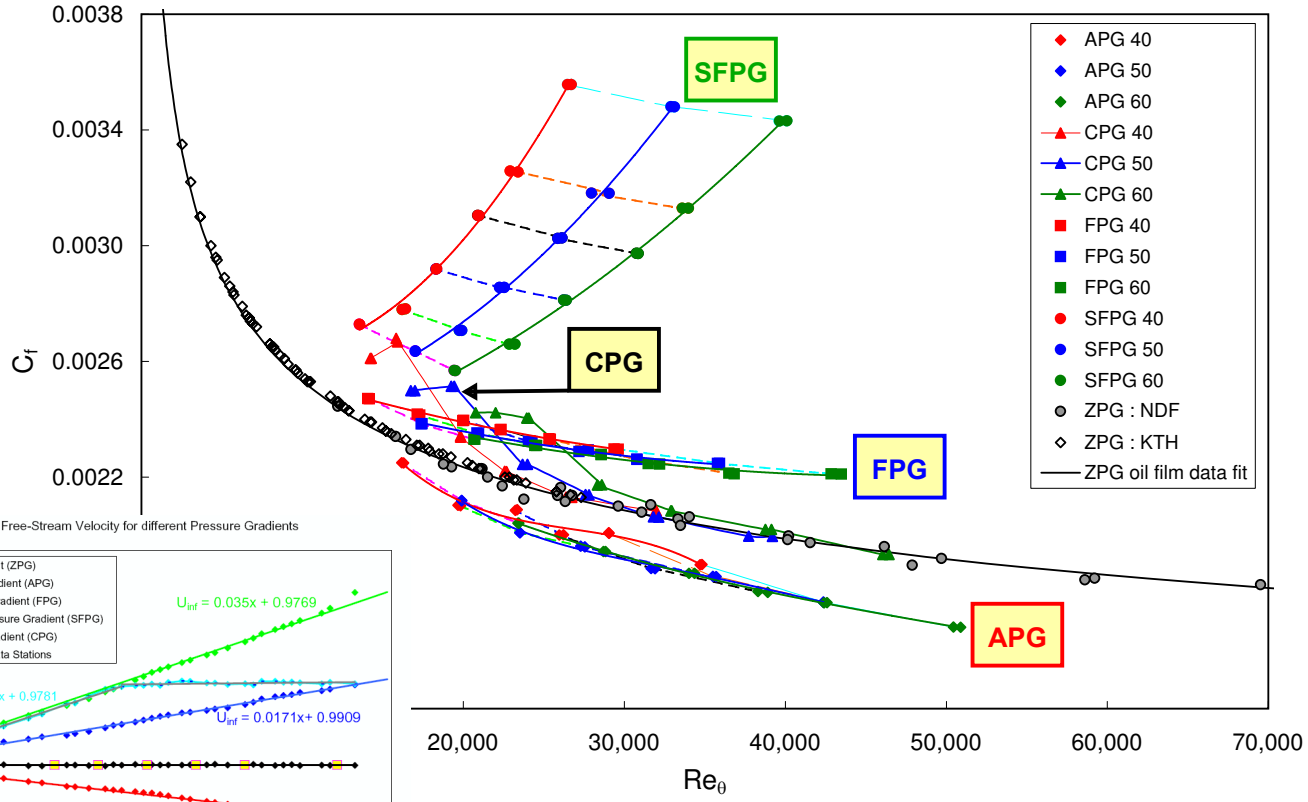

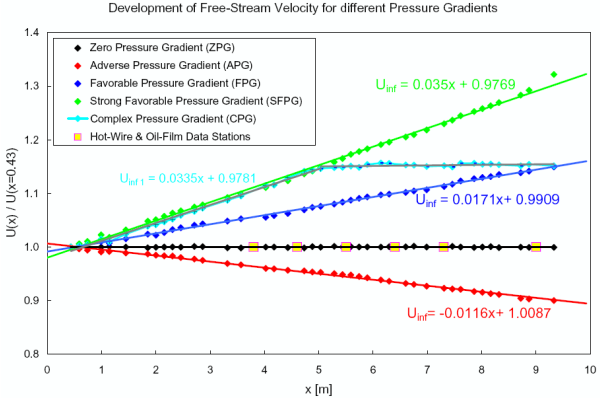

Presence of pressure gradient changes the structure of mean flow.

Changes in κ, B and Π along with U_∞^+.

Corresponding changes in $\overline{u^2}$ also observed.

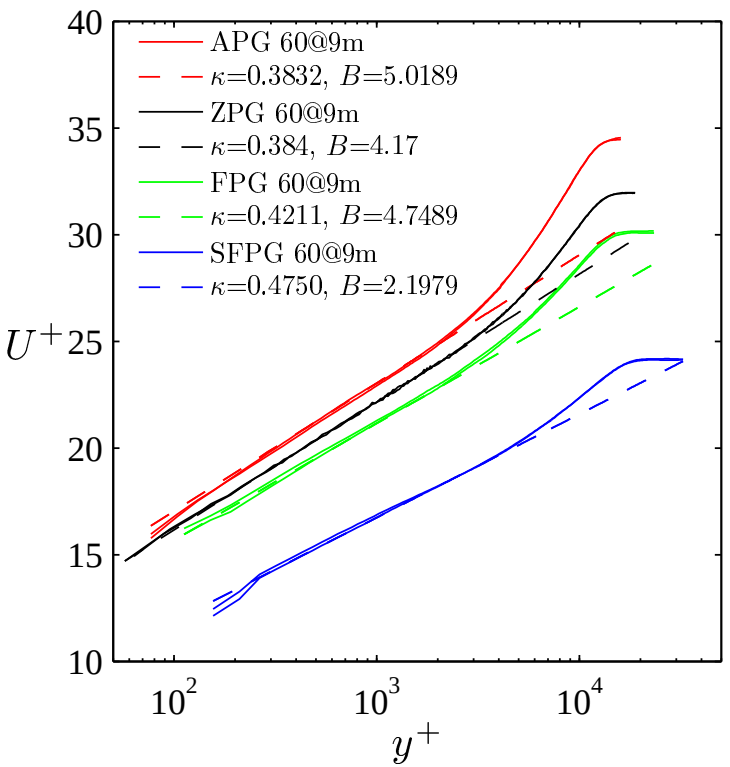

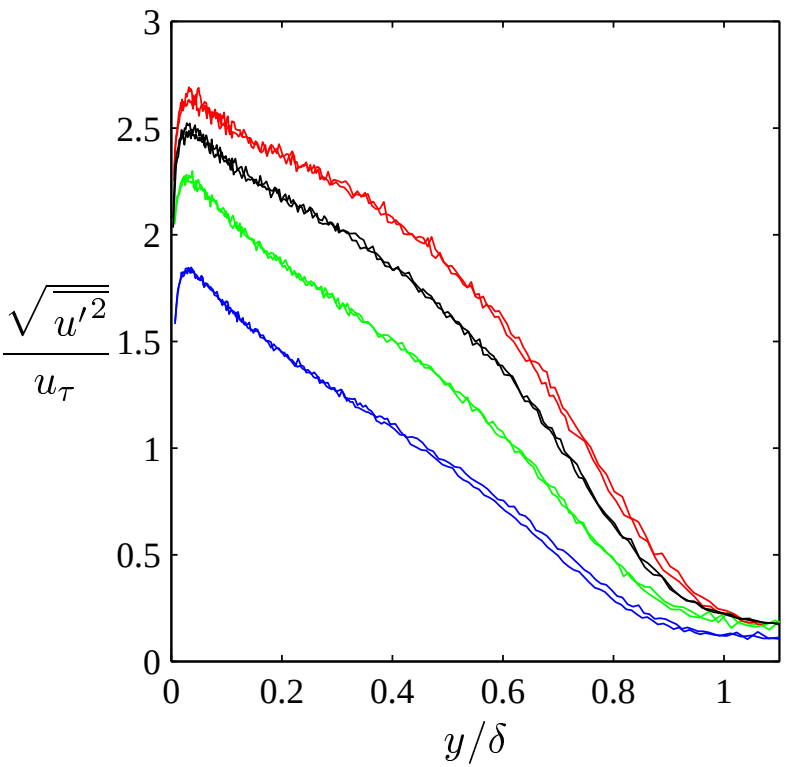

Overlap parameters in all wall-bounded flows studied

The von Kármán coefficient, $\tilde{\kappa}$ and the intercept $\tilde{B}$ for ALL wall-bounded flows have a common behavior.

A simple curve fit to $\tilde{\kappa}\tilde{B}$ versus $\tilde{B}$ can reduce the number of empirical constants in a turbulence model based on the logarithmic law.

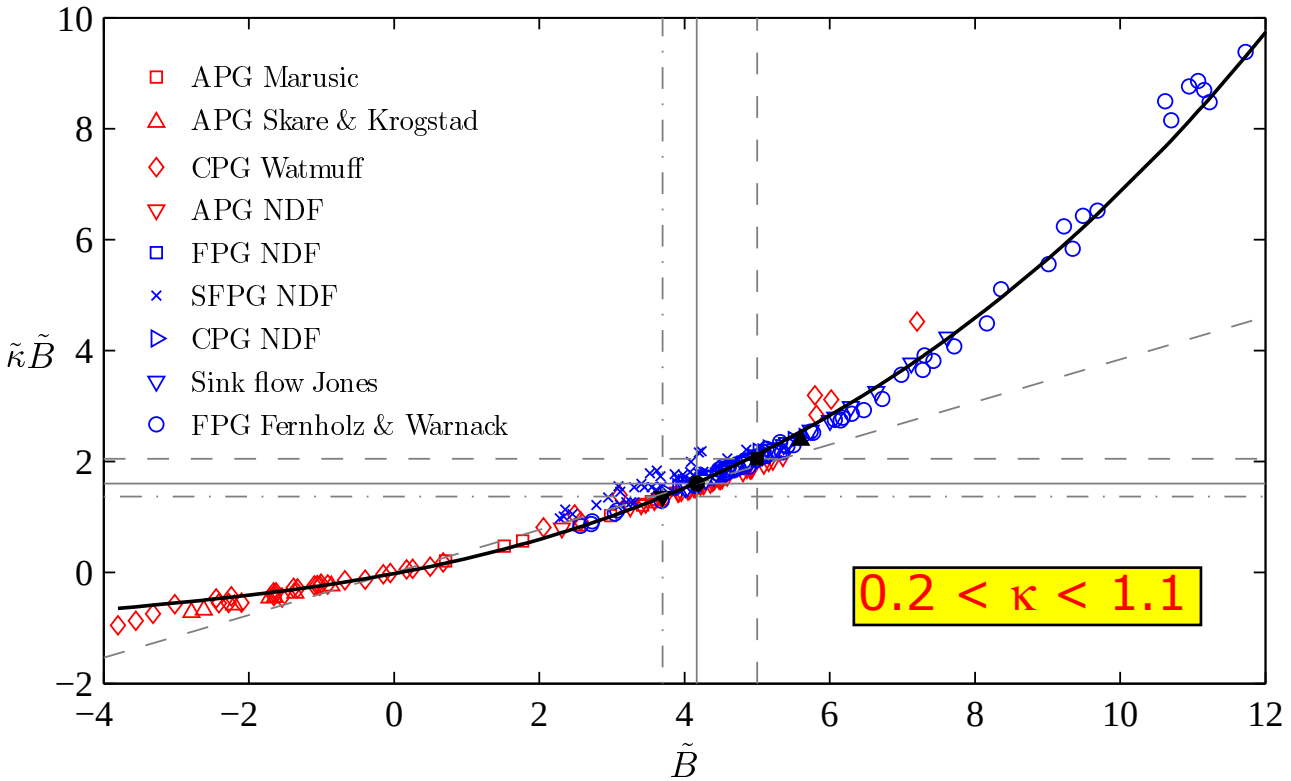

Channel & Pipe Flows

Traditionally the Kármán constant is estimated from the overlap region (log-layer) alone, which leads to a great deal of uncertainty, especially at lower *Re*, and the various approaches used often incorporate assumptions that have not been fully validated (e.g., limits of overlap region).

The uncertainty can be greatly reduced with the help of empirically-based "composite profiles" for the various wall-bounded flows, that are carefully constructed to satisfy several constraints.

$$\text{Channels \& Pipes :} \quad -\frac{\overline{uv}}{u_\tau^2} + \frac{\mathrm{d}U^+}{\mathrm{d}y^+} = 1 - \frac{y^+}{Re_\tau}$$

$$\frac{\mathrm{d}U^+_{\text{inner}}}{\mathrm{d}y^+} = \frac{\frac{1}{s} + \frac{y^{+2}}{\kappa} - \frac{y^+}{s\,Re_\tau}}{\frac{1}{s} + \frac{y^{+2}}{\kappa} + y^{+3}}$$

$$U^+ = U^+_{\text{inner}} + \frac{2\Pi}{\kappa}\mathcal{W}(\eta), \quad \eta \equiv y/H \leq 1$$

$$\left.\frac{\mathrm{d}^n U^+}{\mathrm{d}y^{+n}}\right|_{\eta=1} = 0 \qquad n \text{ is odd}$$

$$\neq 0 \qquad n \text{ is even}$$

$$\mathcal{W}_{\text{pipe}} = \frac{1 - \exp\left[-\frac{1}{3}(4p_2 + 6p_3 + 7p_4)\eta^3 + p_2\eta^4 + p_3\eta^6 + p_4\eta^7\right]}{1 - \exp\left[-(p_2 + 3p_3 + 4p_4)/3\right]}\left(1 - \frac{\ln(\eta)}{2\Pi}\right)$$

where, $p_2 = 4.075$, $p_3 = -6.911$ and $p_4 = 4.876$.

$$\mathcal{W}_{\text{channel}} = \frac{1 - \exp\left[-\frac{1}{2}(3c_2 + 6c_3 + 7c_4)\eta^2 + c_2\eta^3 + c_3\eta^6 + c_4\eta^7\right]}{1 - \exp\left[-(c_2 + 4c_3 + 5c_4)/2\right]}\left(1 - \frac{\ln(\eta)}{2\Pi}\right)$$

where, $c_2 = -20.22$, $c_3 = 17.1$ and $c_4 = -11.17$.

The composite profiles for Channels and Pipes fit accurately to both DNS and experimental data. Fit provides the local κ, B and Π.

$$\text{ZPG TBLs}: \quad -\frac{\overline{uv}}{u_\tau^2} + \frac{\mathrm{d}U^+}{\mathrm{d}y^+} = 1 + \left(\frac{\nu}{u_\tau^2}\frac{\mathrm{d}u_\tau}{\mathrm{d}x}\right)\int_0^{y^+} U^{+2}\mathrm{d}y^+ \quad \Rightarrow \quad 1 - \frac{\mathrm{d}U^+}{\mathrm{d}y^+} \approx c_1 y^{+3}$$

$$\text{PG TBLs}: \quad -\frac{\overline{uv}}{u_\tau^2} + \frac{\mathrm{d}U^+}{\mathrm{d}y^+} = 1 + \frac{\nu}{u_\tau^3}\frac{\partial P}{\partial x}\, y^+ \quad \Rightarrow \quad 1 - \frac{\mathrm{d}U^+}{\mathrm{d}y^+} \approx -\frac{\nu}{u_\tau^3}\frac{\partial P}{\partial x}\, y^+ + c_2 y^{+3}$$

$$\text{Channels \& Pipes}: \quad -\frac{\overline{uv}}{u_\tau^2} + \frac{\mathrm{d}U^+}{\mathrm{d}y^+} = 1 - \frac{y}{H} \quad \Rightarrow \quad 1 - \frac{\mathrm{d}U^+}{\mathrm{d}y^+} \approx \frac{y^+}{Re_\tau} + c_3 y^{+3}$$

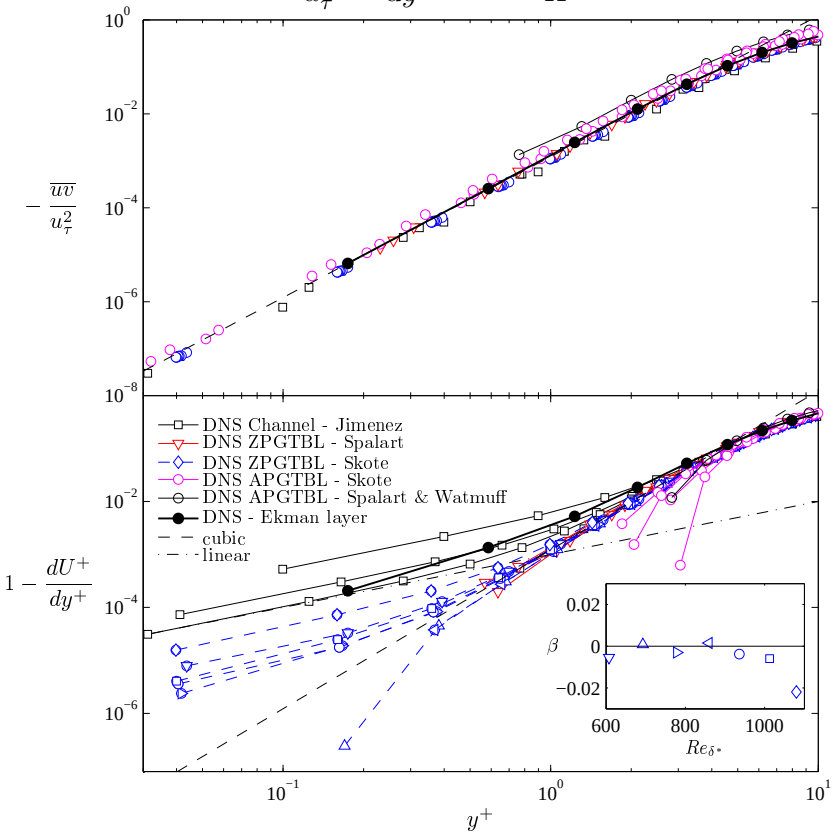

Near the wall DNS of various flows show a cubic behavior for Reynolds shear stress, $-\overline{uv}$.

However, differences between DNS of ZPG TBLs by Spalart (1988) and Skote (2001) are observed for $1 - \mathrm{d}U^+/\mathrm{d}y^+$.

We have also found differences at higher y^+ for the gradient of total stress for these two DNS.

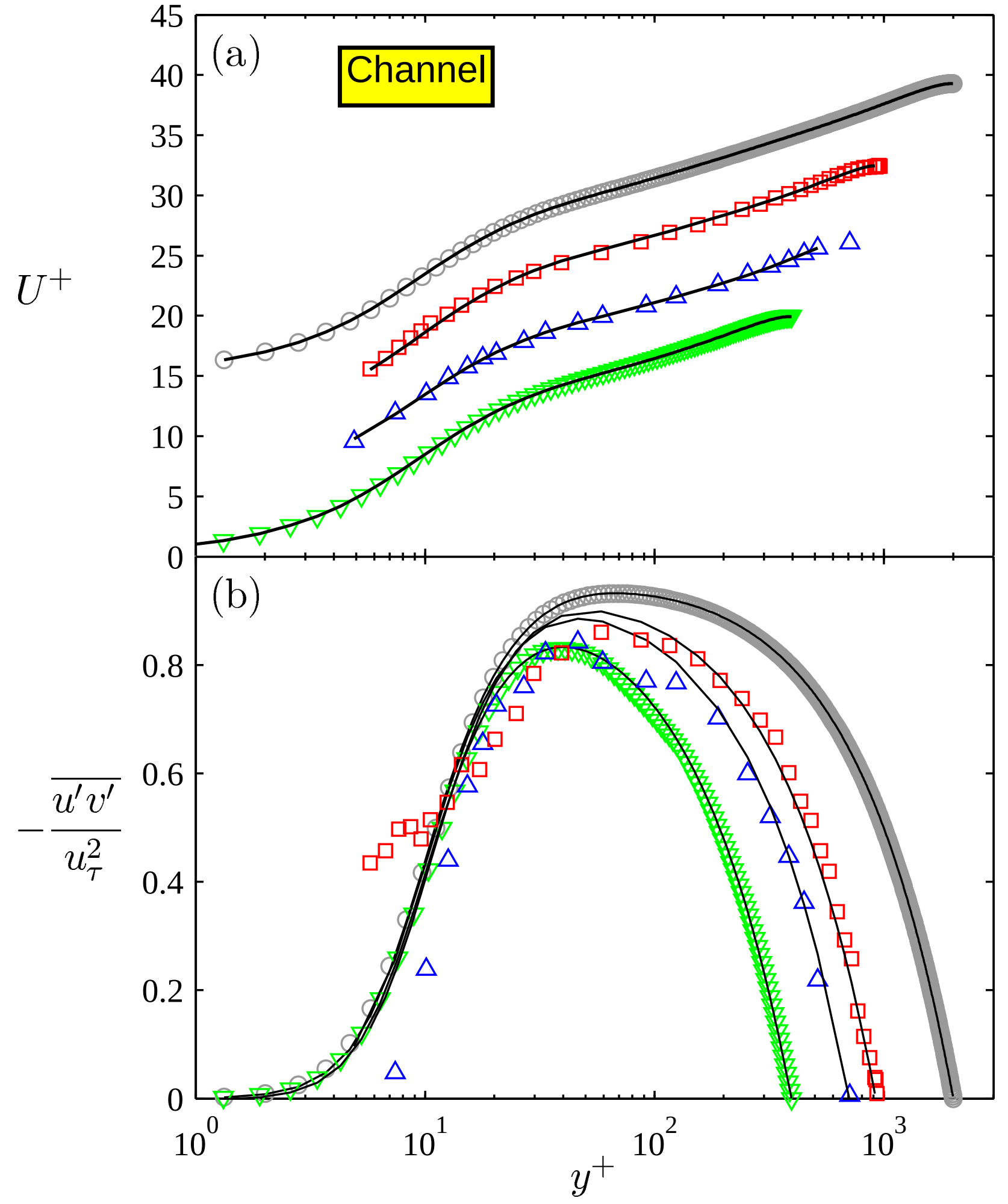
(a)
Channel
U^+
45
40
35
30
25
20
15
10
5
0
(b)
$-\overline{u'v'}/u_\tau^2$
0.8
0.6
0.4
0.2
0
10^0
10^1
10^2
10^3
y^+

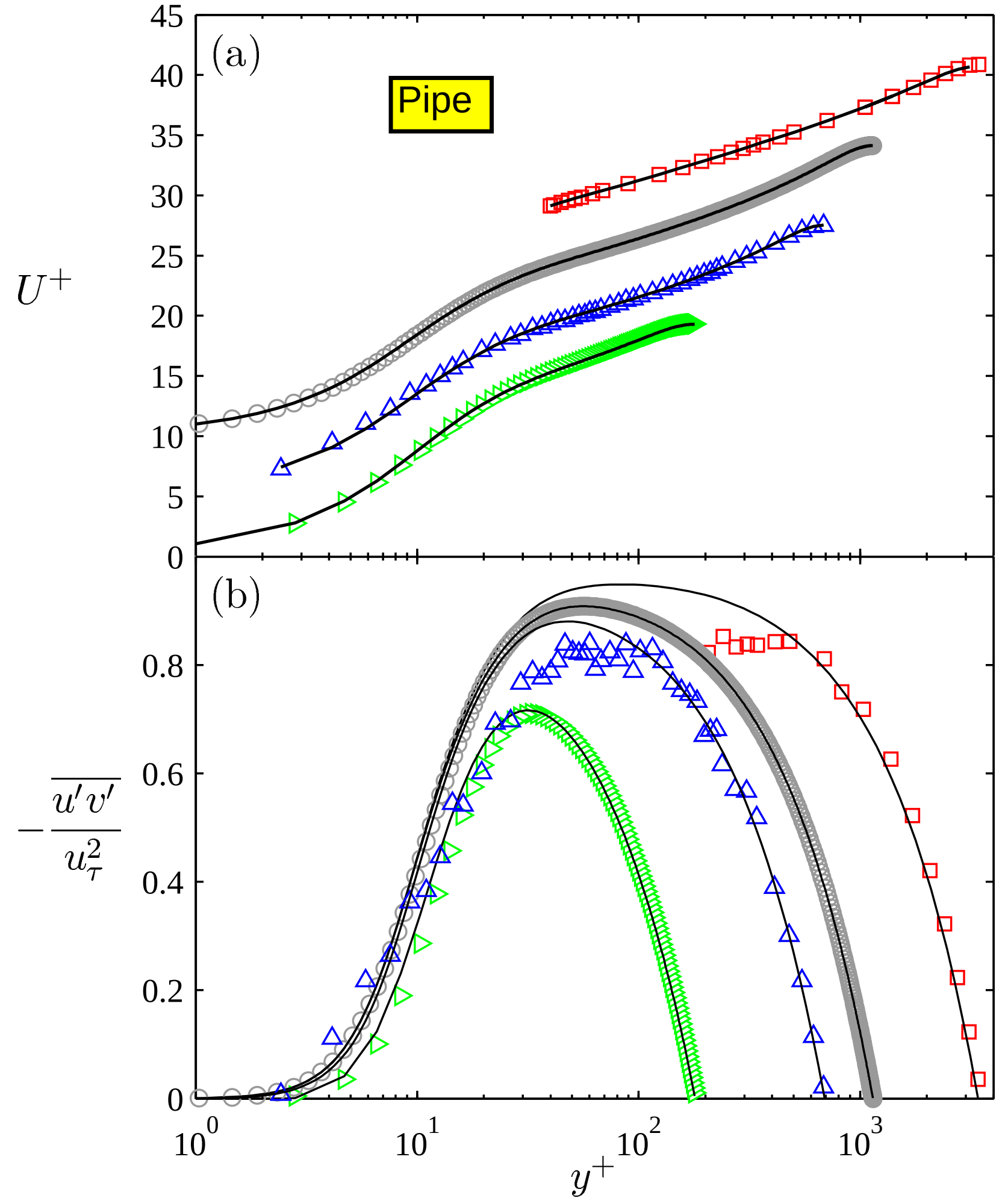
(a)
Pipe
U^+
45
40
35
30
25
20
15
10
5
0
(b)
$-\overline{u'v'}/u_\tau^2$
0.8
0.6
0.4
0.2
0
10^0
10^1
10^2
10^3
y^+

Ψ_i is *almost* constant across y for $\kappa = 0.41$ but the magnitude of Ψ_i decreases with increasing Reynolds number.

Ψ_i for $\kappa = 0.422$ is has a very good constant behavior for $y^+ > 600$. Ψ_o is clearly constant across y/R for $\kappa = 0.41$, except the data with $Re_\tau \lesssim 11,000$.

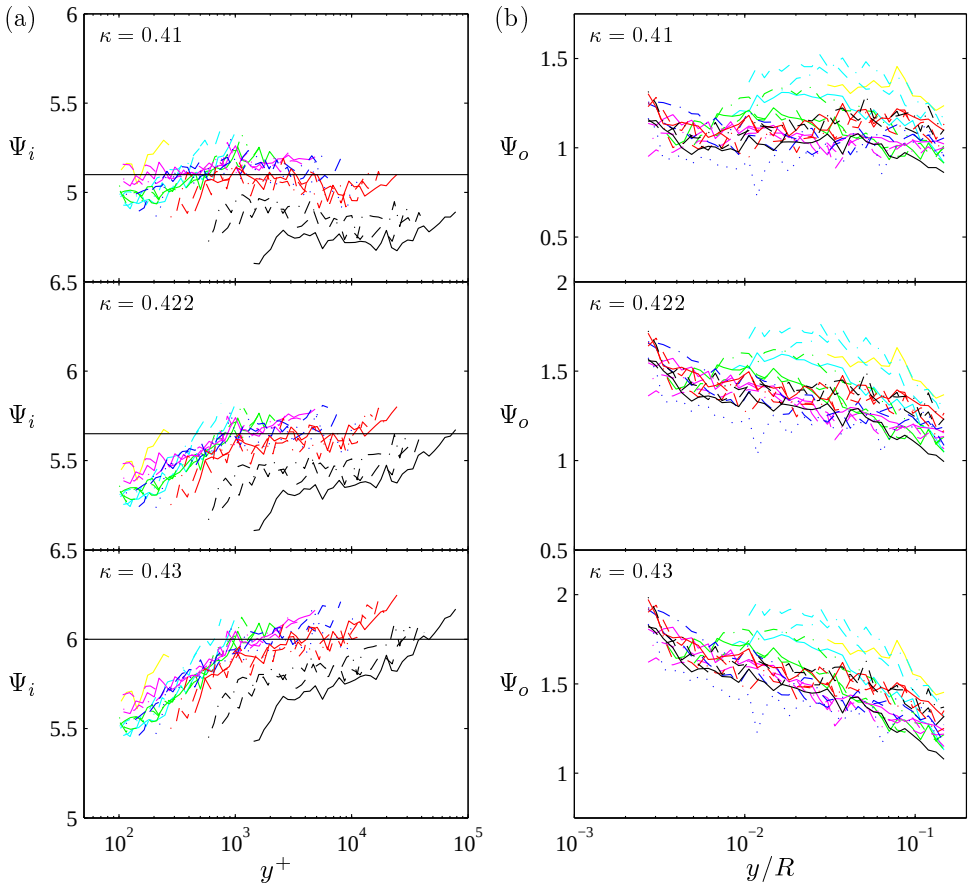

$$\Psi_i = U^+ - \frac{1}{\kappa}\ln(y^+) \equiv B$$

$$\Psi_o = (U_c^+ - U^+) + \frac{1}{\kappa}\ln(y/R) \equiv -B_o$$

$$300 < y^+ < 0.15 Re_\tau$$

Comment on consistency, and single κ for all Re versus composite profile approach yielding κ(Re).

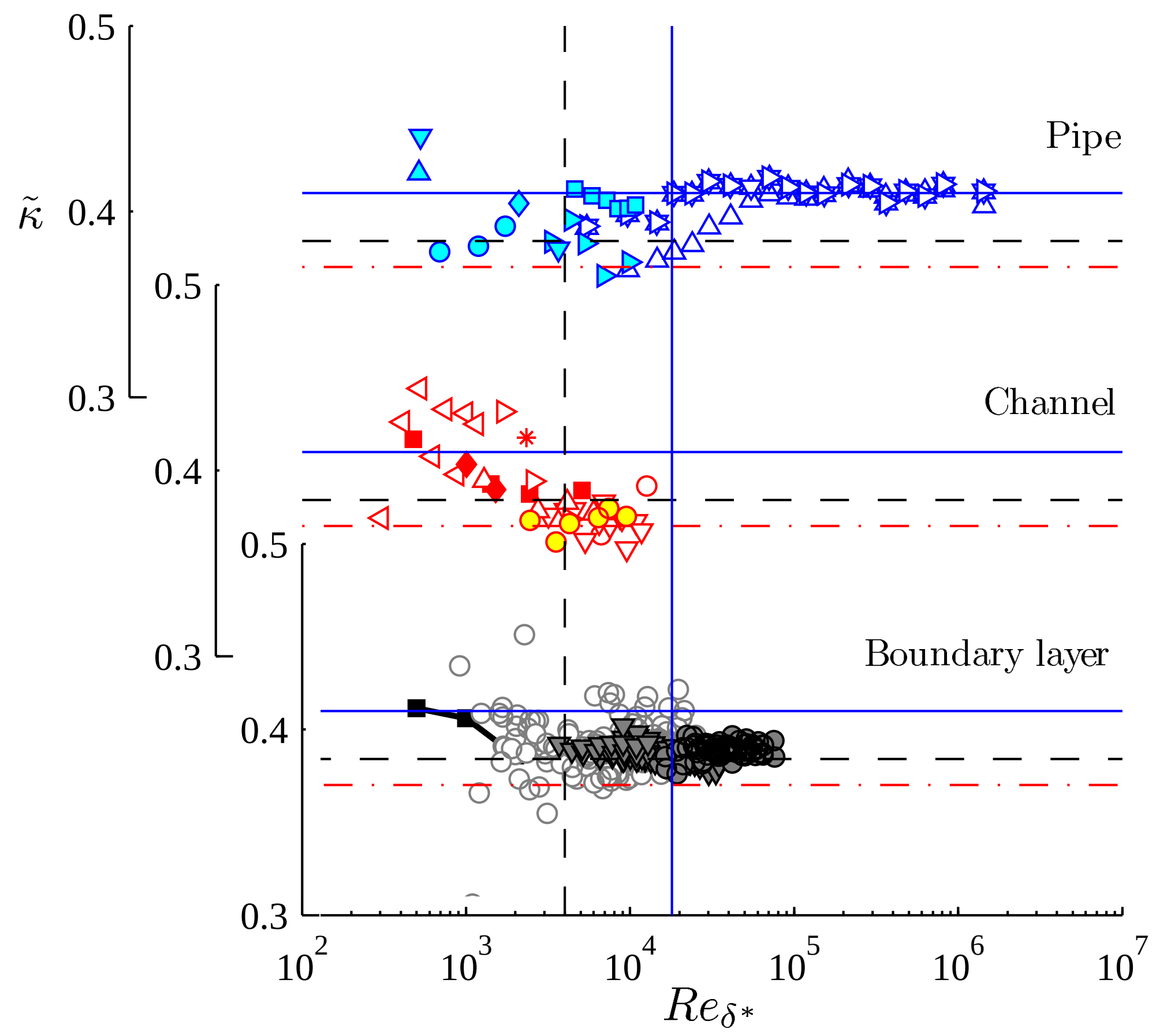
0.5
0.4
0.3
$\tilde{\kappa}$
Pipe
Channel
Boundary layer
10^2
10^3
10^4
10^5
10^6
10^7
$Re_{\delta*}$

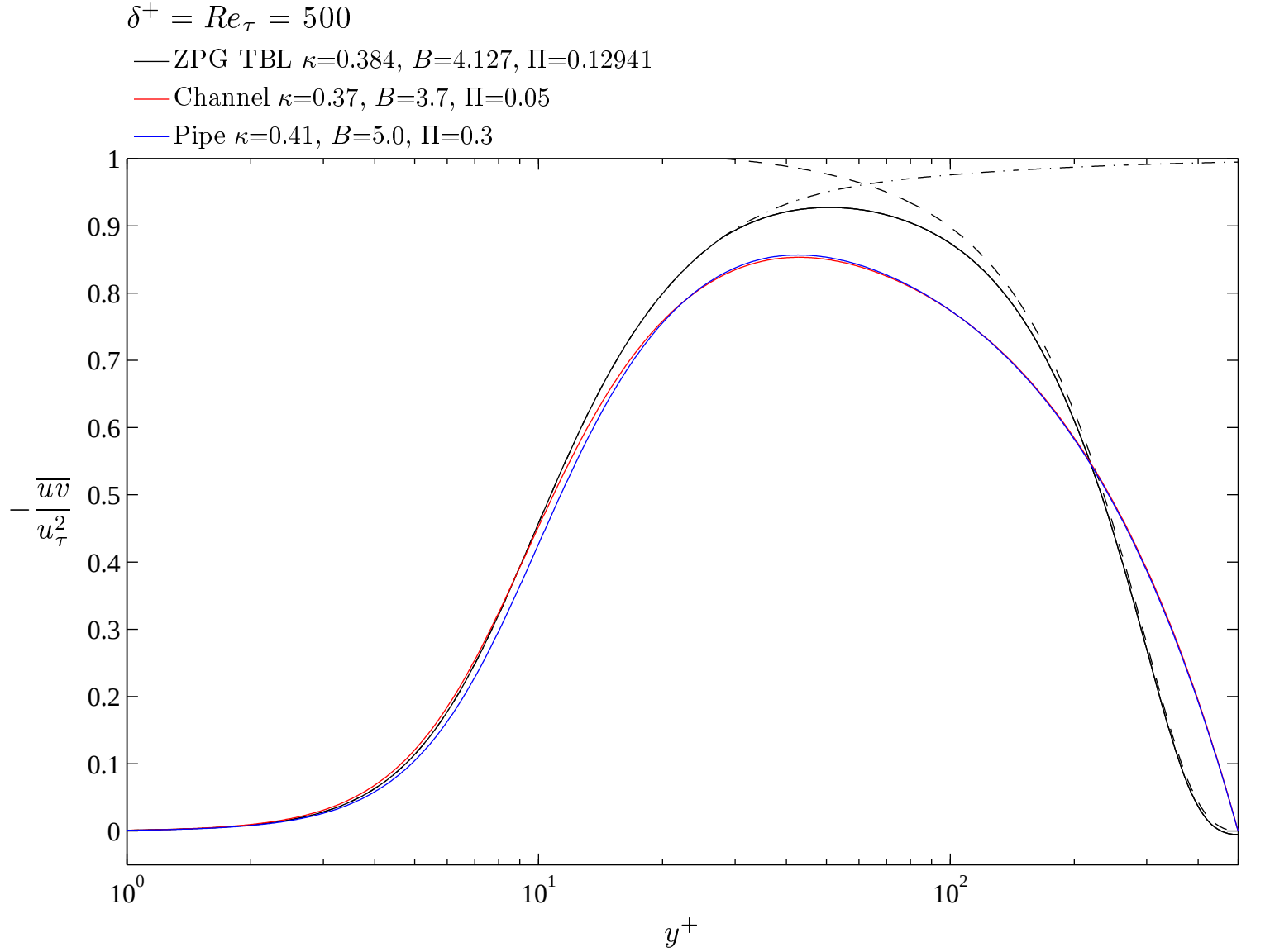
$\delta^+ = Re_\tau = 500$
ZPG TBL κ=0.384, B=4.127, Π=0.12941
Channel κ=0.37, B=3.7, Π=0.05
Pipe κ=0.41, B=5.0, Π=0.3
$-\frac{\overline{uv}}{u_\tau^2}$
y^+
1
0.9
0.8
0.7
0.6
0.5
0.4
0.3
0.2
0.1
0
10^0
10^1
10^2

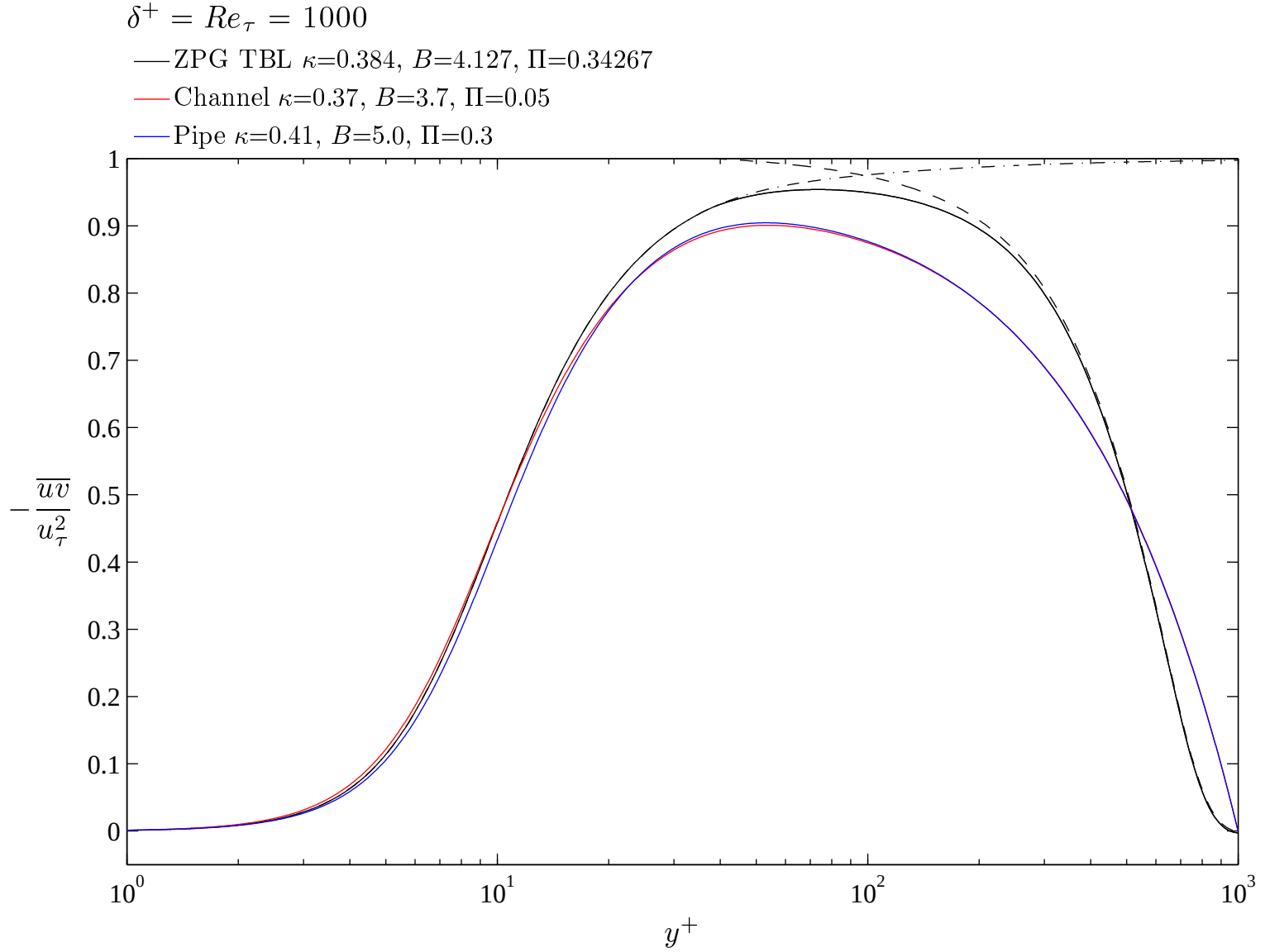
$\delta^+ = Re_\tau = 1000$
ZPG TBL κ=0.384, B=4.127, Π=0.34267
Channel κ=0.37, B=3.7, Π=0.05
Pipe κ=0.41, B=5.0, Π=0.3
$-\frac{\overline{uv}}{u_\tau^2}$
y^+
1
0.9
0.8
0.7
0.6
0.5
0.4
0.3
0.2
0.1
0
10^0
10^1
10^2
10^3

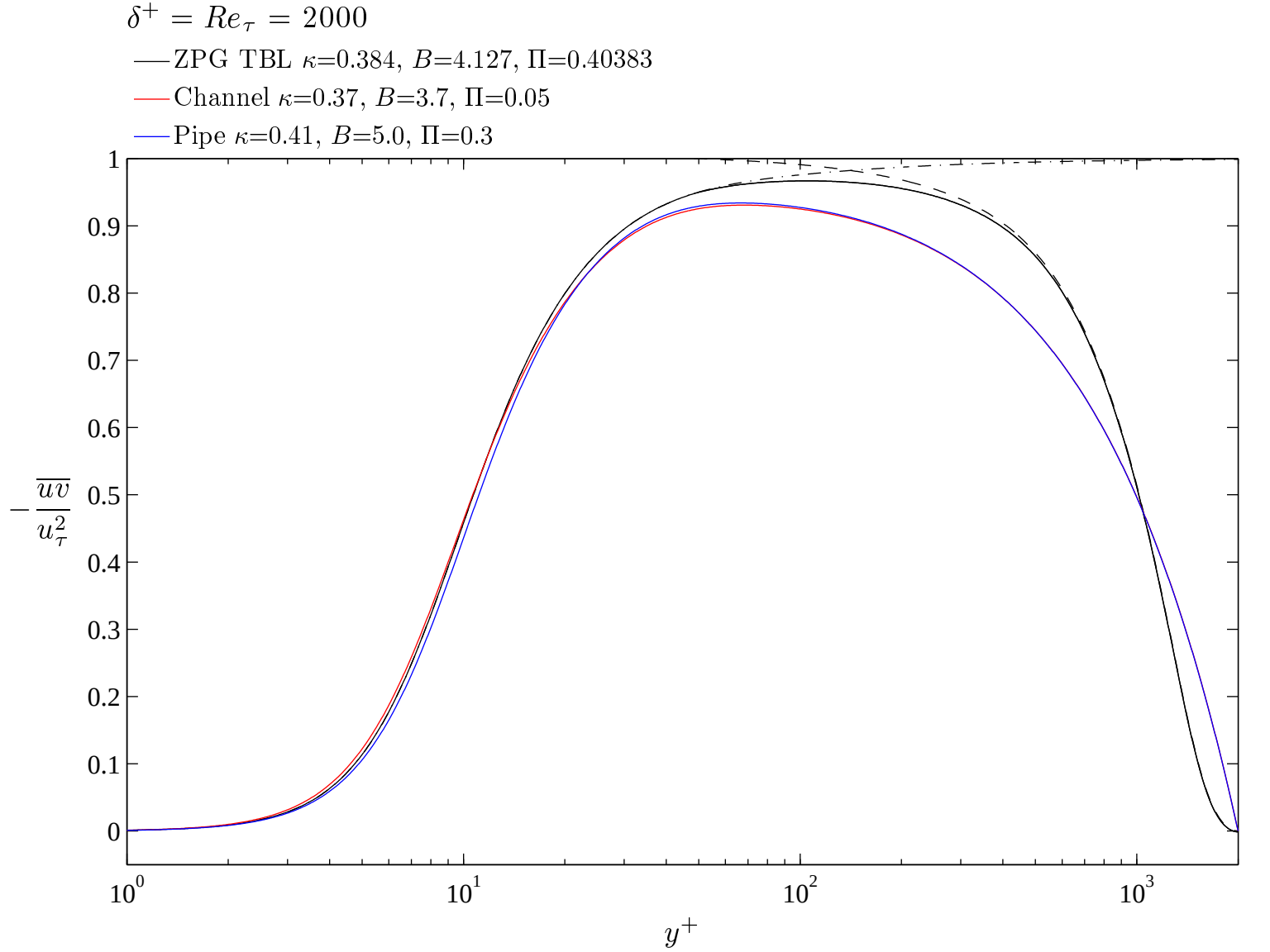
$\delta^+ = Re_\tau = 2000$
ZPG TBL κ=0.384, B=4.127, Π=0.40383
Channel κ=0.37, B=3.7, Π=0.05
Pipe κ=0.41, B=5.0, Π=0.3
$-\frac{\overline{uv}}{u_\tau^2}$
y^+
1
0.9
0.8
0.7
0.6
0.5
0.4
0.3
0.2
0.1
0
10^0
10^1
10^2
10^3

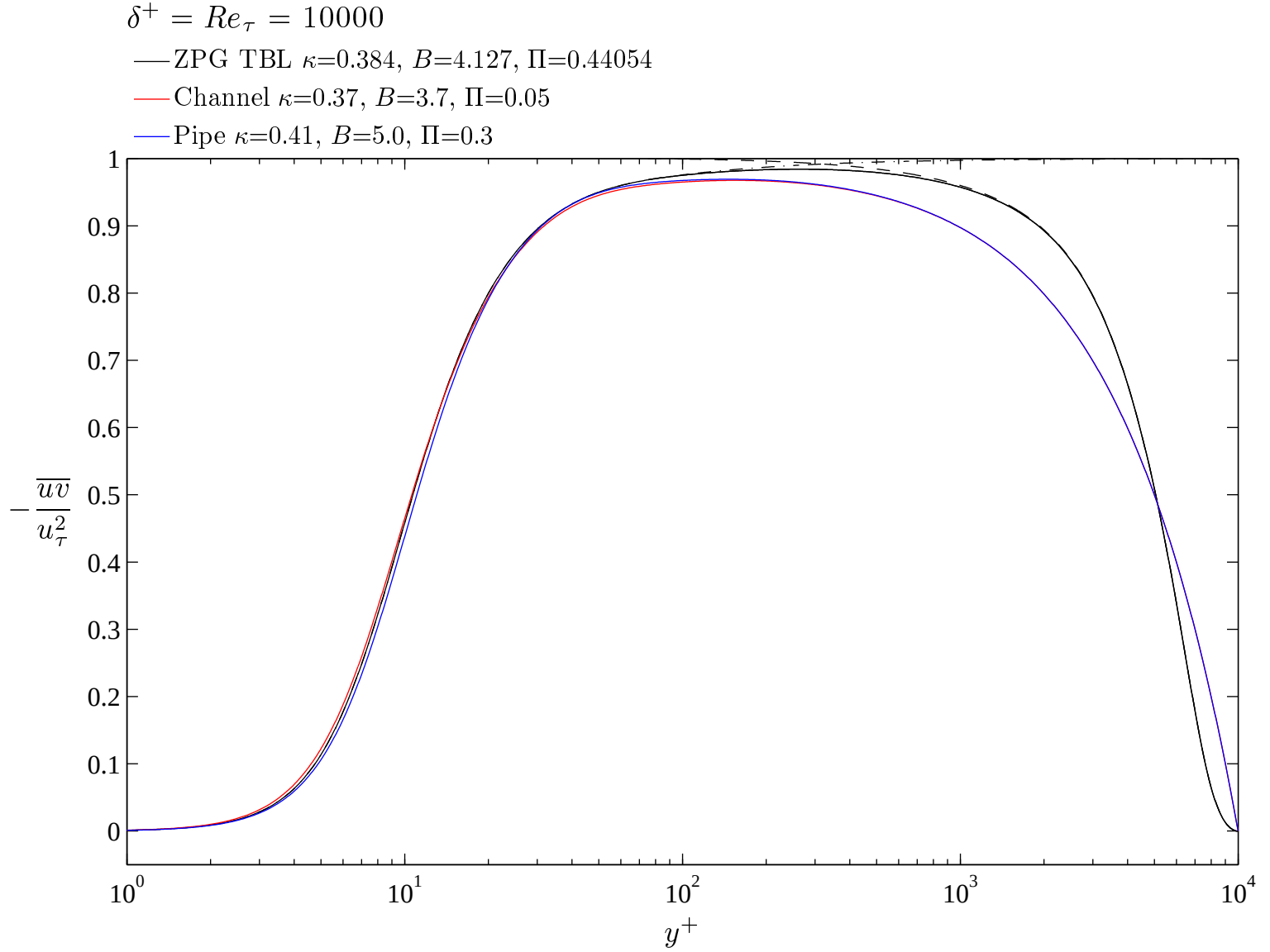
$\delta^+ = Re_\tau = 10000$
ZPG TBL κ=0.384, B=4.127, Π=0.44054
Channel κ=0.37, B=3.7, Π=0.05
Pipe κ=0.41, B=5.0, Π=0.3
$-\frac{\overline{uv}}{u_\tau^2}$
y^+
1
0.9
0.8
0.7
0.6
0.5
0.4
0.3
0.2
0.1
0
10^0
10^1
10^2
10^3
10^4

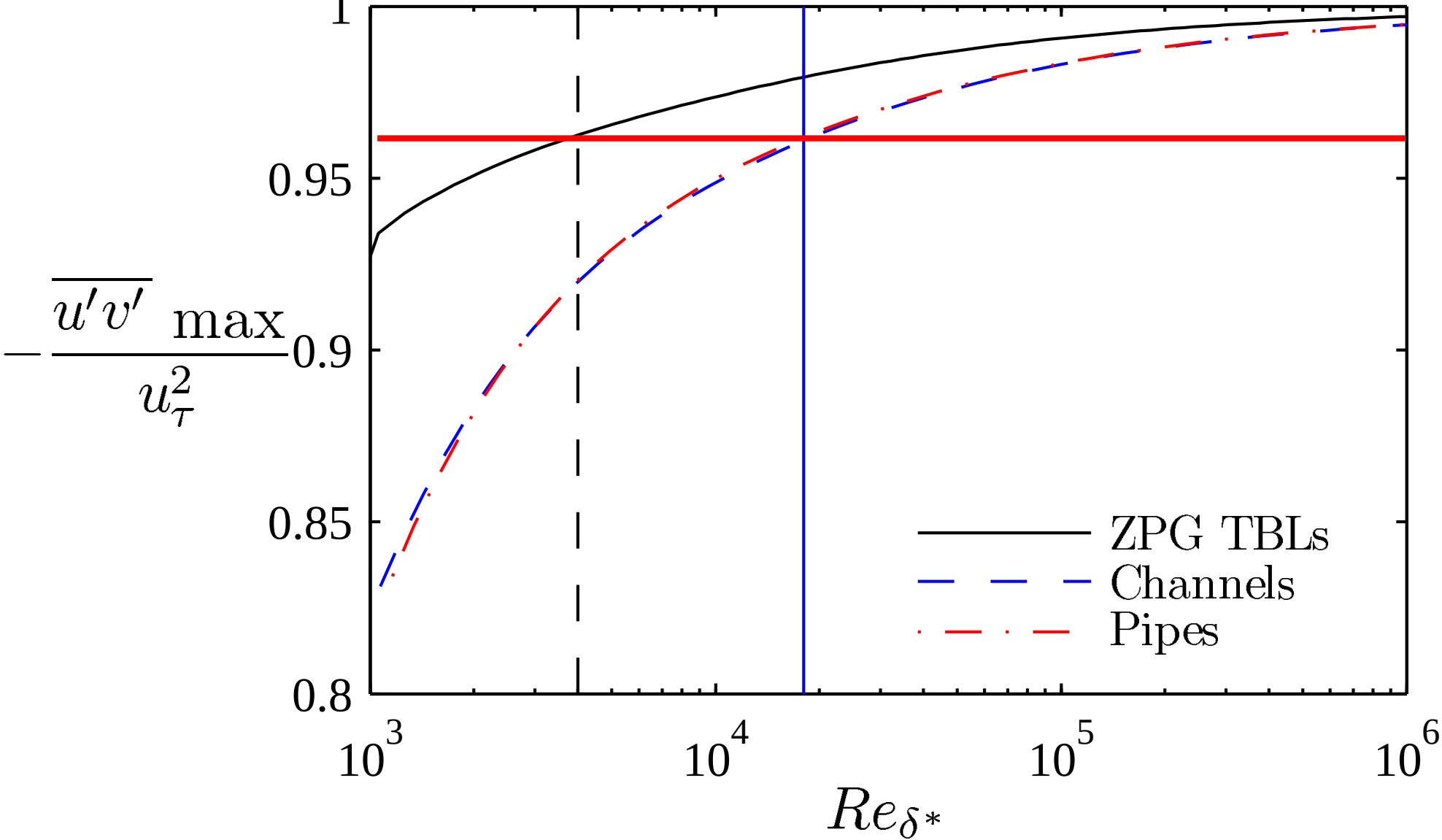
1
0.95
0.9
0.85
0.8
$-\frac{\overline{u'v'}}{u_\tau^2}\max$
10^3
10^4
10^5
10^6
$Re_{\delta*}$
ZPG TBLs
Channels
Pipes

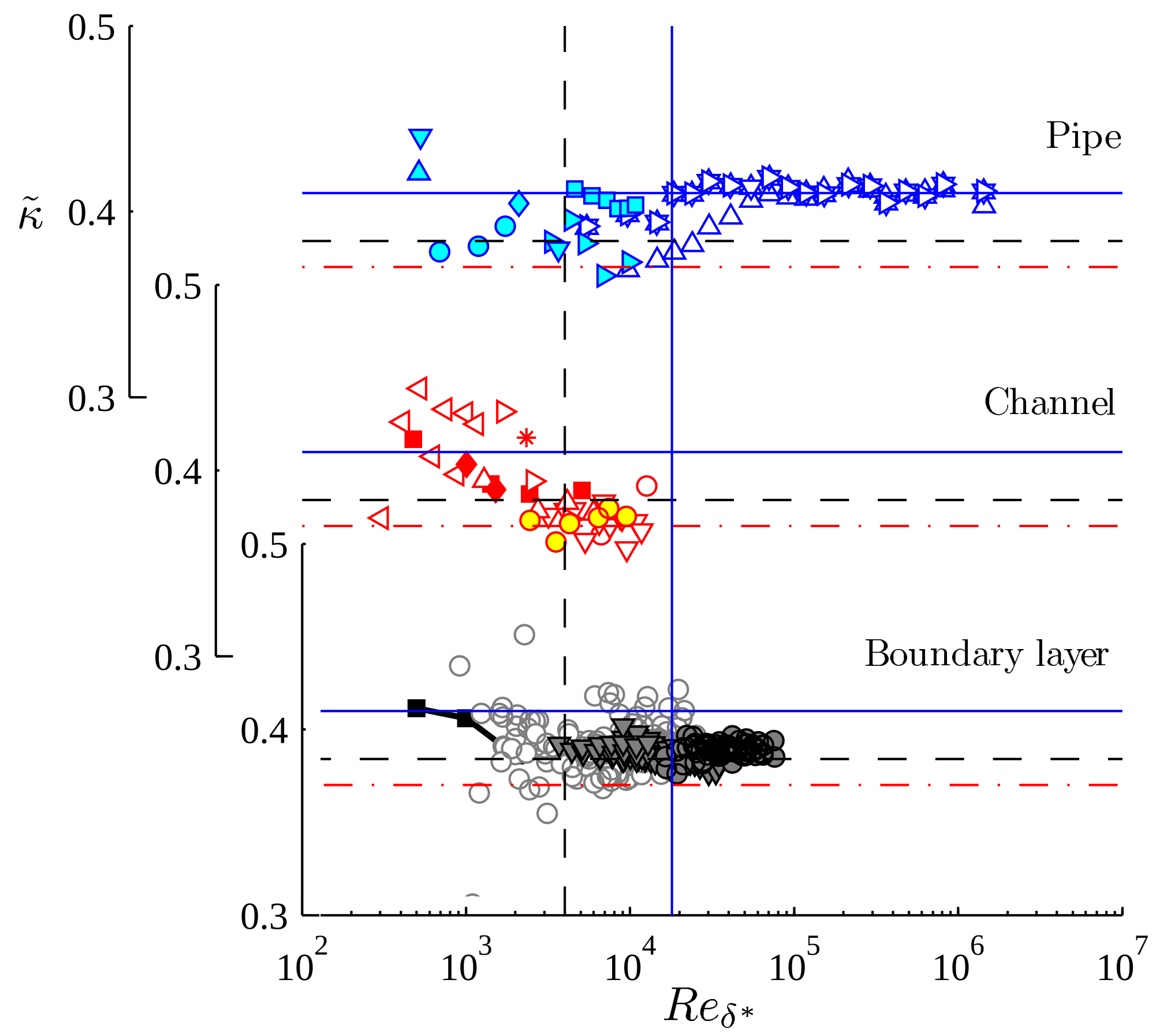
0.5
0.4
0.3
$\tilde{\kappa}$
Pipe
Channel
Boundary layer
10^2
10^3
10^4
10^5
10^6
10^7
$Re_{\delta*}$

Π for pipe flows is higher than that for channel flows, although they have the same governing equation and boundary condition.

Parallel flows do not show the development of Π at low Reynolds numbers.

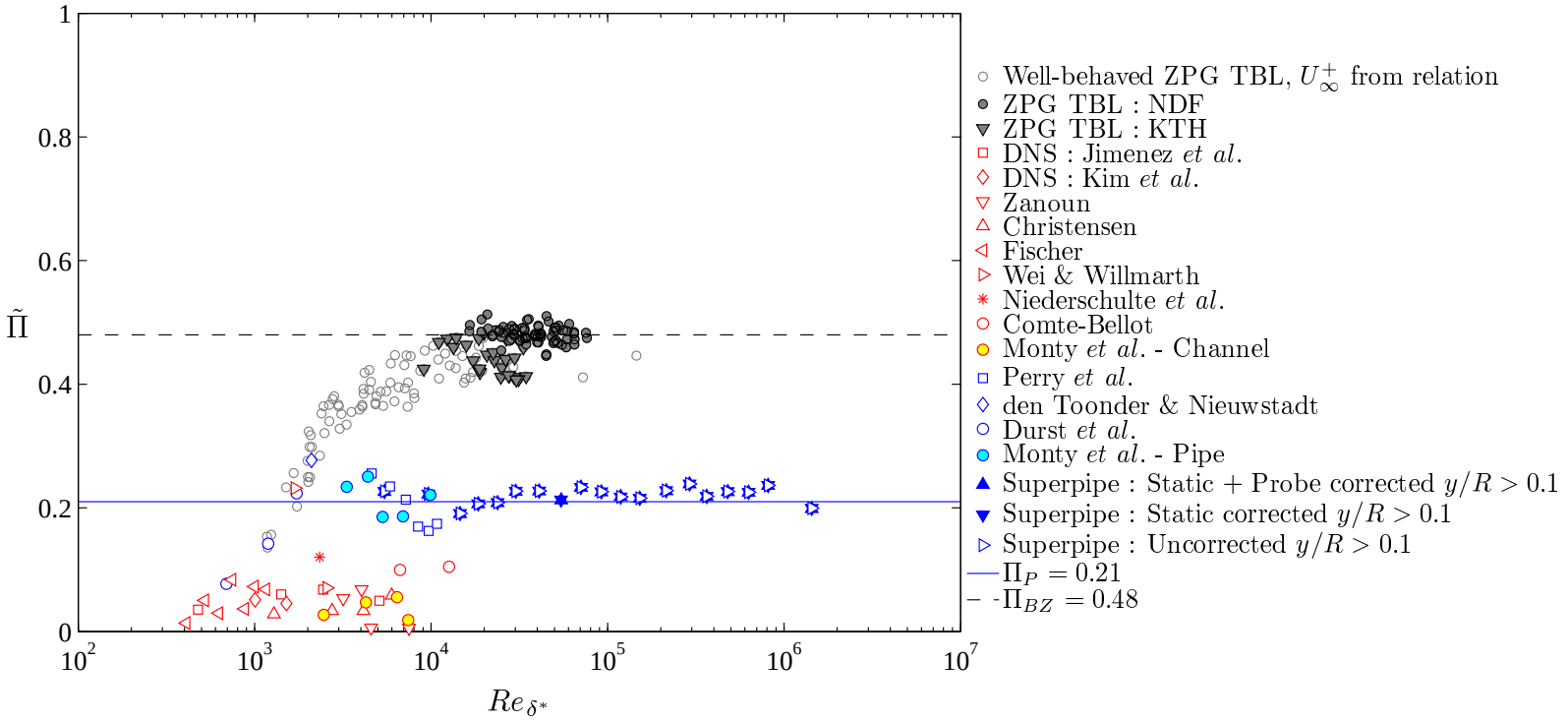

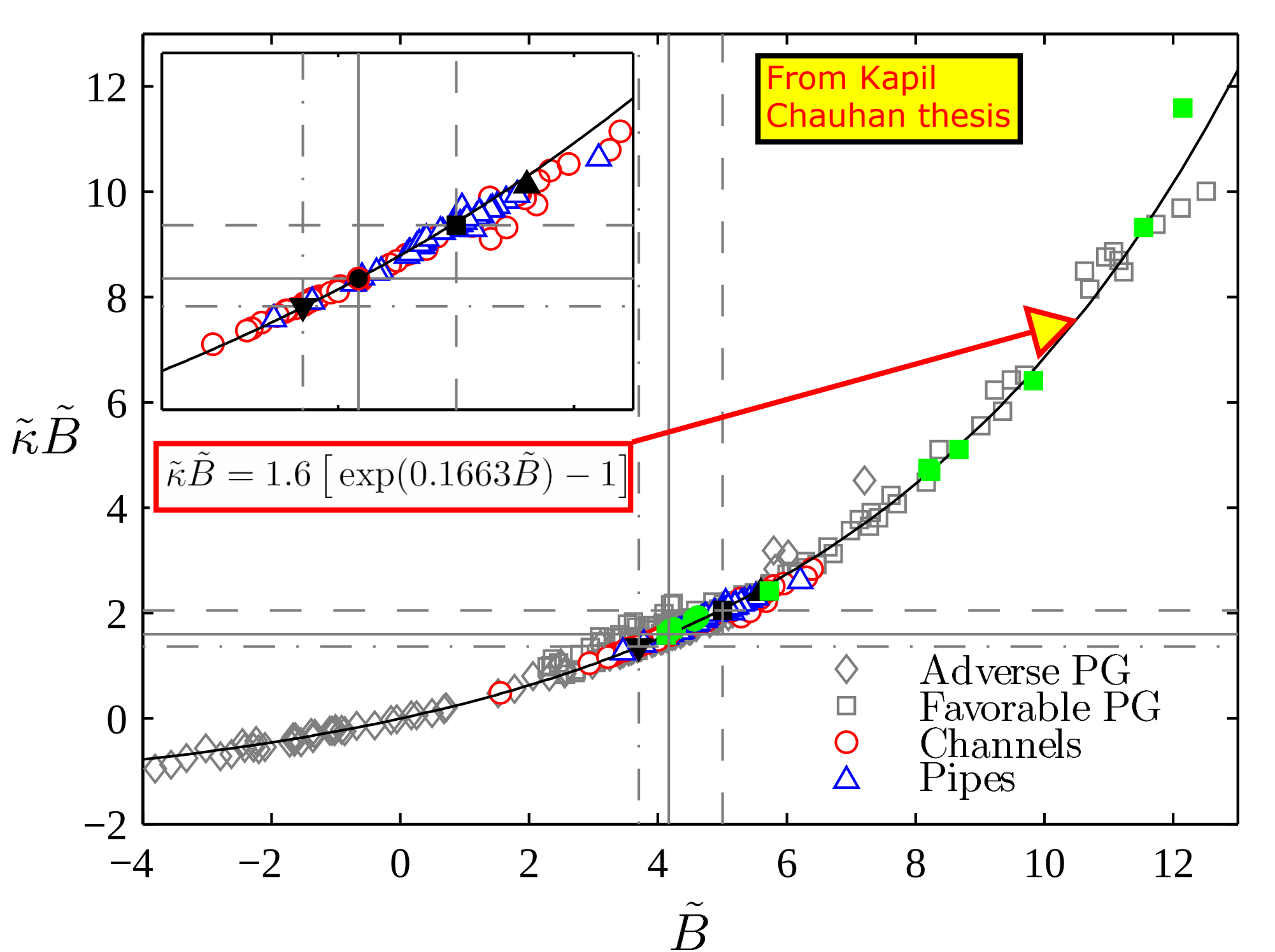
From Kapil Chauhan thesis
$\tilde{\kappa}\tilde{B} = 1.6\left[\exp(0.1663\tilde{B}) - 1\right]$
Adverse PG
Favorable PG
Channels
Pipes
$\tilde{\kappa}\tilde{B}$
$\tilde{B}$
12
10
8
6
4
2
0
−2
−4
−2
0
2
4
6
8
10
12

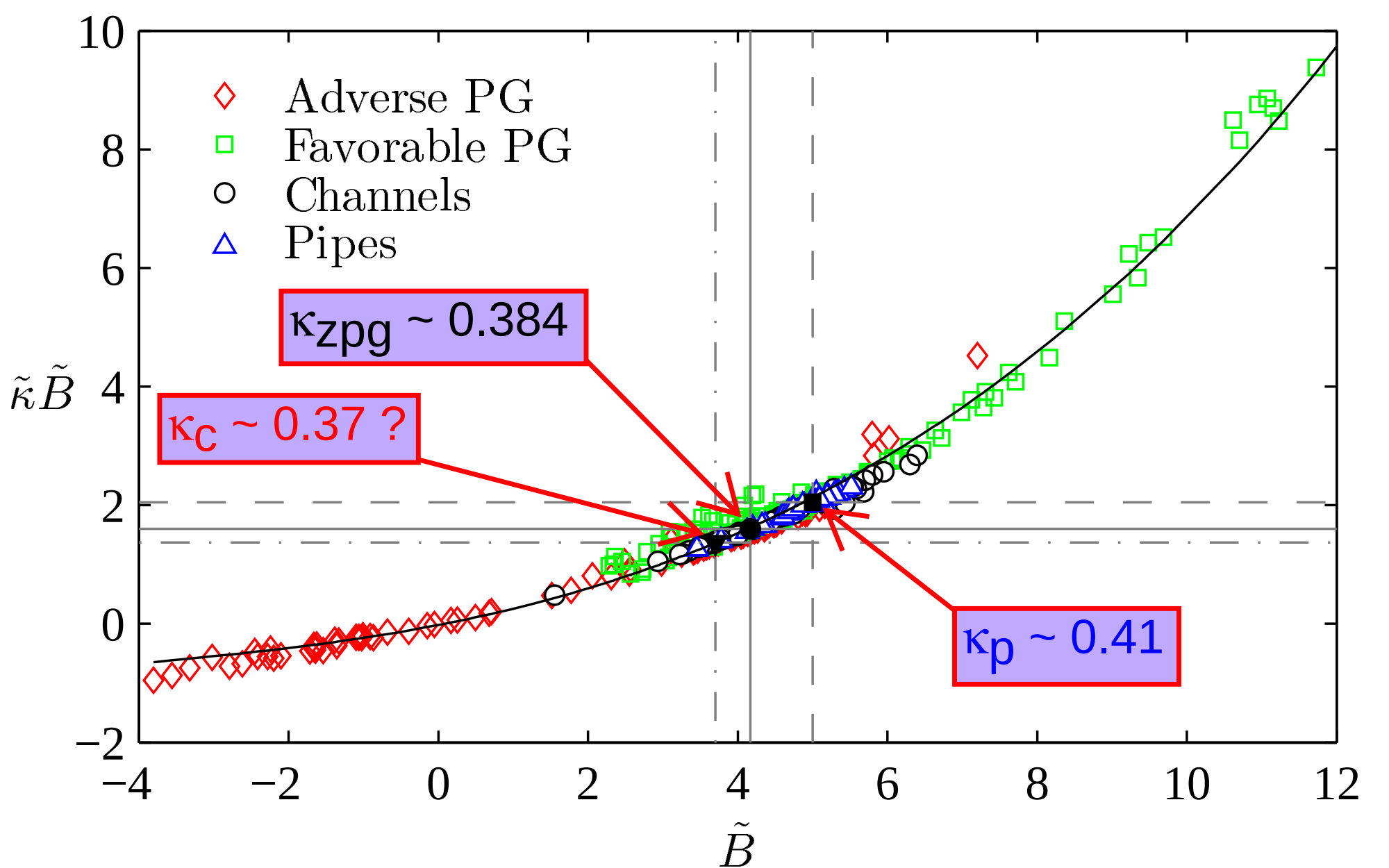
Adverse PG
Favorable PG
Channels
Pipes
κzpg ~ 0.384
κc ~ 0.37 ?
κp ~ 0.41
$\tilde{\kappa}\tilde{B}$
$\tilde{B}$
10
8
6
4
2
0
−2
−4
−2
0
2
4
6
8
10
12

> Overlap parameters for wall-bounded flows, including the von Kármán "*coefficient*," are not universal.

> They appear to at least depend on pressure gradient and flow geometry.

> However, their asymptotic high Reynolds number *values* are different constants for fully developed or near equilibrium flows.

> Full consequences on currently popular models for *prediction* of turbulence should be fully assessed.

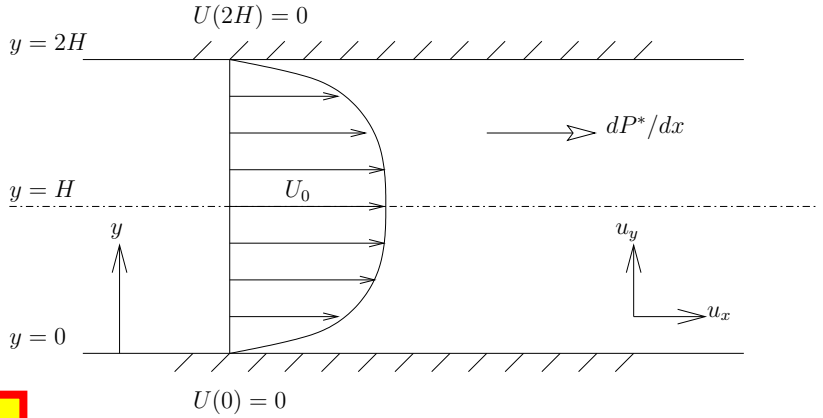

Experiments !!!
Need
High Re
Good Spatial Resolution

Modelling !!!
Need to
Reevaluate

$$\text{Continuity} : \frac{\partial u'}{\partial x} + \frac{\partial v'}{\partial y} = 0$$

$$x - \text{momentum} : -\frac{1}{\rho}\frac{\partial P}{\partial x} + \frac{\partial}{\partial y}\left[\nu\frac{\partial U}{\partial y} - \overline{u'v'}\right] = 0$$

$$y - \text{momentum} : -\frac{1}{\rho}\frac{\partial P}{\partial y} + \frac{\partial \overline{v'^2}}{\partial y} = 0$$

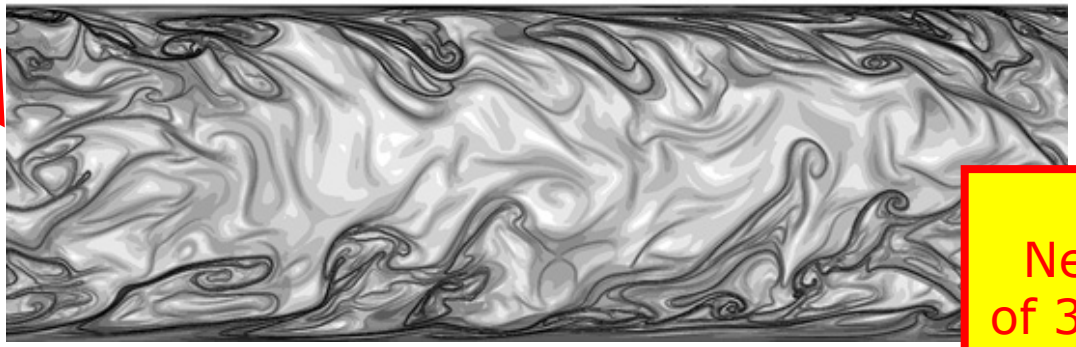

DNS !!!
Need factor
of 3 to 5 in Re
(Computing?)

l_c = Relevant Viscous Length Scale = ν / u_τ = R / R^+; Independent of Fluid, Pressure, etc.

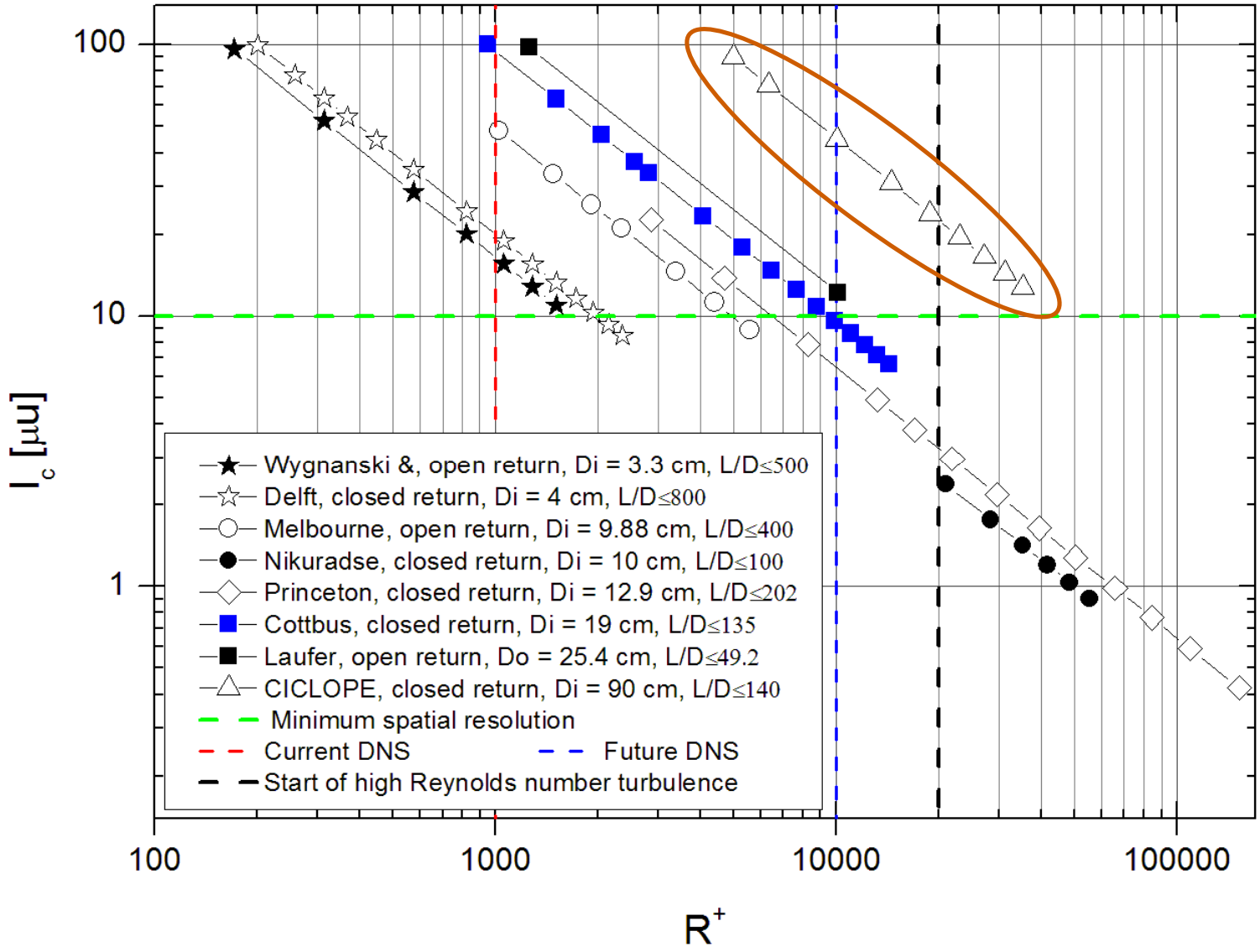

I C E T

International Collaboration on Experiments in Turbulence: Coordinated Measurements in High Reynolds Number Turbulent Boundary Layers from Three Wind Tunnels

Hassan Nagib – IIT
Alexander Smits – Princeton University
Ivan Marusic – University of Melbourne
P. Henrik Alfredsson – KTH
and
ICET Team

62nd Annual Meeting of the APS Division of Fluid Dynamics
Minneapolis, MN, November 22-24, 2009

APS Session
on

Turbulent Boundary Layers: Experimental Studies

1. ICET - International Collaboration on Experiments in Turbulence: Coordinated Measurements in High Reynolds Number Turbulent Boundary Layers from Three Facilities. H. NAGIB, A. SMITS, I. MARUSIC, P. H. ALFREDSSON and ICET Team.

2. Accurate and Independent Measurements of Wall-Shear Stress in Turbulent Flows. J-D. RÜEDI, R. DUNCAN, S. IMAYAMA, K. CHAUHAN and ICET Team.

3. Pitot Probe Corrections for Measurements in Turbulent Boundary Layers. J. MONTY, S. BAILEY, M. HULTMARK, B. McKEON and ICET Team.

4. Challenges in Hot Wire Measurements in Wall-Bounded Turbulent Flows. R. ÖRLU, N. HUTCHINS, T. KURIAN, A. TALAMELLI and ICET Team.

5. Mean Flow Measurements with Pitot Probes in High Reynolds Number Boundary Layers. S. BAILEY, M. HULTMARK, R. DUNCAN, B. McKEON and ICET Team.

6. Mean Flow Measurements with Hot Wires in High Reynolds Number Boundary Layers. R. DUNCAN, N. HUTCHINS, A. SEGALINI, J. MONTY and ICET Team.

7. Turbulence Measurements with Hot Wires in High Reynolds Number Boundary Layers. J. FRANSSON, N. HUTCHINS, R. ÖRLU, M. CHONG and ICET Team.

Scope

- Zero pressure gradient (ZPG) boundary layers at high Reynolds numbers are the focus.
- Over the past few years, four groups have made systematic comparison between several measurement techniques and three facilities.
- The development length of the boundary layers and the free-stream velocity in the three facilities range from 5.5 to 22 m, and from 10 to 60 m/s, respectively.
- Various arrangements for adjustable test section ceilings are employed to generate ZPG boundary layers over the range of momentum thickness Reynolds numbers from 11,000 to 70,000.
- Oil film interferometry (OFI) is employed to directly measure the wall shear stress, and various sizes of Pitot probes and types of hot-wire sensors are used.

Objectives

- Compare the high Reynolds number, ZPG boundary layers formed in three facilities.
- Establish a reliable estimate for the accuracy and repeatability of OFI.
- Evaluate the performance of hot-wire probes with different characteristics and of various anemometer units.
- Compare the mean velocity profiles measured by hot wires and Pitot probes.
- Explain differences between overlap region parameters measured by hot wires and Pitot probes; e.g., the value of κ

Set-up at KTH / MTL wind-tunnel

0.8m x 1.2m x 7m

Adjustable Ceiling

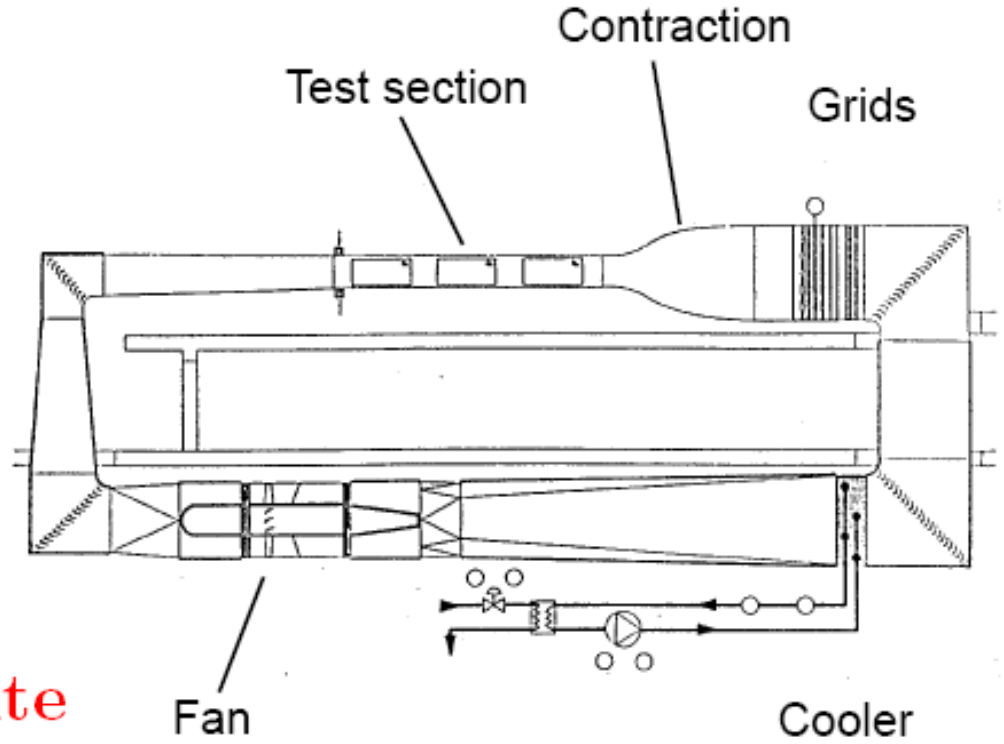

Flat Boundary Layer Plate

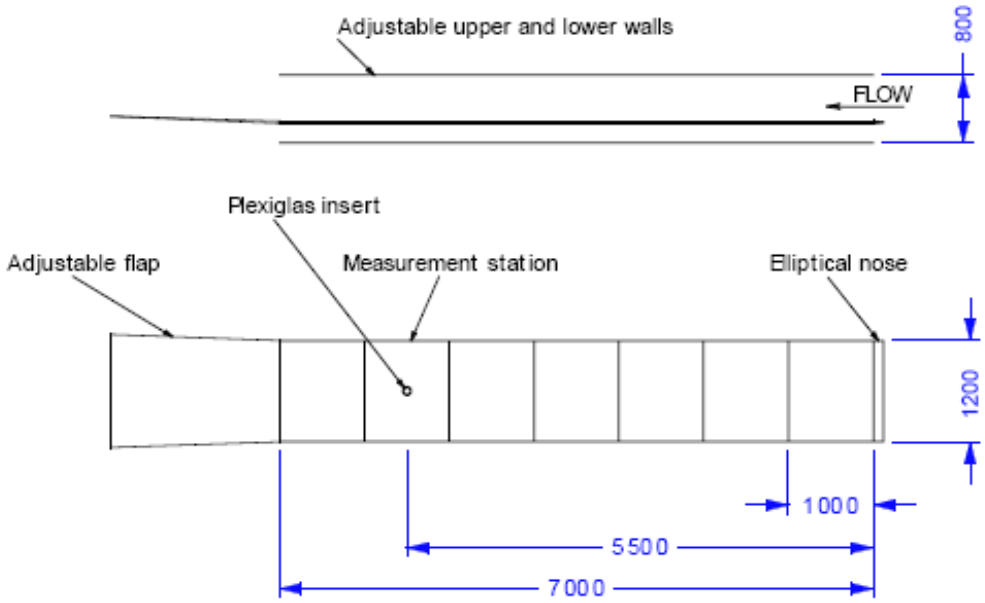

High Re wind tunnel, University of Melbourne

Pressure Adjustment Scheme
for Test Section

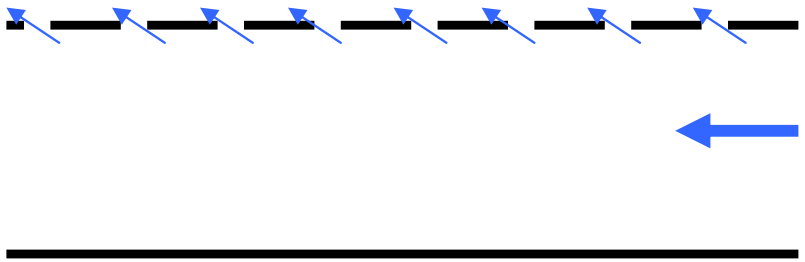

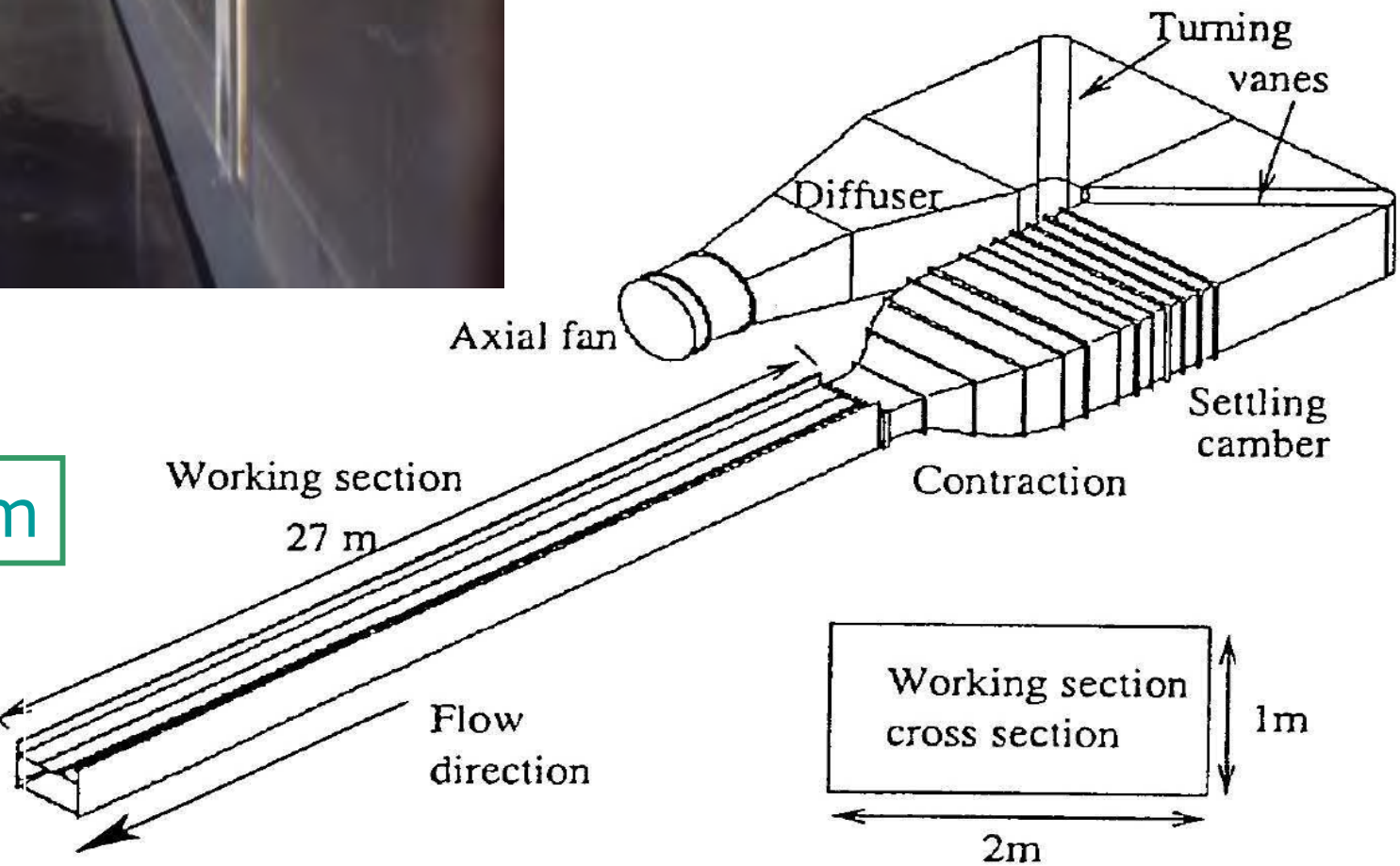

1m x 2m x 27m

Fixed Ceiling with
Transverse Slots for
Pressure Gradient
Relief

Higher Reynolds Number Boundary Layer Data
on a Flat Plate in the NDF
with Pressure Gradient by Chris Christophorou

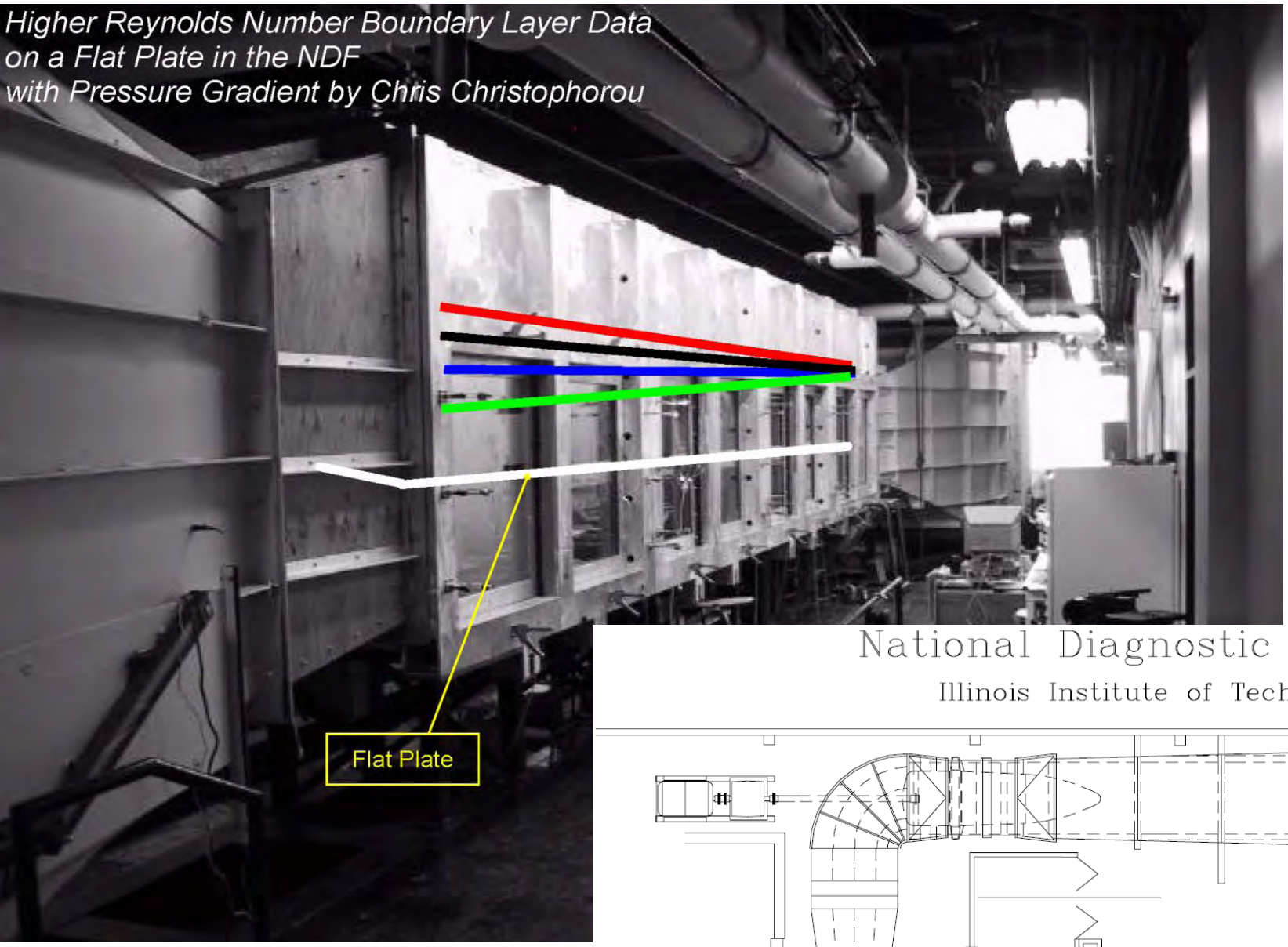

National Diagnostic Facility

Illinois Institute of Technology

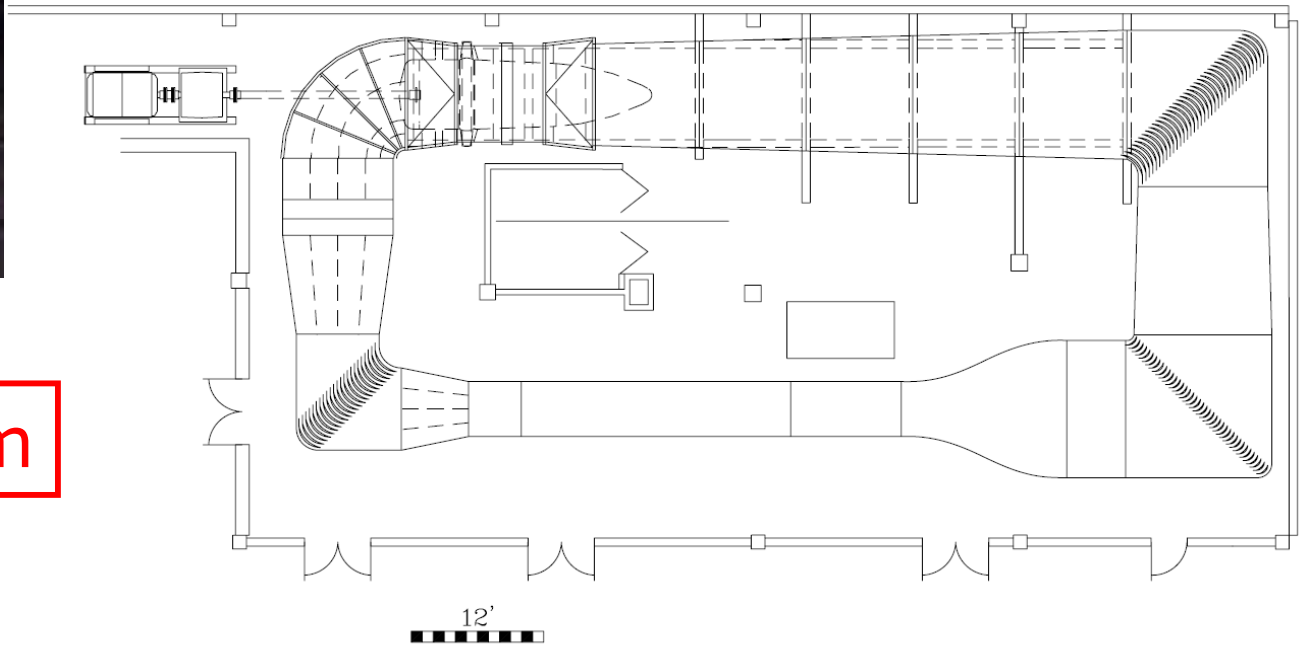

1.3m x 1.5m x 10m

Adjustable Ceiling

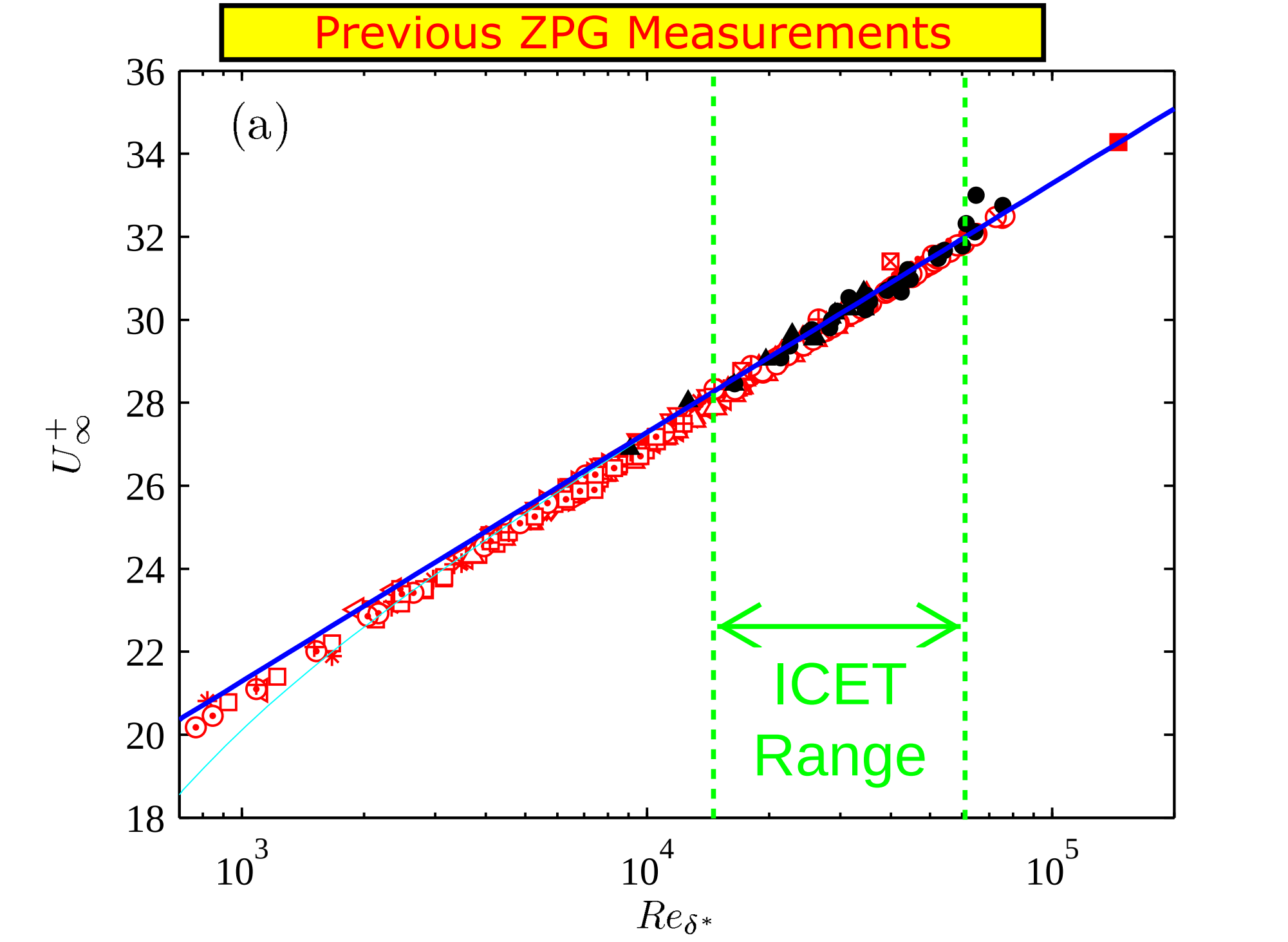
Previous ZPG Measurements
(a)
36
34
32
30
28
26
24
22
20
18
U_∞^+
10^3
10^4
10^5
$Re_{\delta*}$
ICET
Range

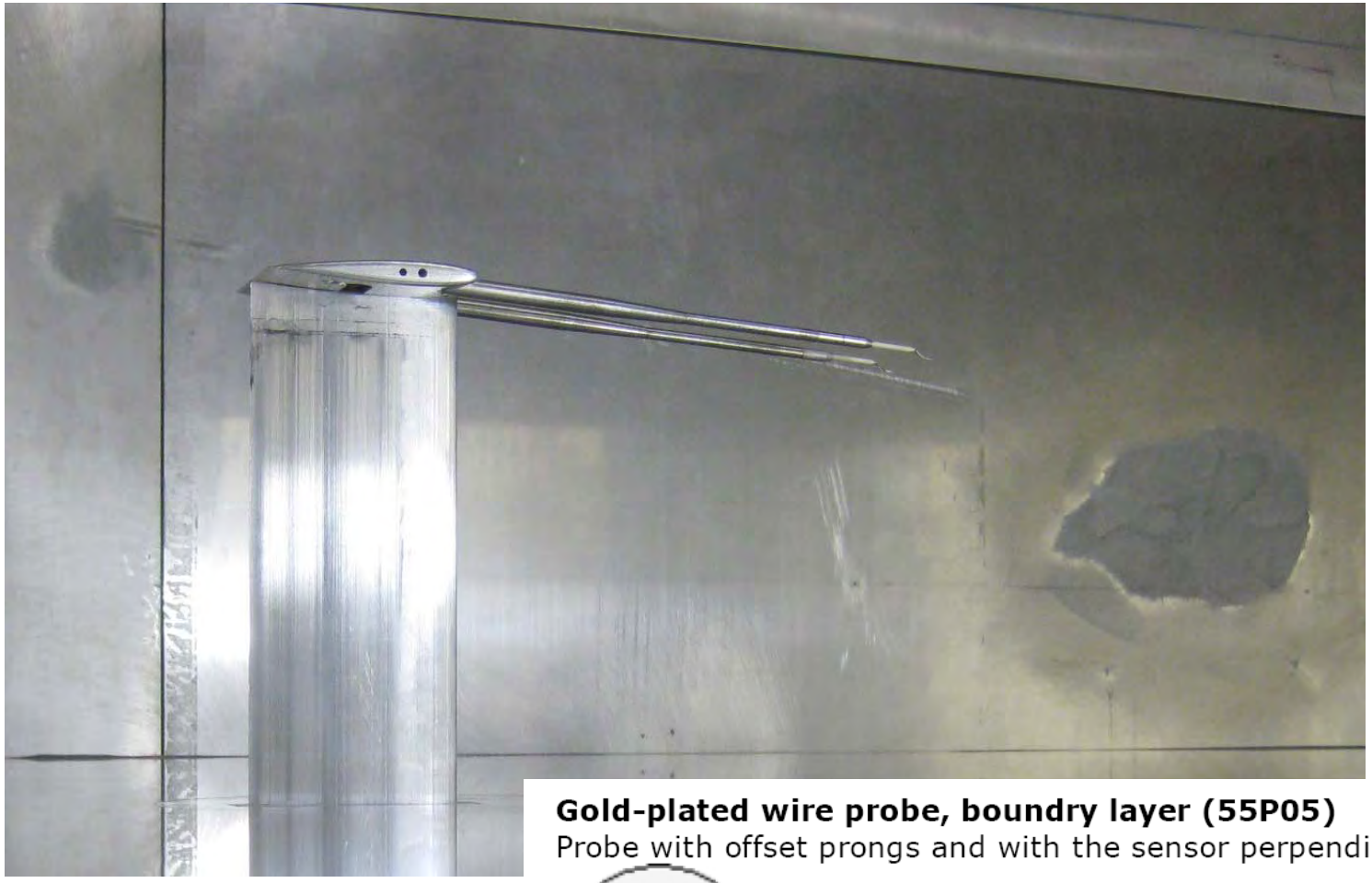

Gold-plated wire probe, boundry layer (55P05)

Probe with offset prongs and with the sensor perpendicular to probe axis.

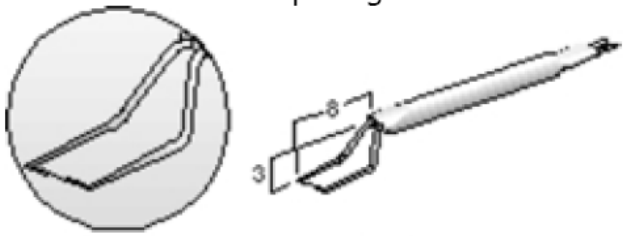

55P05 Boundary layer type

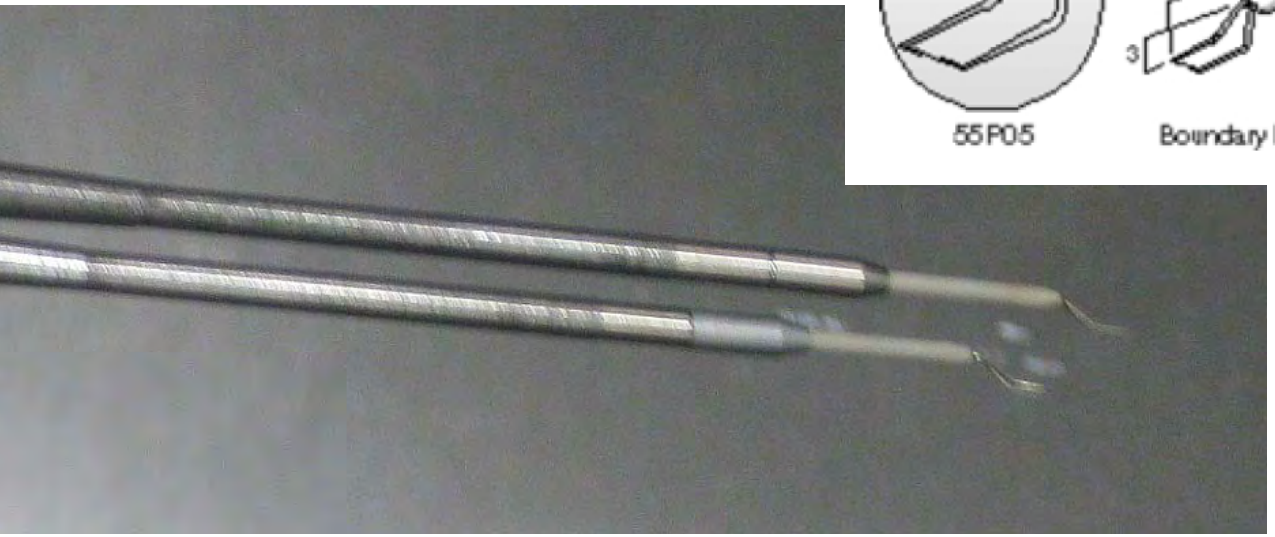

Hot-Wire Probes

Requirements for Accurate Measurements of Wall Distance in High Reynolds Number Wall-Bounded Turbulence

- Continuous and accurate monitoring of wall distance.
- Accurate measurement of velocity near the wall; i.e., minimize probe interference effects.
- Utilize theoretical, DNS or low Re results to correct wall distance:
  - Linear velocity region; often not accessible.
  - Rely on location for peak in rms velocity.
  - Utilize DNS and low Re experimental data in buffer region; e.g., talk AA00007 by Fransson et al.
  - See also talk BN00004 by Alfredsson et al.

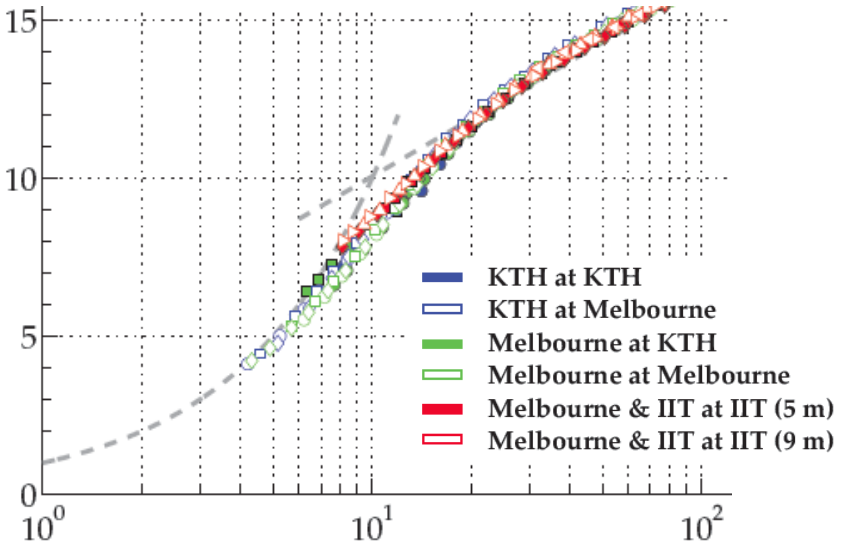

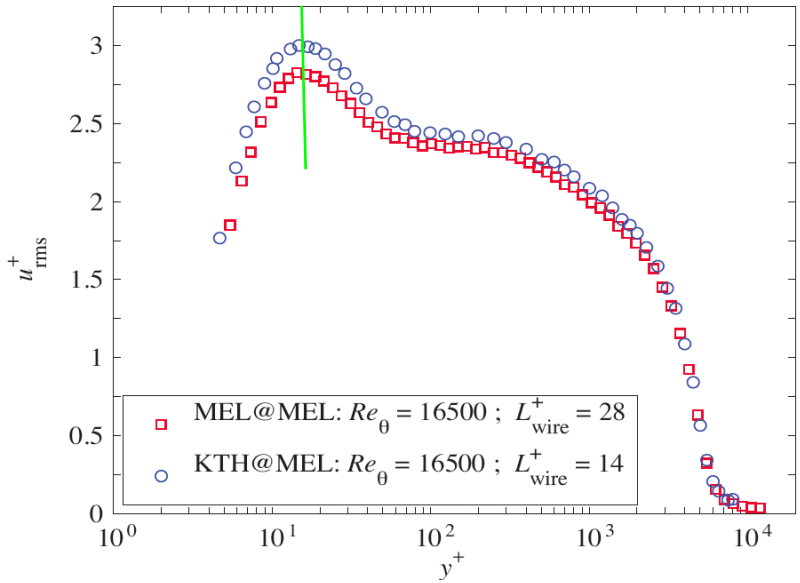

Pitot Probes

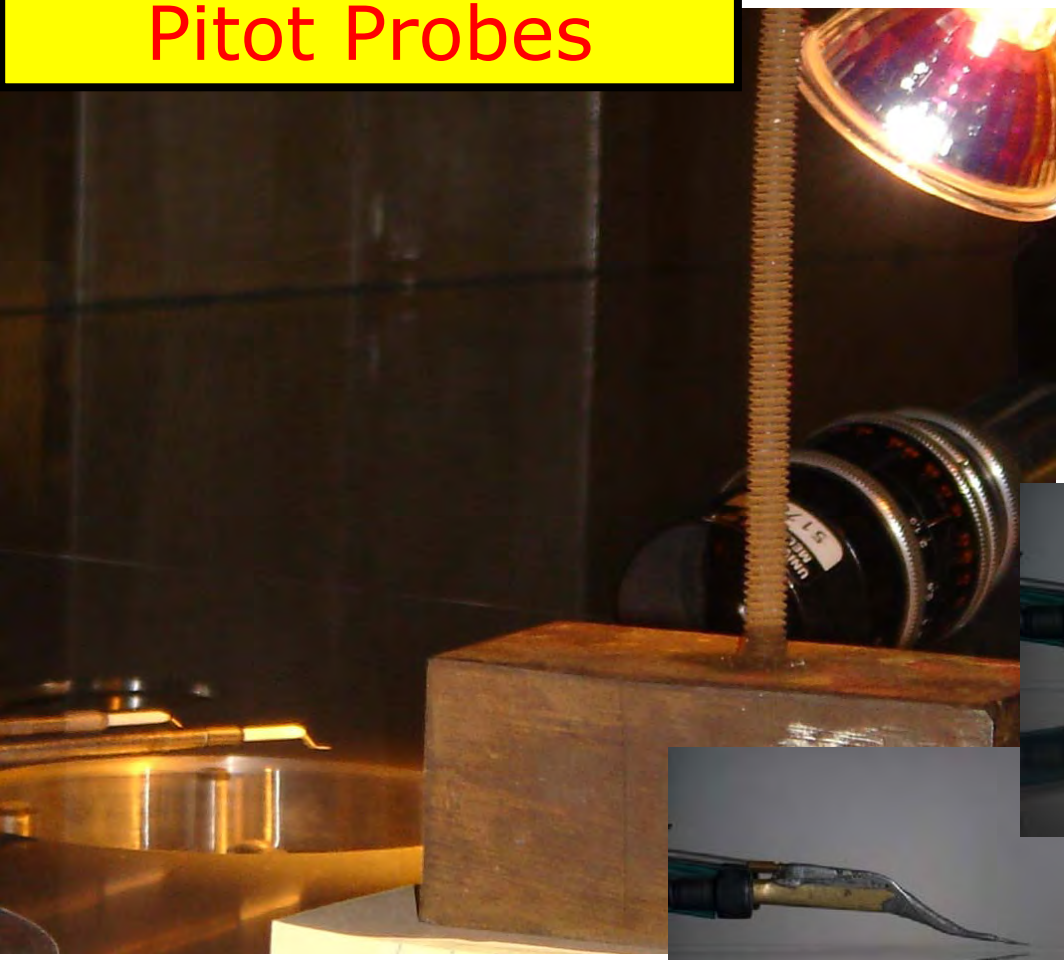

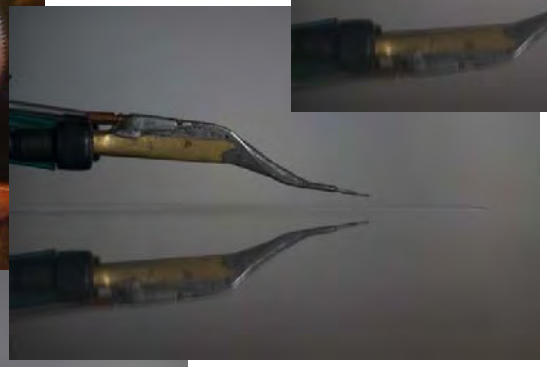

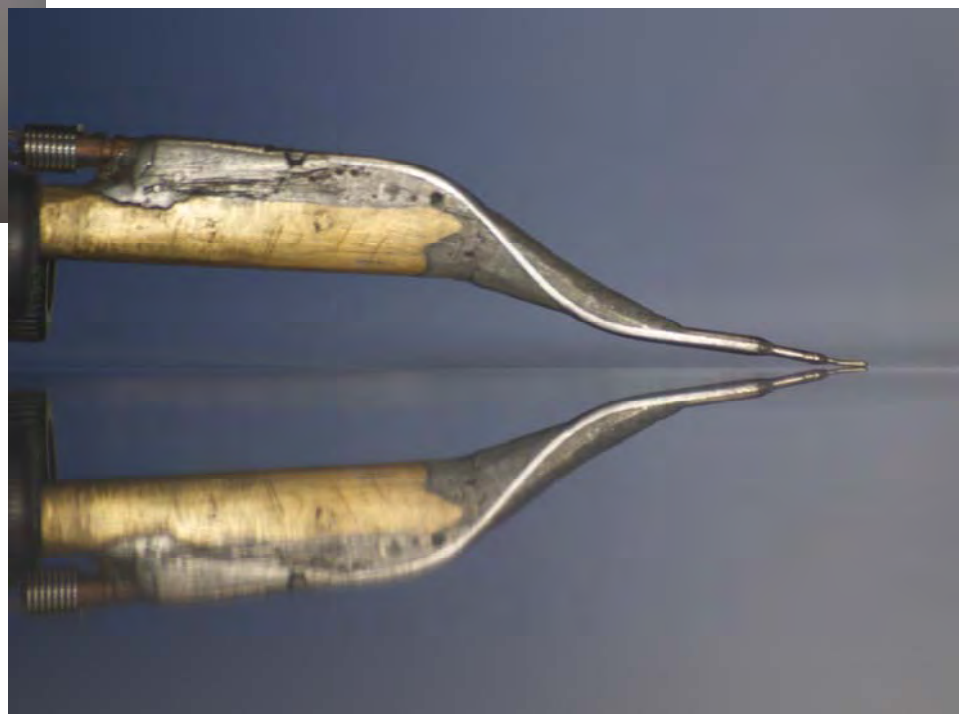

Pressure Gradient in NDF & MTL: Less than 0.2% variation in free stream

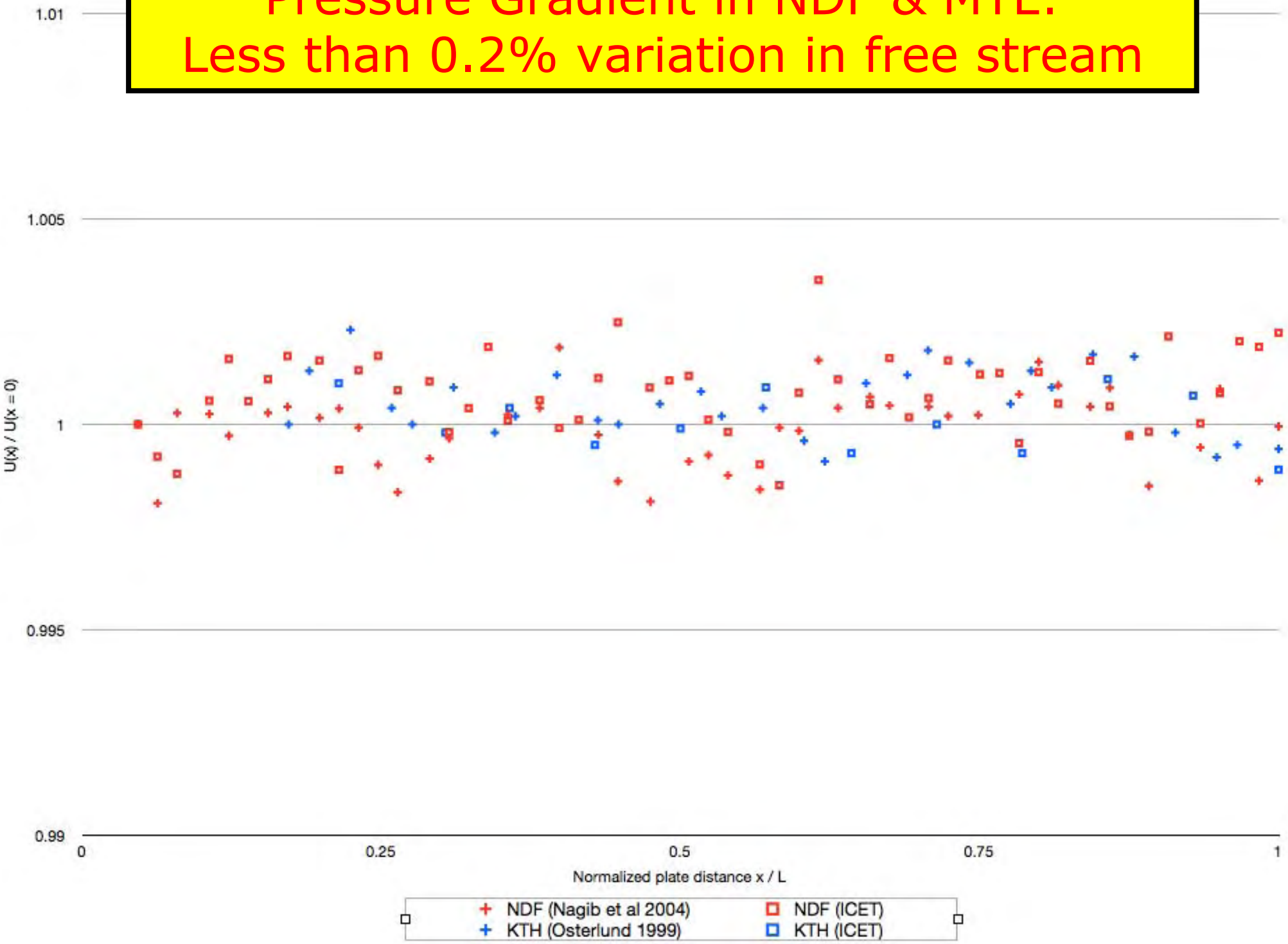

Pressure Gradient in Melbourne: Approximately 2% variation in free stream

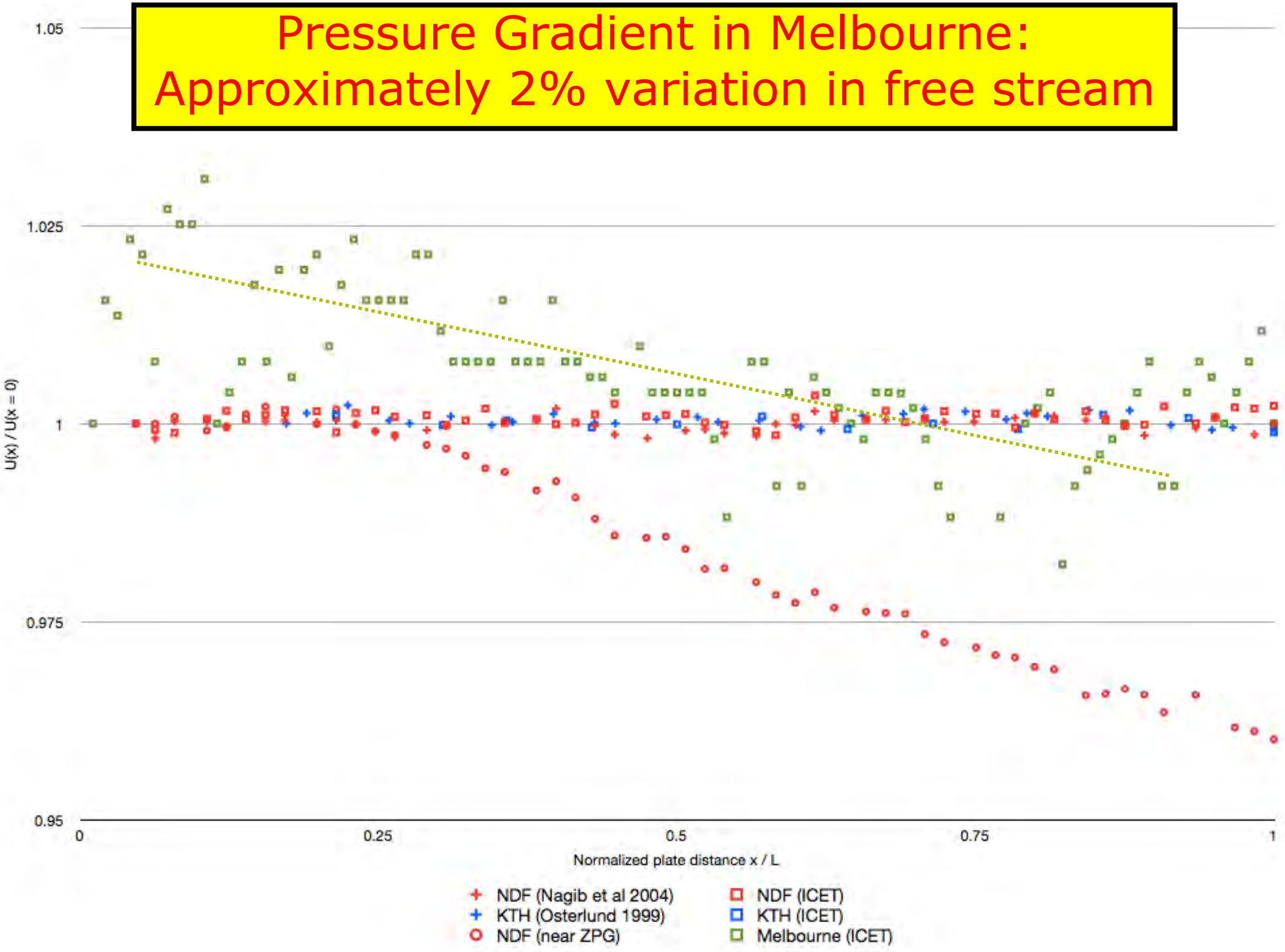

A pressure gradient in NDF with variation of ~4% in free stream, results in a ~4% change in wall-friction velocity. While not accessible with traditional techniques, it is readily measurable with OFI.

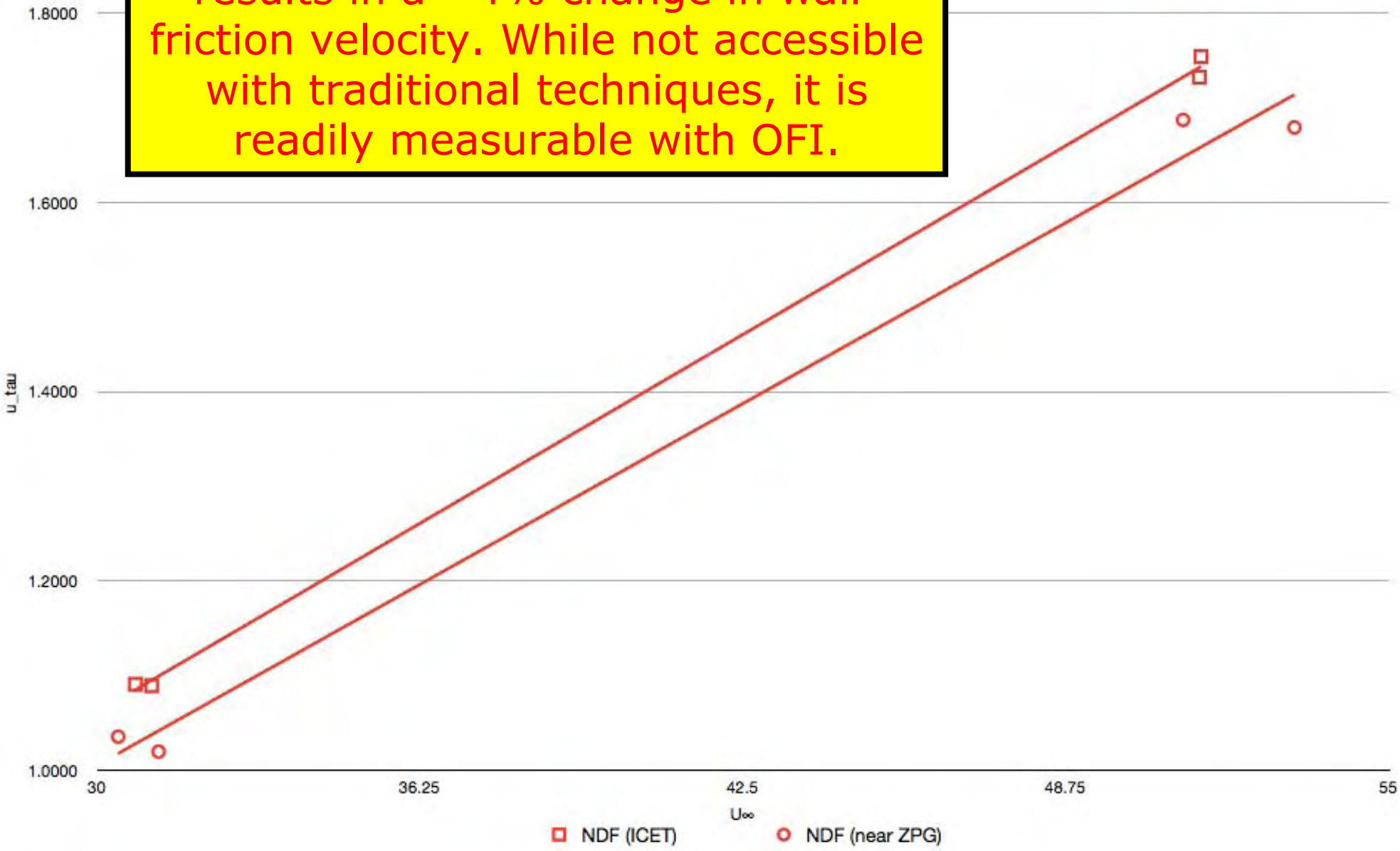

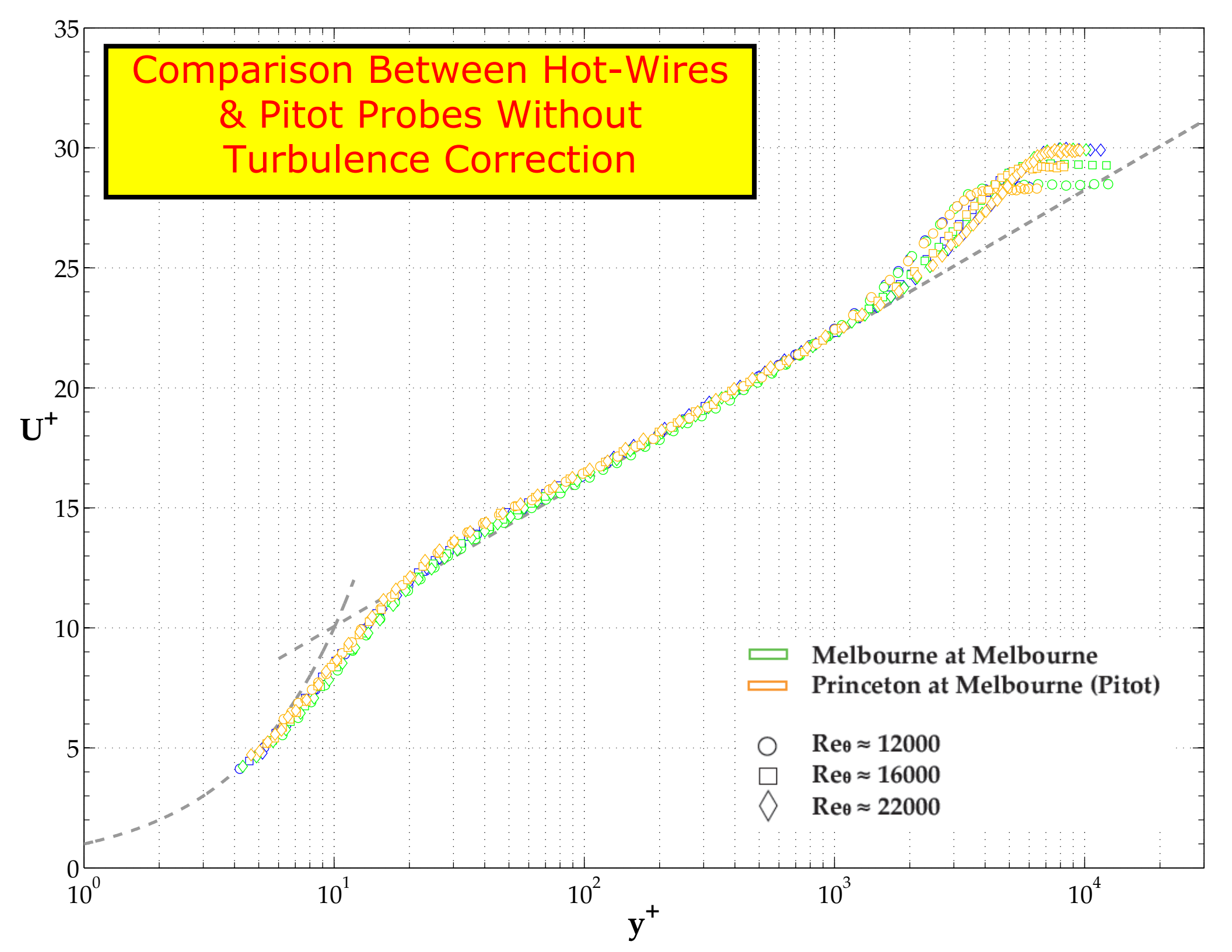
Comparison Between Hot-Wires & Pitot Probes Without Turbulence Correction
U+
y+
0
5
10
15
20
25
30
35
10^0
10^1
10^2
10^3
10^4
Melbourne at Melbourne
Princeton at Melbourne (Pitot)
Reθ ≈ 12000
Reθ ≈ 16000
Reθ ≈ 22000

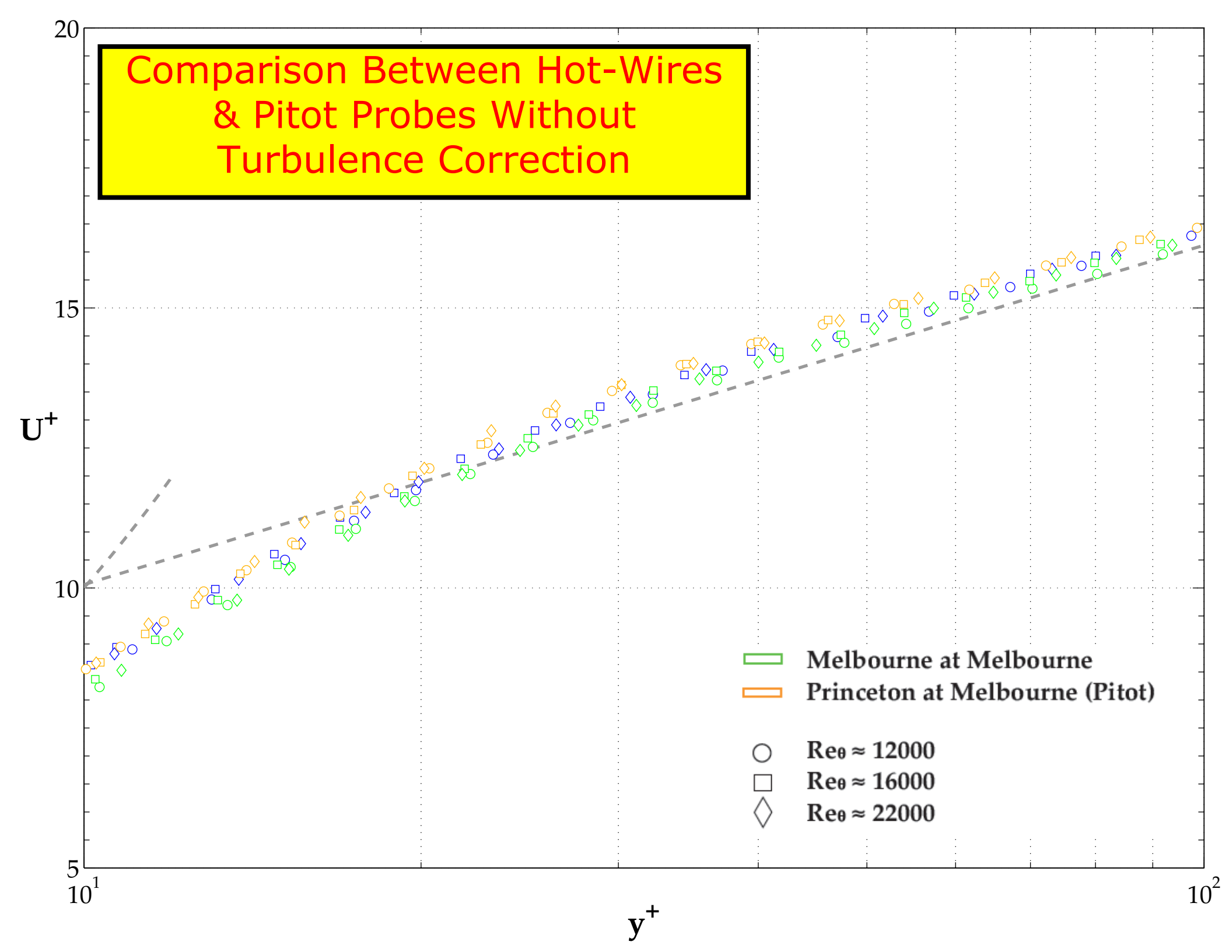
Comparison Between Hot-Wires & Pitot Probes Without Turbulence Correction
20
15
10
5
U^+
10^1
10^2
y^+
Melbourne at Melbourne
Princeton at Melbourne (Pitot)
$Re_\theta \approx 12000$
$Re_\theta \approx 16000$
$Re_\theta \approx 22000$

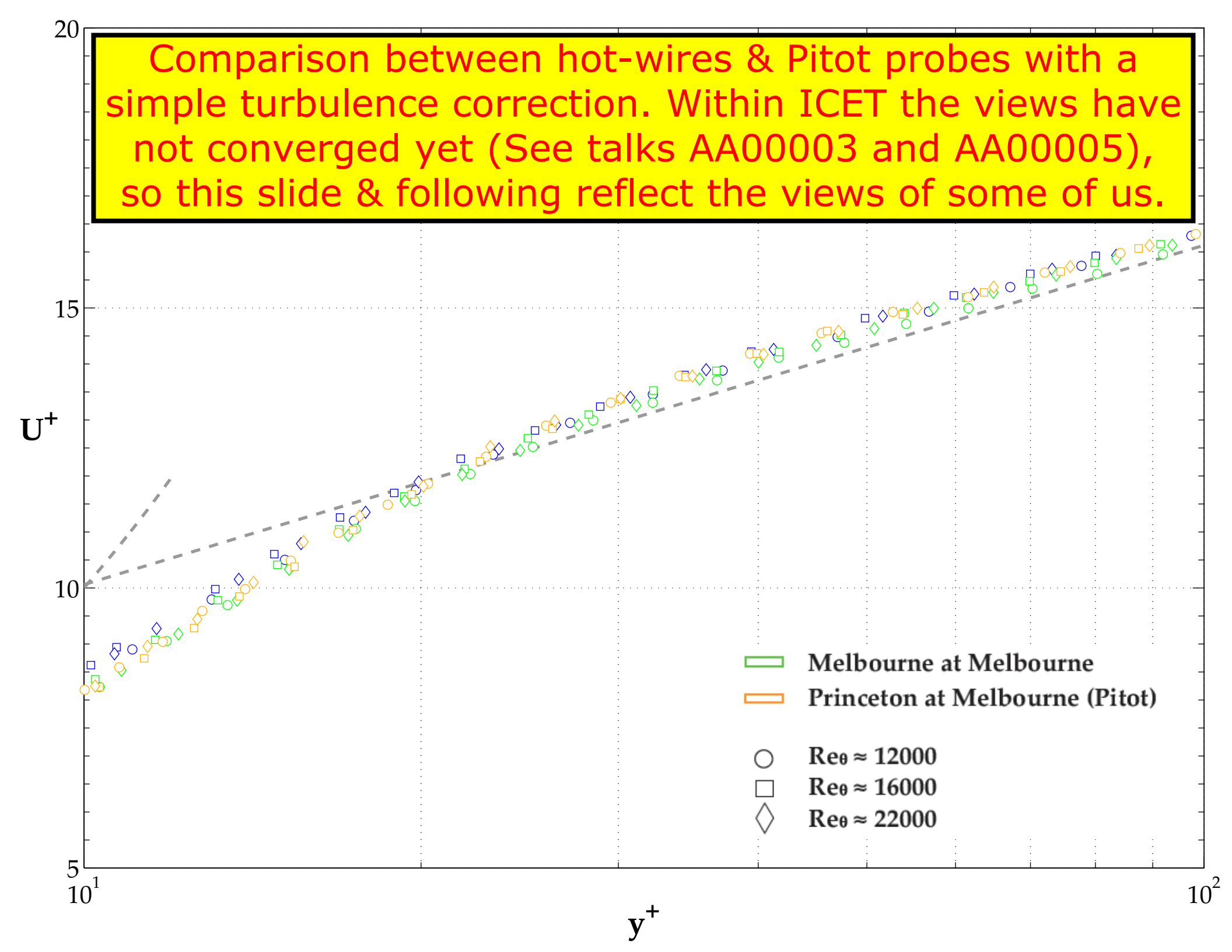
Comparison between hot-wires & Pitot probes with a simple turbulence correction. Within ICET the views have not converged yet (See talks AA00003 and AA00005), so this slide & following reflect the views of some of us.
20
15
10
5
U+
10^1
10^2
y+
Melbourne at Melbourne
Princeton at Melbourne (Pitot)
Reθ ≈ 12000
Reθ ≈ 16000
Reθ ≈ 22000

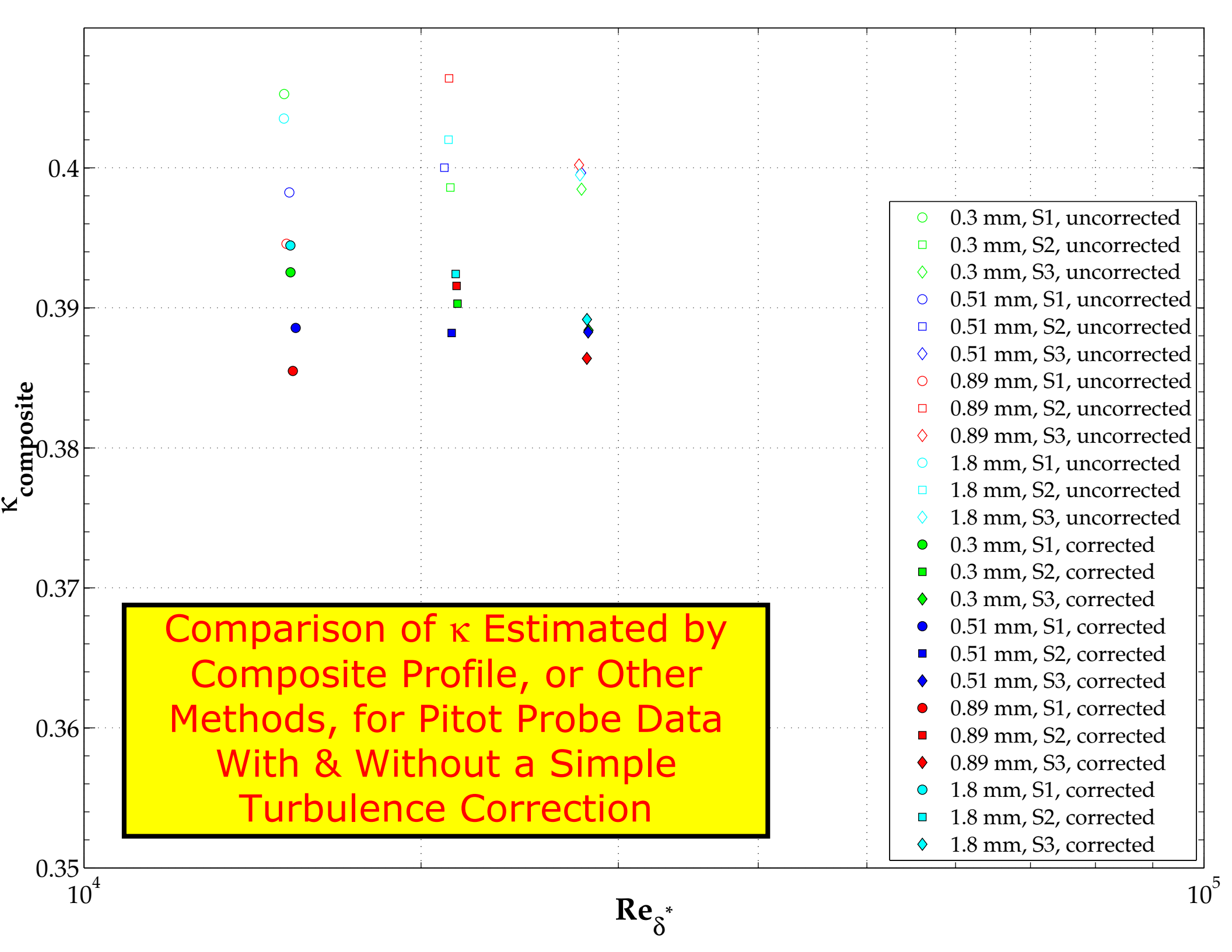
Comparison of κ Estimated by Composite Profile, or Other Methods, for Pitot Probe Data With & Without a Simple Turbulence Correction
κcomposite
Reδ*
0.4
0.39
0.38
0.37
0.36
0.35
10^4
10^5
0.3 mm, S1, uncorrected
0.3 mm, S2, uncorrected
0.3 mm, S3, uncorrected
0.51 mm, S1, uncorrected
0.51 mm, S2, uncorrected
0.51 mm, S3, uncorrected
0.89 mm, S1, uncorrected
0.89 mm, S2, uncorrected
0.89 mm, S3, uncorrected
1.8 mm, S1, uncorrected
1.8 mm, S2, uncorrected
1.8 mm, S3, uncorrected
0.3 mm, S1, corrected
0.3 mm, S2, corrected
0.3 mm, S3, corrected
0.51 mm, S1, corrected
0.51 mm, S2, corrected
0.51 mm, S3, corrected
0.89 mm, S1, corrected
0.89 mm, S2, corrected
0.89 mm, S3, corrected
1.8 mm, S1, corrected
1.8 mm, S2, corrected
1.8 mm, S3, corrected

Conclusions

- See next six talks.
- Criteria regarding the acceptable tolerance in streamwise pressure gradient for ZPG boundary layers have been better defined.
- The requirement of direct and accurate measurements of wall-shear has been reinforced, and caution has again been demonstrated for use of correlations based on other experiments, that may not be representative.
- We have a great deal more to learn from the data we have gathered over last two years and their comparison to other measurements and recent DNS results.
- The need for turbulence correction for Pitot measurements is an important aspect of continuing efforts within ICET. These turbulence corrections could bring the values of the estimated κ closer to those based on hot-wire measurements in the same boundary layer.

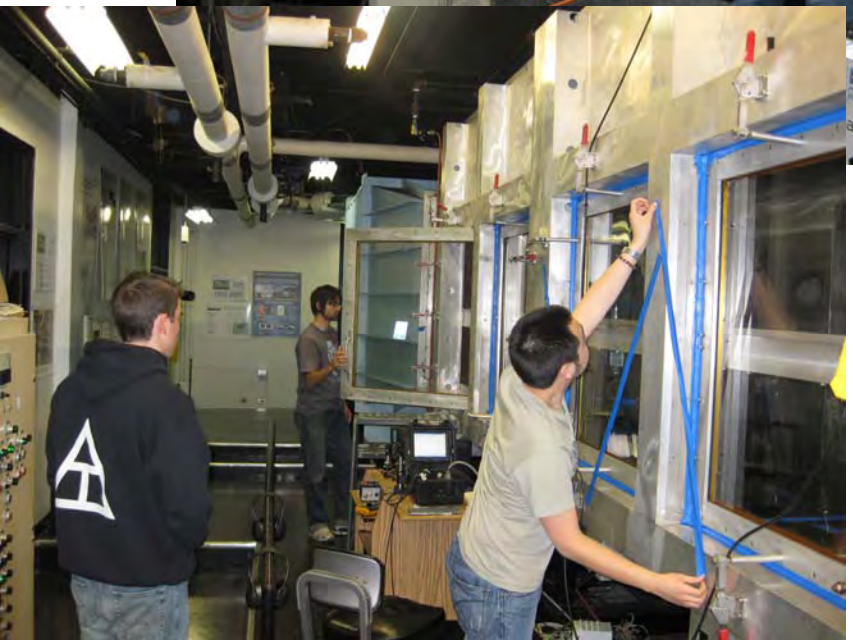

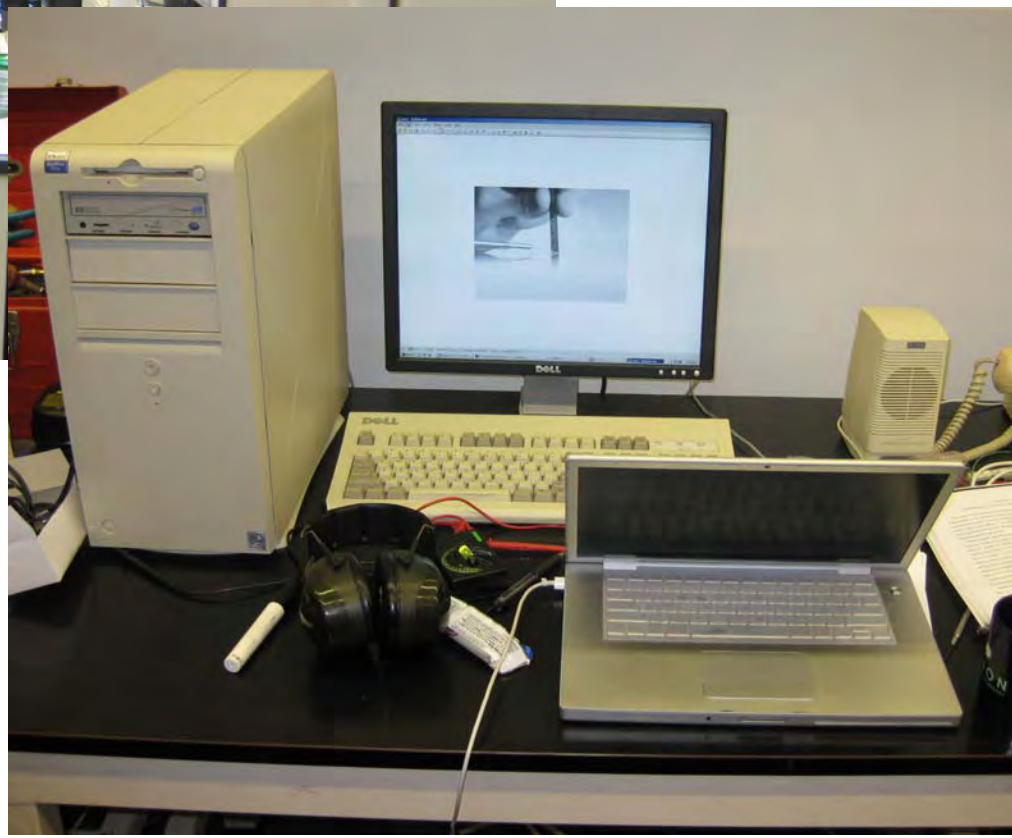

???